**Report Title:**

# Geological and Geotechnical Site Investigation for the Design of a $CO_2$ Rich Flue Gas Direct Injection and Storage Facility

**Final Scientific/Technical Report**

**Reporting Period Start Date: March 31, 2010**

**Reporting Period End Date: June 30, 2013**

**Principal Authors: Paul A. Metz and Patricia Bolz**

**Date Report was Issued: June 2013**

**DOE Award Number: Grant FE0001833**

**University of Alaska Fairbanks**

**P.O. Box 755800**

**Fairbanks, Alaska 99775-5800**

## DISCLAIMER

**Abstract**

With international efforts to limit anthropogenic carbon in the atmosphere, various $CO_2$ sequestration methods have been studied by various facilities worldwide. Basalt rock in general has been referred to as potential host material for mineral carbonation by various authors, without much regard for compositional variations due to depositional environment, subsequent metamorphism, or hydrothermal alteration. Since mineral carbonation relies on the presence of certain magnesium, calcium, or iron silicates, it is necessary to study the texture, mineralogy, petrology, and geochemistry of specific basalts before implying potential for mineral carbonation. The development of a methodology for the characterization of basalts with respect to their susceptibility for mineral carbonation is proposed to be developed as part of this research. The methodology will be developed based on whole rock data, petrography and microprobe analyses for samples from the Caledonia Mine in Michigan, which is the site for a proposed small-scale demonstration project on mineral carbonation in basalt. Samples from the Keweenaw Peninsula will be used to determine general compositional trends using whole rock data and petrography. Basalts in the Keweenaw Peninsula have been subjected to zeolite and prehnite-pumpellyite facies metamorphism with concurrent native copper deposition. Alteration was likely due to the circulation of $CO_2$-rich fluids at slightly elevated temperatures and pressures, which is the process that is attempted to be duplicated by mineral carbonation.

**Table of Contents**



Figures

Tables



Appendices

# Executive Summary


The primary objectives of the project are: a) to develop a methodology for geological and geotechnical site characterization for direct inject of carbon dioxide enriched flue gas streams from stationary sources into large underground cavities in mafic rocks thereby defining the parameters that enhance carbonation of the rocks and permanent sequestration, b) complete characterization of at least one potential mine site suitable for a small demonstration project for the storage of at least 100 tons of carbon dioxide, c) development a design and cost estimate for a direct injection facility at the selected mine site.

The site characterization work includes defining the mineralogical, petrological, chemical composition of the basalts and the determination of the physical properties of the mafic rocks. From project inception approximately 250 samples were collected from 29 mine tailings sites in the Keweenaw Copper Belt (KCB). Of the total, 181 samples were processed for whole rock, trace element, and rare earth element geochemical analyses. Optical mineralogy and petrology examinations and electron microprobe analyses were conducted on selected material from the mine tailing sites and the Caledonia Mine site.

The critical geological parameters for site characterization are defined as: a) the mineralogy, petrology, and geochemistry of the mafic and or ultramafic rocks, b) the geological structures of the host rocks including flow thickness, folding, faulting, jointing and joint spacing, c) rock mechanical properties including compressive strength, and rock mass strength, and d) total volume of rock mass available to mineral carbonation.

The results also support previous investigations that demonstrate that the large native copper deposits were formed as a consequence of $CO_2$-bearing metamorphic fluids migrating through the relatively high porosity sections of the amygdaloidal flow tops of the volcanic sequences. These fluids resulted in the formation of zeolite and prehnite-pumpellyite facies mineral assemblages. These mineral assemblages represent temperature and pressure conditions similar to those that would be produced by the direct injection of a flue gas stream from a coal or natural gas fired power plant.

The large volumes of basaltic rocks of the Portage Lake Volcanics of the Keweenaw Peninsula provide the potential to the storage of very large volumes of carbon dioxide through mineral carbonation. The Portage Lake Volcanic constitute but a very small portion of the extrusive and intrusion mafic and ultramafic rocks of Mid-Continental Rift System including the Duluth Gabbro of Minnesota and the Logan Sills of northwestern Ontario. In aggregate these rocks provide potential storage capacity for extremely large quantities of $CO_2$.

**Experimental Methods:**

**Introduction**

The purpose of this study is to develop a methodology for the characterization of site for the direct injection of a $CO_2$ rich flue gas into basalts and the permanent storage of the gas through mineral carbonation. The basaltic rocks of the Keweenaw Peninsula of northern Michigan were selected due to the large past production of native copper and the vast amount of published research that strongly supports the hypothesis that the mineral deposits were formed by low temperature $CO_2$ rich metamorphic fluids. The estimated temperature and pressure ranges of these mineralizing metamorphic fluids is within the range of the flue gas temperatures of coal and natural gas fired power plants. Thus nature is providing evidence that mineral carbonation may be technically feasible.

The primary objectives of the project are: (1) to develop a methodology for geological and geotechnical site characterization for direct inject of carbon dioxide enriched flue gas streams from stationary sources into large underground cavities in mafic rocks thereby defining the parameters that enhance carbonation of the rocks and permanent sequestration, (2) complete characterization of at least one potential mine site suitable for a small demonstration project for the storage of at least 100 tons of carbon dioxide, (3) examination, sampling, and testing of mine tailings throughout the Keweenaw Copper Belt to estimate the extent of carbonation of the waste material as a consequence of exposure to atmospheric carbon dioxide over the past 100 years, (4) estimate the volume of atmospheric carbon dioxide that has been naturally sequestered in the mine tailings, (5) from the mine and tailings site characterization work, establish instrumentation to monitor the direct injection facility in the basalts, (6) development a design and cost estimate for a direct injection facility at the selected mine site. The site characterization work includes defining the mineralogical, petrological, chemical composition of the bas alts and the determination of the physical properties of the mafic rocks.

The pre-requisite for any geological site characterization of an engineering work is to develop at least a conceptual design for the engineering work that is to be sited. With that conceptual design in hand, critical geological parameters can then be defined and the site investigation can then proceed to determine if the site can meet the specifications for those critical parameters.

**Conceptual Design of a Flue Gas Direct Injection Facility**

The concept is to inject an entire flue gas stream into a large opening in the mafic rocks similar to that developed for the Block Caving mining method. The opening would be at the deepest feasible level and would be sized as constrained by mechanics of the host rocks. In a fully operating system multiple cavities would be created. The number being a function of the volume of the gas stream (size of the power plant) and the reaction rate of the carbonation process. Flue gas streams from coal fired power plants are generally composed of 72-77% $N_2$, 13-15% $CO_2$, and the remainder $H_2O$. Once the $CO_2$ concentration of the gas stream in a cavity reached an acceptable level, the compressed $N_2$ is released back to the power plant and then to the atmosphere. The exothermal heat of the carbonation reactions then could be utilized.

As the surfaces of the fractured and caved rock become coated the reaction products, the back of the cavity would be drilled, blasted, and allowed to cave. Thus the cavity would migrate upward to a level below that of groundwater extraction and below that at which fractures may propagate to the surface. Proper design of the initial cavity taking into account the swell factor for the rock and the volume of reaction products, the cavity should be filled as it reaches its design life. Thus mine subsidence would be prevented.

The major attributes of the concept include: a) permanent sequestration of $CO_2$ without the potential for future releases of supercritical fluids, b) avoidance of costly $CO_2$ recovery systems in the power plant design, c) potential recovery of additional energy from the power plant and from the heat released by the carbonation reactions, d) potential for the permanent sequestration of other deleterious elements in the flue gas stream such as mercury and uranium as these form mineral deposits under similar temperature and pressure conditions as the mineral carbonation reactions, and e) potential recovery of additional copper from formation waters in which the pH is reduced below 5.5 by the formation of carbonic acid.

Thus the critical geological parameters are: a) the mineralogy, petrology, and geochemistry of the mafic and or ultramafic rocks, b) the geological structures of the host rocks including flow thickness, folding, faulting, jointing and joint spacing, c) rock mechanical properties including compressive strength, and rock mass strength, and d) total volume of rock mass available to mineral carbonation.

The general assumptions and cost estimate for the design of a direct injection demonstration project at the Caledonia Mine is included as Appendix B. The total estimated cost for the direct injection of 100 tons of $CO_2$ into the mine is $1.9 million.

**Background**

Many authors have mentioned basalts in general as potential host rocks for in-situ mineral carbonation (McGrail et al., 2006; Goldberg et al., 2008; Matter et al., 2009; Rosenbauer et al., 2012); numerous aqueous phase studies for pure minerals and $CO_2$ have been conducted (Wogelius and Walther, 1991; Guthrie et al., 2001; Oelkers and Gislason, 2001; Gerdemann et al., 2003; Gíslason and Oelkers, 2003; Bearat et al., 2006; Chen et al., 2006; Krevor and Lackner, 2009); and studies on thermodynamics and kinetics of mineral carbonation have been performed (Königsberger et al., 1999; Marini, 2007; Krupka et al., 2010; Aradóttir et al., 2012; Rosenbauer et al., 2012). Most of the work mentioned above is based on either specific basalts, or some kind of assumed basalt composition that is believed to be typical. Maps showing basalt distributions have been developed, inferring the mapped basalts could be feasible for mineral carbonation (e.g. see Figure 1.1).

Figure 1. Distribution of major basalt formations and $CO_2$ sources (from McGrail et al., 2006).

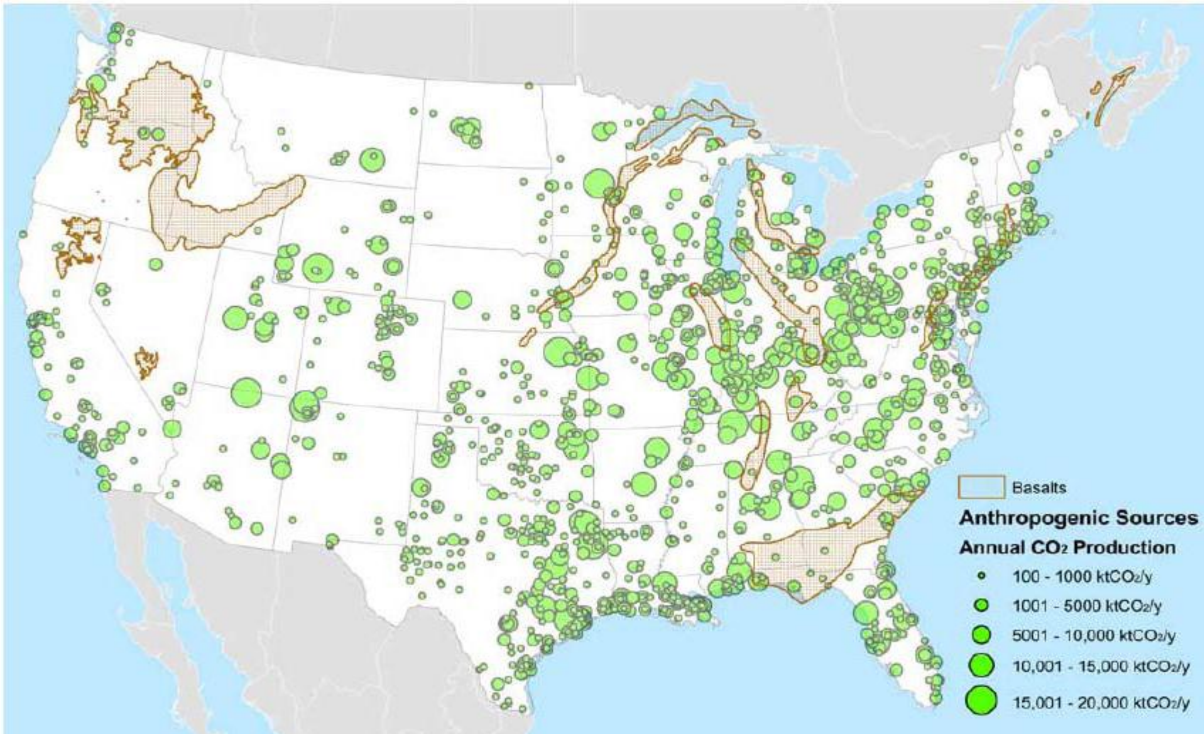


A first step in determining the feasibility of specific basalt for mineral carbonation should involve detailed studies on its mineralogy, petrology, and geochemistry. The thermodynamics and kinetics of reactions between calcium, magnesium, or iron silicate minerals with $CO_2$ depend on many factors such as the mineralogy, texture, and geochemistry of the given basalt. The mineralogy of basalts can vary widely due to depositional environment and presence and extent of alteration. Naturally occurring alteration due to hydrothermal fluids or metamorphism may deplete silicate minerals in calcium and magnesium, or form silicate minerals that are less likely to react with $CO_2$ to form carbonates and thus decrease the potential for mineral carbonation.

With the attempt of limiting anthropogenic carbon emissions as part of international efforts to reduce global warming, several carbon sequestration options have been proposed and are currently studied by various research facilities (Beecy and Kuuskraa, 2001; Aradóttir et al., 2011; McGrail et al., 2011; Zevenhoven et al., 2011). Successful carbon sequestration could reduce anthropogenic carbon emissions without necessitating a substantial decrease of fossil fuel usage. One type of geologic sequestration is generally referred to as mineral carbonation. Mineral carbonation is defined as the reaction of certain calcium, magnesium and iron bearing silicate minerals with carbon dioxide to form thermodynamically stable carbonates such as calcite, magnesite, and siderite (Lackner et al., 1995). The mineral carbonation process occurs naturally, and is commonly known as a form of weathering or alteration. Ultramafic and mafic rocks are typically rich in calcium, magnesium, and iron silicates (e.g. olivine, calcic plagioclase, and pyroxene) and have been studied by numerous authors with respect to their potential for mineral carbonation (Lackner et al., 1997; Gerdemann et al., 2003; Bearat et al., 2006; Chen et al., 2006; Oelkers et al., 2008; Brown et al., 2010). Alteration products of ultramafic rocks include hydrous silicates (e.g. serpentine), which have been observed to react with atmospheric $CO_2$ to form hydrous carbonates on mine tailings (Wilson et al., 2006; 2009).

Basalts form in a wide variety of tectonic environments including mid-ocean ridges, island arcs, back-arc basins, intra-plate oceanic islands, large igneous provinces and intra-continental rifts. Not surprisingly, basalts are the most common volcanic rock by volume at the earth's surface (Gill, 2010). Major basalt formations in the United States are shown in Figure 1.1. One of the shown basalt formations is located just north and south of Lake Superior in Michigan. The samples used for this project were collected from the major basalt formation located along the southern flank of Lake Superior. These basalts are known as Keweenaw Volcanics. The Keweenaw Volcanics formed in a relatively short-lived midcontinent rift system during the Mesoproterozoic in the North American craton. The rift length has been estimated to about 2,000 km with an extensional width of no more than 100 km and a thickness of up to 20 km (Ojakangas et al., 2001) (see Figure ). Large extents of the Keweenawan Volcanics have been covered by sedimentary deposits, but remain exposed in the study area along the Keweenaw Peninsula.

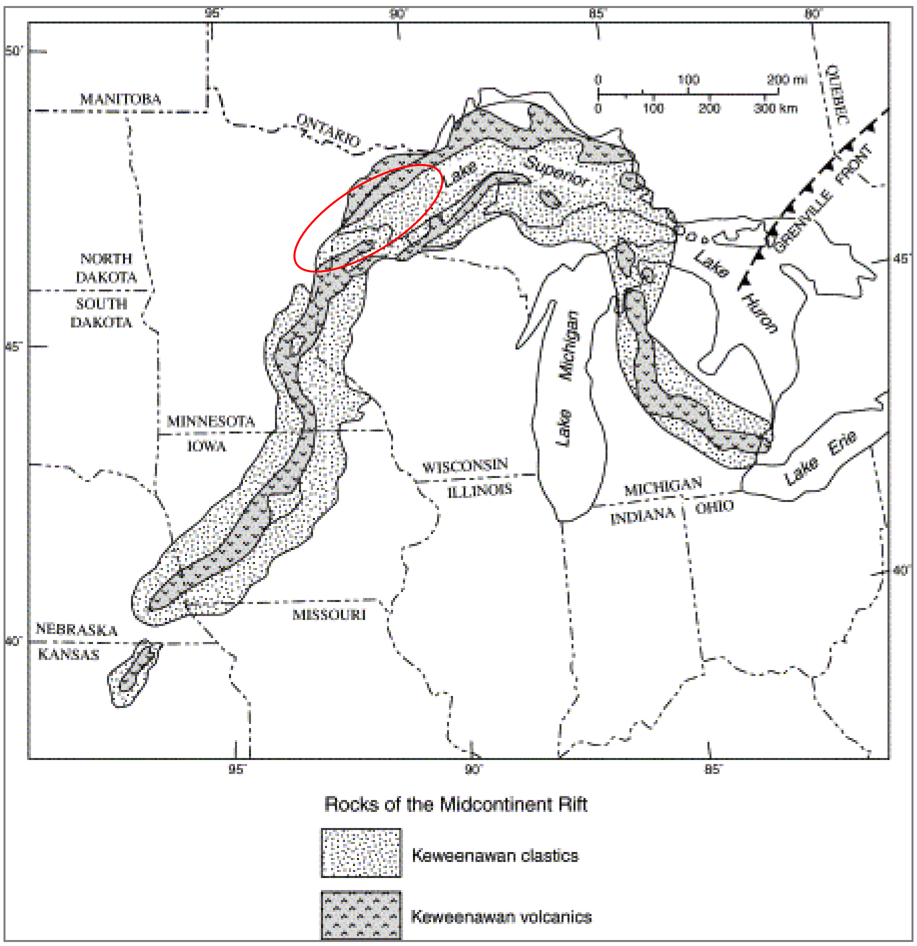


Figure 2 Midcontinent rift basalts (modified from Ojakangas and others, 2001).

The study focuses on the basalts from the Keweenaw Peninsula and the Caledonia Mine. These basalts have been variedly metamorphosed and show signs of hydrothermal alteration that is believed to have occurred concurrently with the deposition of native copper (Cornwall, 1951; Stoiber and Davidson, 1959; Paces and Bornhorst, 1985; Pueschner, 2001; Brown, 2006).

## Sampling for Rock Characterization

Samples were collected from mine tailings of the Keweenaw Copper Belt during the field seasons of 2010 and 2011 by P.A. Metz, P. Bolz and J. Dezelski. Sample locations are shown in Figure 3.

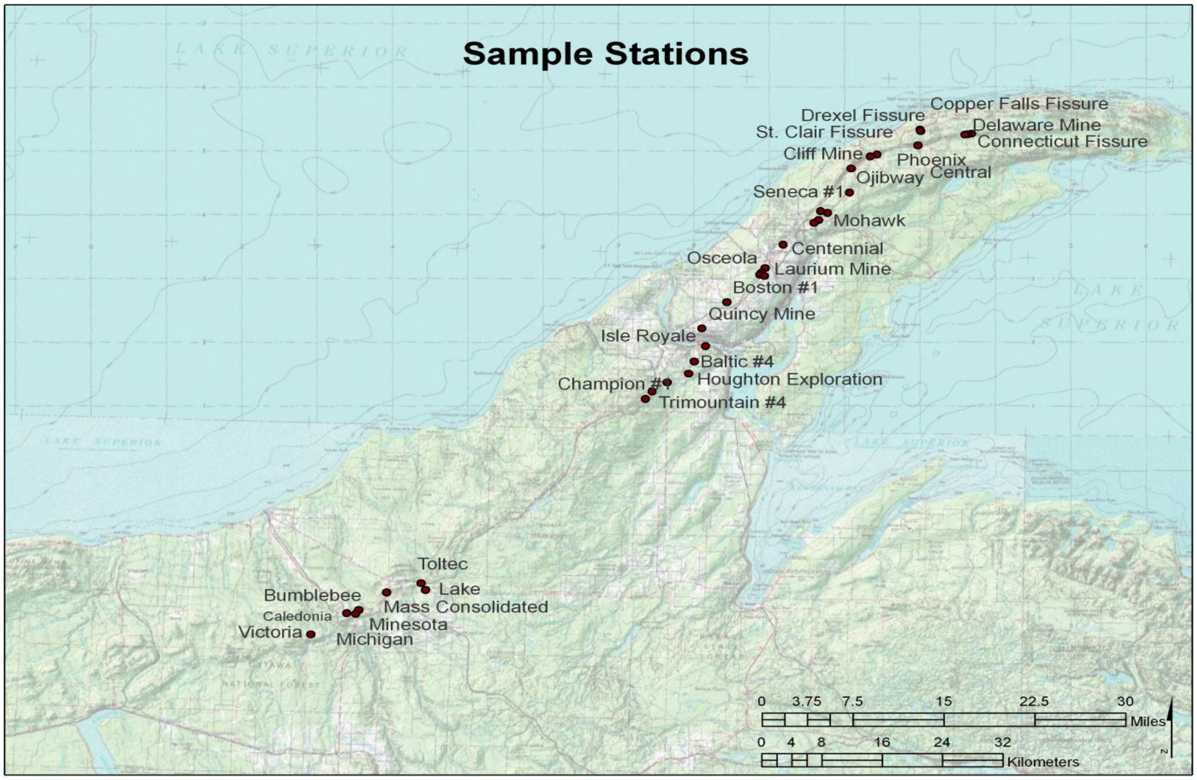


Figure 3 Sample station locations (Keweenaw Peninsula, including Caledonia)

A total of 181 samples were collected for rock characterization of which eight were hand specimen only. For each sample station, four to six samples were collected including amygdaloidal, fine-grained, medium-grained, ophitic, granitic and brecciated samples if present. For each station samples were collected to include the main textures present at the location. Whole rock laboratory analysis was done on 173 samples by *ALS Minerals*. Analytes included major elements, C, S, base metals, trace elements and rare earth elements (REE) as well as volatiles. Whole rock analyses were done using lithium metaborate fusion, by leco, four acid analysis, lithium borate fusion and aqua regia (ALS Minerals Service Schedule, 2010). The complete set of data for all samples is included in this report in the appendix. Samples names were based on year, location and sample number. Sample names with mine names, lode and location (Northing and Easting based on UTM coordinates in Zone 16T) are shown in Table 2.

Table 1. Whole rock sample, mine and lode names and location.

| Sample | Mine | Lode | UTM Zone 16T | |
|---|---|---|---|---|
| | | | Northing | Easting |
| BA | Baltic #4 | Baltic Amygdaloid | 5213657 | 376437 |
| BB | Bumblebee | - | 5178023 | 335590 |
| CC | Mohawk #6 | Kearsarge Amygdaloid | 5238639 | 395919 |
| CE | Central | Fissure | 5250807 | 409721 |
| CF | Copper  Falls Fissure | Fissure | 5253261 | 410018 |
| CH | Champion #1 | Baltic Amygdaloid | 5211127 | 373617 |
| CL | Cliff Mine | Fissure | 5247189 | 400866 |
| CN | Centennial | Calumet & Hecla Conglomerate | 5235262 | 391861 |
| CO | Connecticut Fissure | Fissure | 5252538 | 416292 |
| DE | Delaware Mine | Allouez Conglomerate | 5252635 | 416814 |
| DR | Drexel Fissure | Fissure | 5252490 | 415977 |
| FJ | Boston #1 | Allouez Conglomerate | 5226257 | 384365 |
| FU | Mohawk #5 | Kearsarge Amygdaloid | 5239116 | 396519 |
| GR | Mohawk #1 | Kearsarge Amygdaloid | 5240236 | 397742 |
| HE | Houghton Exploration | Baltic Amygdaloid | 5215044 | 379318 |
| IR | Isle Royale #1 | Isle Royale Amygdaloid | 5219401 | 381553 |
| | Isle Royale #4 | Isle Royale Amygdaloid | 5216962 | 380034 |
| LA | Lake | - | 5181192 | 344416 |
| MC | Mass Consolidated | - | 5180802 | 339252 |
| MG | Michigan | - | 5177421 | 335191 |
| MI | Minesota (?) | - | 5177546 | 333999 |
| OC | Osceola #4 | Osceola Amygdaloid | 5230894 | 388987 |
| | Osceola #5 | Osceola Amygdaloid | 5230554 | 388755 |
| | Osceola # 13 | Osceola Amygdaloid | 5231570 | 389440 |
| OJ | Ojibway | Kearsarge Amygdaloid | 5243453 | 400679 |
| PH | Phoenix | Fissure | 5249104 | 403419 |
| QU | Quincy Mine | Pewabic Amygdaloidal | 5222120 | 381102 |
| SC | St. Clair Fissure | Fissure | 5249381 | 404285 |
| SE | Seneca #1 | Iroquois & Houghton? | 5240534 | 396833 |
| TO | Laurium Mine | Kearsarge Amygdaloid (?) | 5230346 | 389342 |
| TR | Trimountain #4 | Baltic Amygdaloid | 5212289 | 374483 |
| TT | Toltec | - | 5182240 | 343842 |
| VI | Victoria | - | 5174214 | 329226 |
| CBF | Caledonia | - | 5179700 | 337622 |
| CLD | Caledonia | - | 5179700 | 337622 |

## Results and Discussion

### Whole Rock Data

The collected samples were classified using a total alkali silica diagram (TAS) as shown in 4. Data used in 4 was first normalized to 100% excluding volatiles (LOI, $CO_2$, $H_2O$) and then plotted on the diagram.

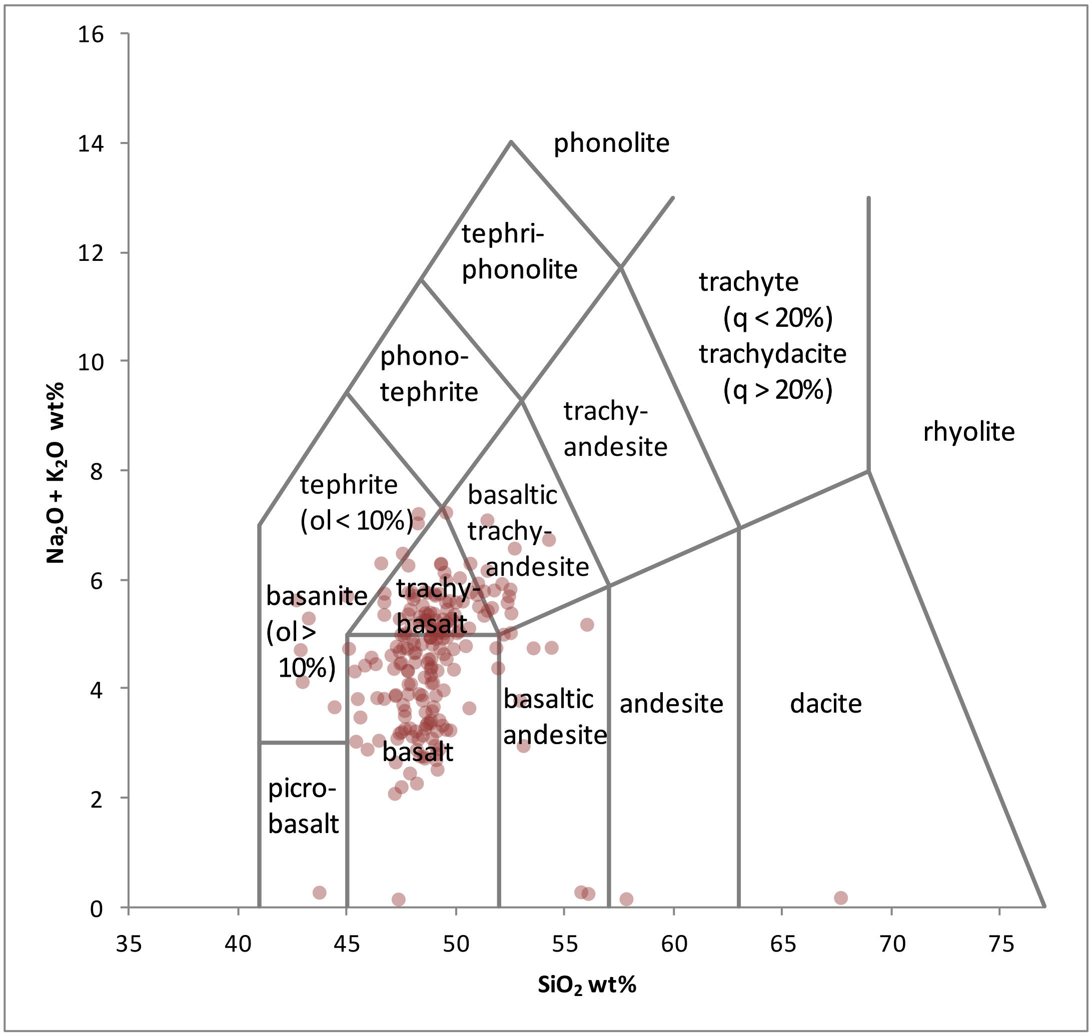


Figure 4. TAS diagram for collected samples (Keweenaw Peninsula, including Caledonia).

Most of the volcanic rocks in the sampled region are classified as basalt or trachy-basalt. Few samples are more or less silica rich then the bulk of the. Samples with low alkali contents ($Na_2O$ + $K_2O$ weight %) were mostly amygdaloidal samples that had been intensely weathered (excluding the dacite sample).

AFM and ACF ternary plots were constructed from the whole rock data to visualize potential alteration. The AFM diagram shows alkalis (Na2O + K2O), iron oxide (total Fe as FeO) and magnesium oxide (MgO). All values are expressed as mol proportions (see Figure ).

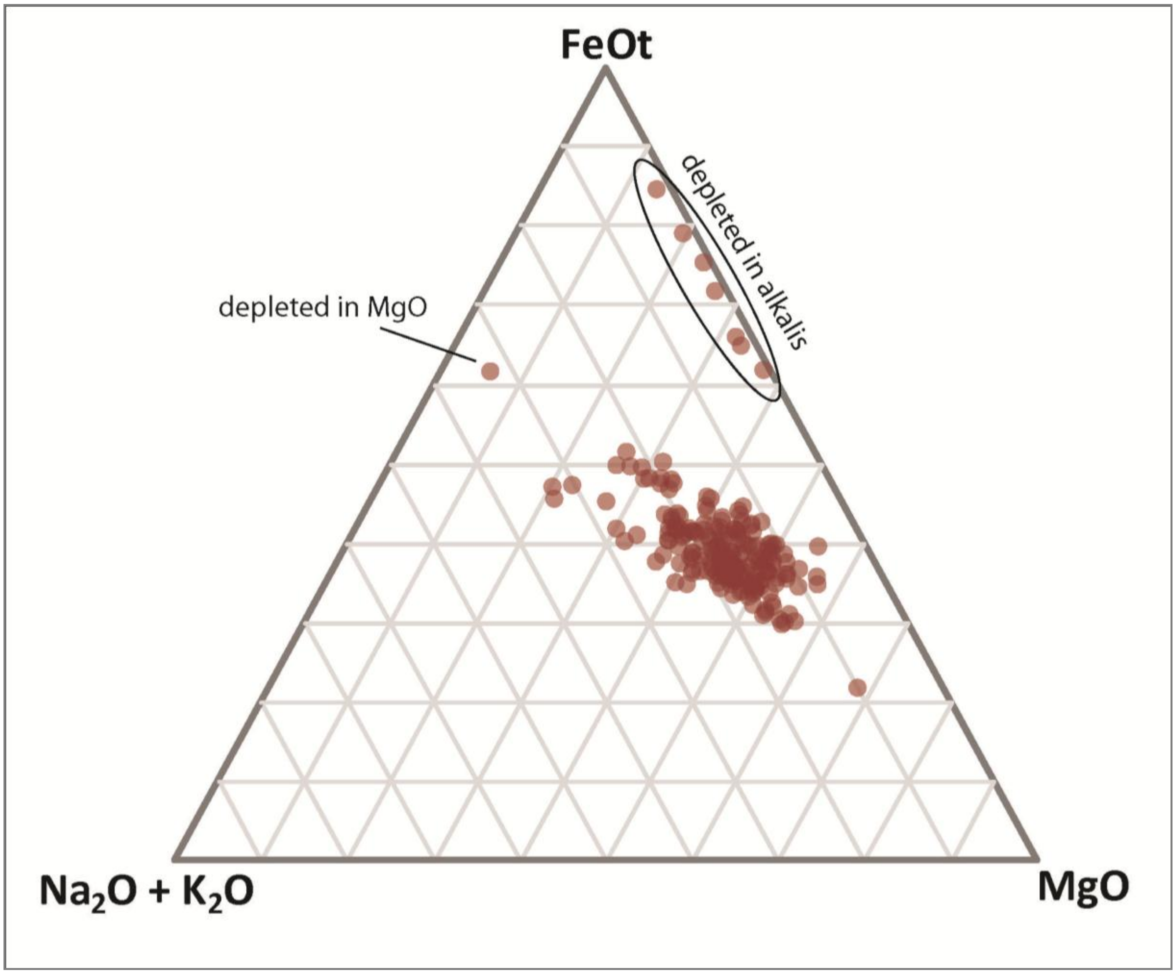


Figure 5. AFM diagram (all in mol proportions)

Most samples in the AFM diagram appear to be grouped fairly close together. One sample appears to be depleted in MgO and a group of samples appears to be depleted in alkalis. The samples depleted in alkalis are the same samples that showed up with low alkali contents in 4. All samples with depleted alkali contents were amygdaloidal (other than the dacite, sample 11CLD005).

The ACF diagram is shown in Figure 6.

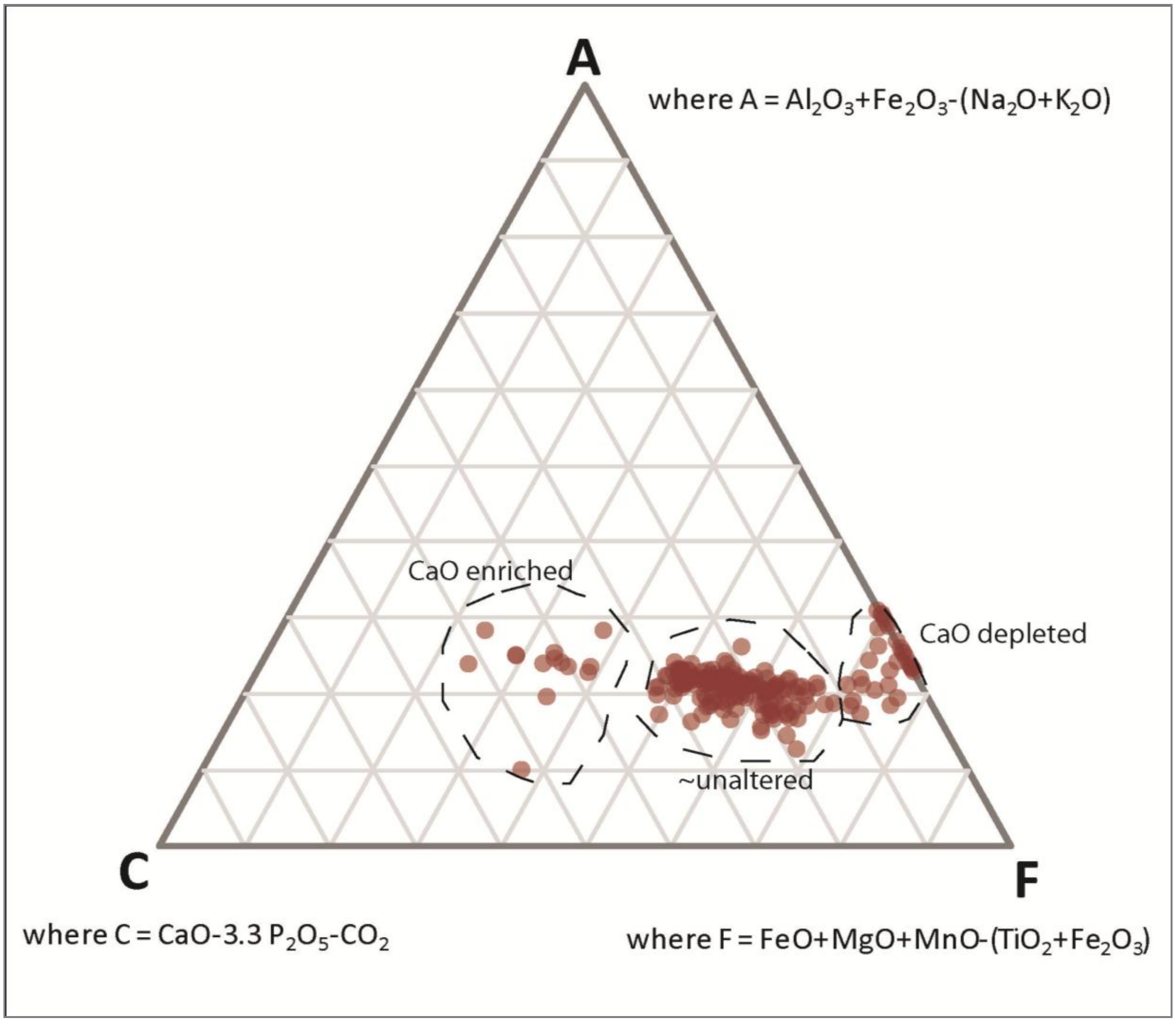


Figure 6. ACF diagram for whole rock data.

In the ACF diagram, three major groupings can be identified: calcium enriched samples, calcium depleted samples and samples that remain mostly unaltered regarding CaO. The calcium enriched sample group includes all of the alkali depleted samples and additional samples. All samples within the calcium enriched group were either amygdaloidal (and then also alkali depleted) or mostly breccias. Few medium-grained samples also appeared to be CaO enriched.

**Microprobe Analyses**

Microprobe analyses were conducted by P. Bolz on six samples from the Caledonia mine. Five of these samples were basaltic and one sample was dacitic. Samples were collected by P.A. Metz during the 2011 field season in the Caledonia mine with permission of Richard Whiteman, of Red Metal Minerals which is the mine owner. Thin sections were prepared by J. Deininger Jr. in Fairbanks, Alaska and carbon coated by P. Bolz.

Samples were first studied under the microscope and various general sampling areas were selected and photographed using a microscope kindly provided by R.J. Newberry. Sample locations were recorded and converted to microprobe coordinates. Photographs were printed and used to mark specific sample locations using the microprobe. Microprobe work was conducted using Energy Dispersive X-ray Spectroscopy (EDS) with the CAMECA SX-50 at the Advanced Instrumentation Laboratory (AIL) at the University of Alaska Fairbanks (UAF).

The quality of achieved results was first tested using several standards, including one chlorite standard, two albite standards, an augite standard and a plagioclase standard.

The first few analyses were made using 15 kV, 10nA and 20 Liveseconds. For later samples, the voltage was increased to 20kV in order to to produce better images of sample points.

Tested samples, the dates that they were tested and the testing voltage and current are shown in Table 3.

Table 2. Microprobe samples.

| Date | Samples | Voltage (kV) | Current (nA) |
|---|---|---|---|
| 10-22-2012 | 11CLD001 | 15/20 | 10 |
| 10-29-2012 | 11CLD003, 11CLD001 | 20 | 10 |
| 11-06-2012 | 11CBF006, 11CLD007 | 20 | 10 |
| 02-25-2013 | 11CLD005, 11CBF004 | 20 | 10 |

The data was analyzed using SEM QuantZAF software. Parameters used were: 20 kV (or10kV where applicable), 20nA, Take-off 40°, and 0° Tilt.

The microprobe data is presented by sample and by mineral (see Appendix A). Microprobe data for the feldspars was used to calculate the mole fractions of the three end-member feldspars: potassium feldspar, albite and anorthite. The ternary diagram is shown in Figure 7.

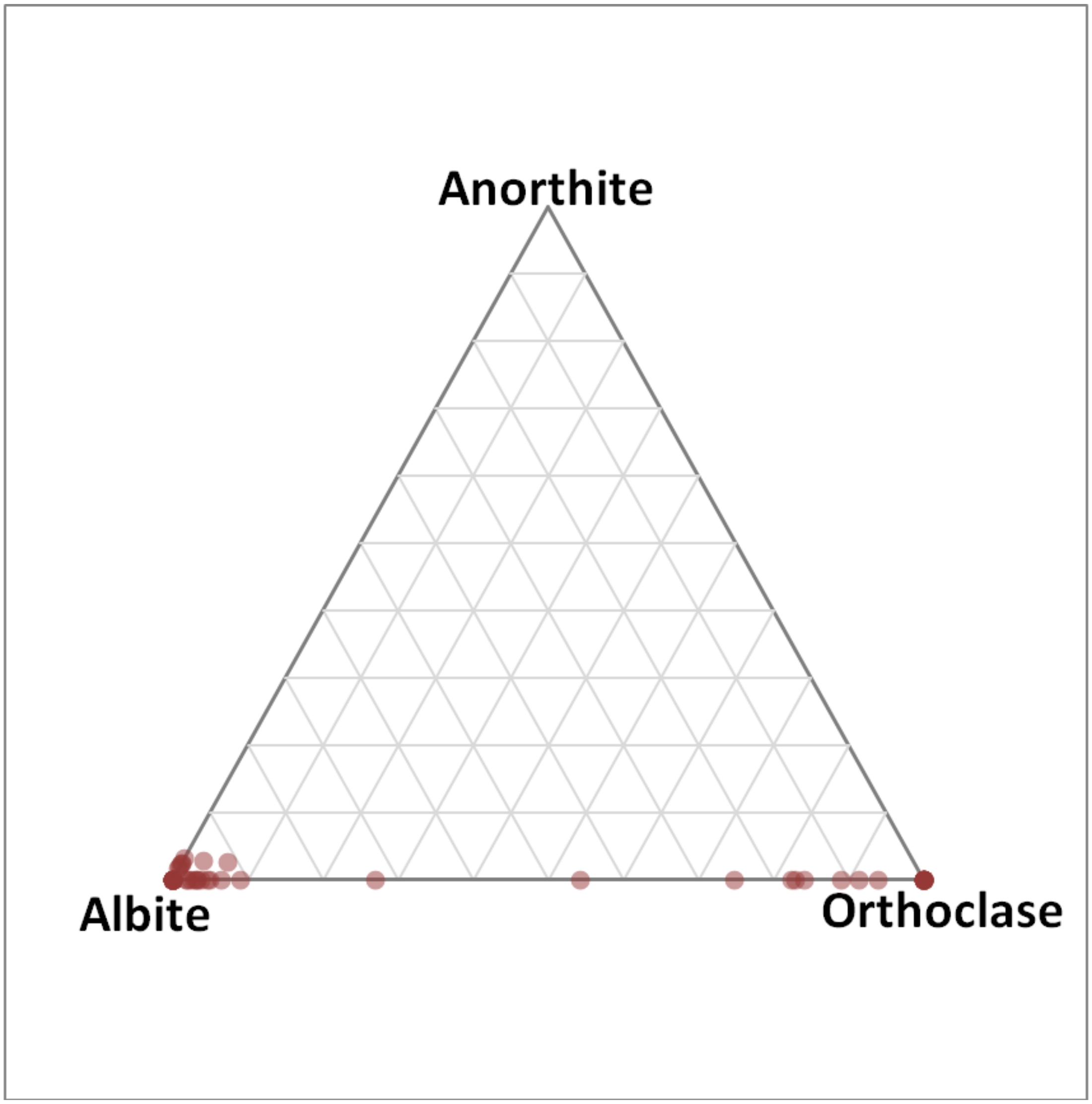


Figure 7. Ternary diagram for sampled feldspars.

**District Mine Tailings Examination for Secondary Hydrous Carbonates**

Wilson et al (2009) report major secondary hydrous carbonate mineral forming on the mine tailings of the closed Cassiar and Clinton Creek asbestos mines in northwestern British Columbia and Yukon Territory, Canada respectively. The host rocks to the deposits are ultramafic rocks that have undergone intense carbonate alteration and serpentinization. The asbestos was extracted from the ore by fine crushing and vacuum separation of the fibrous minerals. The finely crushed waste rock was placed in tailings sites at or near the groundwater level. The indentified secondary minerals are as follows:

1. Nesquehonite [$MgCO_3 \cdot 3H_2O$}
2. Dypingite [$Mg_5(CO_3)_4(OH)_2 \cdot 5H_2O$]
3. Hydromagnesite [$Mg_5(CO_3)_4(OH)_2 \cdot 4H_2O$]

4. Lansfordite [$MgCO_3 \cdot 5H_2O$]

Wilson et al (2009) demonstrate that the $CO_2$ forming the secondary carbonates is of atmospheric origin. Furthermore they demonstrate that the volumes of carbon dioxide extracted from the atmosphere probably exceeded the production of $CO_2$ from the mining and milling operations. The near surface mineral carbonation occurred at Alpine and Sub-Arctic climatic environments.

The Keweenaw Mine sites shown in Figure 3 were also examined and sampled for the detection of secondary carbonate minerals. As noted above, only the amygdaloidal flow tops of the Portage Lake Volcanics contain significant copper mineralization. The native copper was extracted by crushing the ore to sand size fractions in stamp mills and then separating the liberated copper by gravity methods. The “stamp sand” was then disposed subaqueously in either Portage Lake or Lake Superior. Thus the stamp sand was generally not exposed to atmospheric carbon dioxide.

During the mining process large volumes of the non-mineralized portions of the basaltic flows were removed and placed in tailings piles. This waste rock ranged in size from 10 to 50 cm. These mine tailings piles form a near continuous series of mounds from Copper Harbor to the Caledonia Mine, a distance of approximately 160 km. The tailings piles are generally well drained and many have been partially removed for construction material or disturbed by mineral collectors. None of the sites shown in Figure 3 yielded any secondary carbonate minerals.

The major differences between the mine tailings at Cassiar and Clinton Creek and those of the Keweenaw Copper Belt are: the original bulk chemical composition host rocks, degree of alteration, grain size distribution after mineral processing, and methods of mine waste disposal. Secondary hydrous carbonate minerals may occur in the Keweenaw however the most probable sites are in the near surface of the residual soils formed by chemical weathering of the more primitive olivine basalts of the Portage Lake Volcanics.

**Caledonia Mine General Geology**

The Caledonia Mine is located on the southwestern end of the Keweenaw Copper Belt (see Figure 3). The area was the site of the first mine developments in the region. After the discovery of the major deposits to the northeast, this portion of the district was not an area interest until the development of the White Pine Mine in 1957. As a consequence, the Caledonia Mine area has not been the subjected to modern mineral exploration techniques.

A 1938 vintage mine map and field notes provided by Red Metal Minerals, the current mine owner and operator, was examined and field checked during the current investigation. The map covers approximately 800 feet of the main Caledonia crosscut and accurately portrays the extent of the amygdaloidal flow tops and the porphyritic and ophitic textured portions of the unaltered flows. Regionally the Portage Lake Volcanic strike NE-SW and dip to the NW at 50-70 degrees. Calumet & Helca staff accurately described the mineralogy of the flow tops in the adit as epidote, calcite, chlorite, adularia ("red feldspar"), laumontite, prehnite and quartz (chalcedonic) with minor native copper and datolite. Over the 800 feet of the mapped adit there 17 flow tops recorded for a total of 160 feet. As the adit is oblique to the direction of dip and the recorded lengths of intercepts are horizontal, the intersections do not represent true thickness of the sections of the flows. The total recorded length of the unaltered portions of the flows is 628 feet. Thus the amygdaloidal zones represent approximately 20 percent and the unaltered zones 80 percent of the volcanic sequence. Cornwall (1951) estimated that for the entire district, 85 percent of the Portage Lake Volcanics are not subject to alteration and mineralization.

Basaltic rocks with similar mineral assemblages to the Portage Lake Volcanics were first described by Brogniard (1827) and were then termed spilites. The origin of spilitic basalts was a major topic of debate amongst petrologists for over 125 years (Amstutz, 1974). However the initial recognition that spilitic basaltic rocks are of metamorphic origin did not occur until the work by Coombs (1954, 1960, and 1961) who further demonstrated that spilitic basalts may encompass two separate low-grade facies of regional metamorphism. Fyfe et al (1958) and Miyashiro (1973) have made major contributions to the pressure, temperature, and compositional constraints on the zeolite and the prehnite-pumpellyite facies of regional metamorphism. The Portage Lake Volcanics are classic examples of what has been termed spilitic basalts. Although large amounts of P-T-X data exists for the zeolite facies, the metastability of zeolites makes the prediction to P-T conditions less certain than that of the prehnite-pumpellyite facies.

Fyfe et al (1960) and Miyashiro (1973) also noted the significance of $CO_2$ in the evolution of the mineral assemblages of basaltic rocks to the zeolite and prehnite-pumpellyite facies. Miyashiro (1973) also presents data on the stability of heulandite and laumantite in the presence of $CO_2$ with the formation of laumontite at approximately $150^0$C and the upper boundary of the zeolite facies at $200^0$C. The upper boundary of the prehnite-pumpellite facies is approximately $250^0$C. Both facies have wide ranges in baric conditions from 1 to 4 kilobars for the zeolite facies and 2 to 6 kilobars for the prehnite pumpellyite facies.

The temperature boundaries for the facies are well within the range of the flue gas temperatures of coal and natural gas power plants. Thus P-T-X conditions that formed the mineralization in the Portage Lake Volcanic may well provide the sufficient conditions for mineral carbonation and carbon sequestration. The necessary condition is the rates at which these reactions shall take place.

**Rock Quality Designator (RQD) Analysis for Caledonia Mine**

One scan line was established in each of the two drifts of the Caledonia Mine that were selected for the proposed direct inject site. Joint data was collect for the length of the drifts. At each location the basalt is porphyritic to ophitic textured and has very wide joint spacing ranging from greater than 10 cm to several meters, thus the RQD analyses were 100% for each location. The field notes that accompany the map of the Caledonia crosscut lists 12 underground drill holes. The holes were drilled at or near horizontal and the logs do not include discontinuity data. Since there is no data in the vertical direction, the RQD analysis is of limited utility. The data indicates a high rock mass strength which is evident from the size of the stopes in Caledonia Mine and other mines in the district.

Discontinuity surveys are of limited importance to the proposed direct injection demonstration project but are extremely important in the design of a full-scale storage facility. The design of such a facility will require a significant number of vertical and inclined diamond drill holes. The analyses of the data should include block volume calculations as described by Palmstrom (2005)

**Uniaxial Compression Strength of Unaltered Basalt from the Caledonia Mine**

The U.S. Army Corps of Engineers conducted uniaxial compression tests on multiple samples of non-mineralized basalt from the Caldenia Mine in anticipation of the utilization of the basalt in the reconstruction of the Ontonagon Harbor (Richard Whiteman, Red Metal Minerals, *personal communication*). The unpublished data indicate compressive strengths ranging from 58,000 to 62,000 psi. These data are to be expected from the visual inspection of the rock and its resistance to fracture with even a five pound rock hammer.

**Caledonia Mine Water Quality Analyses**

Five one liter samples of water were collected from the Caledonia adit along with a sample from seepage below the Caldenia Mine tailings pile. An additional sample was collected from a flowing water well located approximately one quarter mile northwest of the mine portal. Sample analyses were conducted by ALS Global and are summarized in Table 4. Analyses were conducted for the following elements however only those listed in Table 4 were above the detection limits: Al, Sb, AS, Ba, Be, Bi, B, Cd, Ca, Cs, Cr, Co, Cu, Ga, Fe, Pb, Li, Mg, Mn, Mo, Ni, P, Re, Rb, Se, Si, Ag, Na, Sr, Te, Tl, Th, Sn, Ti, W, U, V, Y, Zn, Zr, and Hardness (as $CaCO_3$) (mg/L).

Table 3. Water samples from the Caledonia Mine and adjacent area.

| Analyte Total (mg/L) | CMW1 | CMW2 | CMW3 | CMW4 | CMW5 | CMW6 Flowing Well | CMW7 Tailings Seep |
|---|---|---|---|---|---|---|---|
| Aluminum | 0.103 | 0.613 | 0.095 | 0.095 | 0.049 | <0.030 | 0.063 |
| Boron | 7.66 | 6.58 | 1.31 | 5.04 | 1.16 | 5.35 | 1.19 |
| Calcium | 11.3 | 15.5 | 38.1 | 132 | 36.4 | 5680 | 35.7 |
| Copper | 0.080 | 0.308 | 0.166 | 0.445 | 0.178 | <0.005 | 0.283 |
| Iron | 0.120 | 0.996 | 0.311 | 0.102 | 0.312 | <0.30 | 0.273 |
| Magnesium | 2.00 | 4.25 | 6.07 | 16.3 | 6.05 | 2.8 | 5.78 |
| Phosphorus | 0.67 | <0.30 | <0.30 | 0.74 | <0.30 | <0.30 | <0.30 |
| Potassium | <2.0 | <2.0 | <2.0 | 124 | <2.0 | <2.0 | <2.0 |
| Silicon | 6.64 | 8.48 | 6.70 | 4.38 | 6.41 | 5.08 | 6.34 |
| Sodium | 74.3 | 113 | 31.5 | 331 | 30.0 | 1710 | 31.8 |
| Strontium | 0.0483 | 0.0811 | 0.134 | 0.741 | 0.123 | 33.7 | 0.120 |
| Hardness | | | | | | | |
| $CaCO_3$ | 36.4 | 56.2 | 120 | 398 | 116 | 14,200 | 113 |

The samples from the underground workings and the sample from the tailings seep show elevated levels of the elements that may be released by mineral reactions of the basaltic rocks during the metamorphism to zeolite and prehnite-pumpellyite facies (Ca, Mg, Si, Na, and calcium carbonate).

The flowing well was drilled as an exploration borehole by the Calumet and Hecla Mining Company. No drill log is available for the borehole. The water from the borehole effervescing and undetermined gas. The discharge from the well has attracted large numbers of whitetail deer probably due to its high salt content. The water contains high concentrations Ca, Na, Sr, and high hardness as calcium carbonate equivalent. The elemental associations are more indicative of the chemistry of the Nonesuch Shale and Freda Sandstone that overlie the Copper Harbor Conglomerate and Portage Lake Volcanics.

**Autoclave Analyses**

Six samples of porphyritic and ophitic textured basalt from the Caledonia Mine were sent to the Pacific Northwest National Laboratory (PNNL) for autoclave experiments. The experiments on the crushed samples were conducted at $160^0$C and 300 psi in a gas mixture similar to a flue gas stream from a coal or natural gas fired power plant as described above. The analyses from sample one did not indicate any reaction products over the period of the experiment. The results from the remaining samples are included in a report that is under review by the PNNL Staff. Upon receipt of this data a supplement will be issued to this report.

Prior to the development of a direct injection demonstration project, additional autoclave experiments must be conducted to further define the mineral reaction rates and products. Adequate sample material (approximately two metric tones) has been collected during this investigation for such experiments.

**Conclusions**

The field and laboratory results of the investigation of the Portage Lake Volcanics of the Keweenaw Peninsula of Northern Michigan and their hosted native copper deposits establishes a baseline for the design of a $CO_2$ rich flue gas direct injection facility. The results also support previous investigations that demonstrate that the large native copper deposits were formed as a consequence of $CO_2$-bearing metamorphic fluids migrating through the relatively high porosity sections of the amygdaloidal flow tops of the volcanic sequences. These fluids resulted in the formation of zeolite and prehnite-pumpellyite facies mineral assemblages. These mineral assemblages represent temperature and pressure conditions similar to those that would be produced by the direct injection of a flue gas stream from a coal or natural gas fired power plant.

The large volumes of basaltic rocks of the Portage Lake Volcanics of the Keweenaw Peninsula provide the potential to the storage of very large volumes of carbon dioxide through mineral carbonation. The Portage Lake Volcanic constitute but a very small portion of the extrusive and intrusion mafic and ultramafic rocks of Mid-Continental Rift System including the Duluth Gabbro of Minnesota and the Logan Sills of northwestern Ontario.

The proposed direct injection technology has the following attributes relative to the injection of supercritical $CO_2$ into porous sedimentary rocks: a) permanent sequestration of $CO_2$ without the potential for future releases of supercritical fluids, b) avoidance of costly $CO_2$ recovery systems in the power plant design, c) potential recovery of additional energy from the power plant and from the heat released by the carbonation reactions, d) potential for the permanent sequestration of other deleterious elements in the flue gas stream such as mercury and uranium as these form mineral deposits under similar temperature and pressure conditions as the mineral carbonation reactions, and e) potential recovery of additional copper from formation waters in which the pH is reduced below 5.5 by the formation of carbonic acid.

**Graphical Materials List – None**

**References**


Amstutz, G.C., Ed., 1974, Spilites and spilitic rocks: International Union of Geological Sciences Series A, Number 4: Springer-Verlag, Berlin, 482 p.

Bearat, H., McKelvy, M.J., Chizmeshya, A.V.G., Gormley, D., Nunez, R., Carpenter, R.W., Squires, K., and Wolf, G.H., 2006, Carbon sequestration via aqueous olivine mineral carbonation: Role of passivating layer formation: Environmental Science Technology, v. 40, p. 7.

Beecy, D.J., and Kuuskraa, V.A., 2001, Status of U.S. geologic carbon sequestration research and technology: Environmental Geosciences, v. 8, no. 3, p. 152-159.

Bradshaw, J., and Cook, P., 2001, Geological sequestration of carbon dioxide: Environmental Geosciences, v. 8, no. 3, p. 149-151.

Brongniart, A., 1827, Classification et caracteres mineralogiques des roches. Paris

Brown, A.C., 2006, Genesis of native copper lodes in the Keweenaw District, Northern Michigan: A hybrid evolved meteoric and metamorphogenic model: Economic Geology, v. 101, no. 7, p. 1437-1444.

Brown, G.E.J., Bird, D.K., Kendelewicz, T., Maher, K., Mao, W., Johnson, N., Rosenbauer, R.J., and Real, P.G.D., 2010, Geological sequestration of CO2: An exploratory study of the mechanisms and kinetics of CO2 reaction with Mg-silicates: Stanford University.

Chen, Z.-Y., O'Connor, W.K., and Gerdemann, S.J., 2006, Chemistry of Aqueous Mineral Carbonation for Carbon Sequestration and Explanation of Experimental Results: Environmental Progress, v. 25, no. 2, p. 6.

Coombs, D.S., 1954, The nature and alteration of some Triassic sediments in Southland New Zealand: Trans. R. Soc. N.Z. 82, 65-109.

Coombs, D.S., Ellis, A.J., Fyfe, W.S., and Taylor, A.M., 1959, The zeolite facies, with comments on the interpretation of hydrothermal synthesis: Geochim. Cosmochim. Acta 17, 53-107.

Coombs, D.S., 1960, Lower grade mineral facies in New Zealand: Internat. Geol. Congr. 21st Sess., Rep. Part 13, p. 339-51., Copenhagen.

Coombs, D.S., 1961, Some recent work on the lower grades of metamorphism: Australian J. Sci. 24, p. 203-15.

Cornwall, H.R., 1951, Differentiation in Lavas of the Keweenaw Series and the Origin of the Copper Deposition of Michigan: Geological Society of America Bulletin, v. 62, no. 2, p. 159-202.

Fyfe, W.S., Turner, F.J., and Verhoogen, J., 1958, Metamorphic Reactions and Metamorphic Facies, Geol. Soc. America Mem. 73, 259 p.

Gerdemann, S.J., Dahlin, D.C., O'Connor, W.K., and Penner, L.R., 2003, Carbon Dioxide Sequestration by Aqueous Mineral Carbonation of Magnesium Silicate Minerals, in Second Annual Conference on Carbon Sequestration, Alexandria, VA, National Energy Technology Laboratory, NETL.

Gill, R., 2010, Igneous Rocks and Processes - a practical guide: West Sussex, John Wiley & Sons.

Goldberg, D.S., Takahashi, T., and Slagle , A.L., 2008, Carbon dioxide sequestration in deep-sea basalt: Proceedings of the National Academy of Sciences.

Hoffert, M.I., Caldeira, K., Benford, G., Criswell, D.R., Green, C., Herzog, H., Jain, A.K., Kheshgi, H.S., Lackner, K.S., Lewis, J.S., Lightfoot, H.D., Manheimer, W., Mankins, J.C., Mauel, M.E., Perkins, L.J., Schlesinger, M.E., Volk, T., and Wigley, T.M.L., 2002, Advanced Technology Paths to Global Climate Stability: Energy for a Greenhouse Planet: Science, v. 298, no. 5595, p. 981-987.

IPCC Special Report on Carbon Dioxide Capture and Storage, 2005, ed. by B. Metz, O. Davidson, H. de Coninck, M. Loos, L. Meyer: Cambridge University Press, New York.

Lackner, K.S., 2003, A Guide to CO2 Sequestration: Science, v. 300, no. 5626, p. 1677-1678.

Lackner, K.S., Butt, D.P., and Wendt, C.H., 1997, Progress on binding CO2 in mineral substrates: Energy Conversion and Management, v. 38, no. Supplement 1, p. S259-S264.

Lackner, K.S., Wendt, C.H., Butt, D.P., Joyce, E.L., and Sharp, D.H., 1995, Carbon dioxide disposal in carbonate minerals: Energy, v. 20, no. 11, p. 1153-1170.

Le Bas, M.J., Le Maitre, R.W., Streckeisen, A., and Zanettin, B., 1986, A Chemical Classification of Volcanic Rocks Based on the Total Alkali-Silica Diagram: Journal of Petrology, v. 27, no. 3, p. 745-750.

Matter, J.M., Broecker, W.S., Stute, M., Gislason, S.R., Oelkers, E.H., Stefánsson, A., Wolff-Boenisch, D., Gunnlaugsson, E., Axelsson, G., and Björnsson, G., 2009, Permanent Carbon Dioxide Storage into Basalt: The CarbFix Pilot Project, Iceland: Energy Procedia, v. 1, no. 1, p. 3641-3646.

McGrail, B.P., Schaef, H.T., Ho, A.M., Chien, Y.-J., Dooley, J.J., and Davidson, C.L., 2006, Potential for carbon dioxide sequestration in flood basalts: J. Geophys. Res., v. 111, no. B12, p. B12201.

Meschede, M., 1986, A method of discriminating between different types of mid-ocean ridge basalts and continental tholeiites with the Nb¸Zr¸Y diagram: Chemical Geology, v. 56, no. 3-4, p. 207-218.

Miyashiro, A., 1973, Metamorphism and Metamorphic Belts: John Wiley & Sons: New York, 479 p.

Oelkers, E.H., Gislason, S.R., and Matter, J., 2008, Mineral Carbonation of CO2: Elements, v. 4, no. 5, p. 333-337.

Ojakangas, R.W., Morey, G.B., and Green, J.C., 2001, The Mesoproterozoic Midcontinent Rift System, Lake Superior Region, USA: Sedimentary Geology, v. 141-142, p. 421-442.

Paces, J.B., and Bornhorst, T.J., 1985, Geology and geochemistry of lava flows within the Copper Harbor Conglomerate, Keweenaw Peninsula, Michigan, in 31st Annual Institute on Lake Superior Geology Kenora, Ontario, p. 71-72.

Palmstrom, Arild, 2005, Measurements of and correlations between block size and Rock Quality Designation (RQD): Tunnels and Underground Space Technology 20 (2005).

Pueschner, U.R., 2001, Very low-grade metamorphism in the Portage Lake Volcanics on the Keweenaw Peninsula, Michigan, USA: Basel, Universitaet Basel, 163 p.

Rosenbauer, R.J., Thomas, B., Bischoff, J.L., and Palandri, J., 2012, Carbon sequestration via reaction with basaltic rocks: Geochemical modeling and experimental results: Geochimica et Cosmochimica Acta, v. 89, p. 116-133.

Stoiber, R.E., and Davidson, E.S., 1959, Amygdule mineral zoning in the Portage Lake Lava series, Michigan copper district; Part 1: Economic Geology, v. 54, no. 7, p. 1250-1277.

Turner, F.J., and Verhoogen, John, 1960, Igneous and metamorphic petrology: McGraw-Hill, New York, 694 p.

Wilson, S.A., Dipple, G.M., Power, I.M., Thom, J.M., Anderson, R.G., Raudsepp, M., Gabites, J.E., and Southam, G., 2009, Carbon Dioxide Fixation within Mine Wastes of Ultramafic-Hosted Ore Deposits: Examples from the Clinton Creek and Cassiar Chrysotile Deposits, Canada: Economic Geology, v. 104, no. 1, p. 95-112.

Wilson, S.A., Raudsepp, M., and Dipple, G.M., 2006, Verifying and quantifying carbon fixation in minerals from serpentine-rich mine tailings using the Rietveld method with X-ray powder diffraction data: American Mineralogist, v. 91, no. 8-9, p. 1331-1341.

Winchester, J.A., and Floyd, P.A., 1977, Geochemical discrimination of different magma series and their differentiation products using immobile elements: Chemical Geology, v. 20, p. 325-343.

Zevenhoven, R., Fagerlund, J., and Songok, J.K., 2011, CO2 mineral sequestration: developments toward large-scale application: Greenhouse Gases: Science and Technology, v. 1, no. 1, p. 48-57.

**Bibliography**

Bearat, H., McKelvy, M.J., Chizmeshya, A.V.G., Gormley, D., Nunez, R., Carpenter, R.W., Squires, K., and Wolf, G.H., 2006, Carbon Sequestration via Aqueous Olivine Mineral Carbonation: Role of Passivating Layer Formation: Environmental Science Technology, v. 40, p. 7.

Beecy, D.J., and Kuuskraa, V.A., 2001, Status of U.S. Geologic Carbon Sequestration Research and Technology: Environmental Geosciences, v. 8, no. 3, p. 152-159.

Bradshaw, J., and Cook, P., 2001, Geological Sequestration of Carbon Dioxide: Environmental Geosciences, v. 8, no. 3, p. 149-151.

Brown, A.C., 2006, Genesis of native copper lodes in the Keweenaw District, Northern Michigan: A hybrid evolved meteoric and metamorphogenic model: Economic Geology, v. 101, no. 7, p. 1437-1444.

Brown, G.E.J., Bird, D.K., Kendelewicz, T., Maher, K., Mao, W., Johnson, N., Rosenbauer, R.J., and Real, P.G.D., 2010, Geological Sequestration of CO2: An Exploratory Study of the Mechanisms and Kinetics of CO2 Reaction with Mg-Silicates: Stanford University.

Chen, Z.-Y., O'Connor, W.K., and Gerdemann, S.J., 2006, Chemistry of Aqueous Mineral Carbonation for Carbon Sequestration and Explanation of Experimental Results: Environmental Progress, v. 25, no. 2, p. 6.

Cornwall, H.R., 1951, Differentiation in Lavas of the Keweenaw Series and the Origin of the Copper Deposition of Michigan: Geological Society of America Bulletin, v. 62, no. 2, p. 159-202.

Gerdemann, S.J., Dahlin, D.C., O'Connor, W.K., and Penner, L.R., 2003, Carbon Dioxide Sequestration by Aqueous Mineral Carbonation of Magnesium Silicate Minerals, in Second Annual Conference on Carbon Sequestration, Alexandria, VA, National Energy Technology Laboratory, NETL.

Gill, R., 2010, Igneous Rocks and Processes - a practical guide: West Sussex, John Wiley & Sons.

Goldberg, D.S., Takahashi, T., and Slagle , A.L., 2008, Carbon dioxide sequestration in deep-sea basalt: Proceedings of the National Academy of Sciences.

Hoffert, M.I., Caldeira, K., Benford, G., Criswell, D.R., Green, C., Herzog, H., Jain, A.K., Kheshgi, H.S., Lackner, K.S., Lewis, J.S., Lightfoot, H.D., Manheimer, W., Mankins, J.C., Mauel, M.E., Perkins, L.J., Schlesinger, M.E., Volk, T., and Wigley, T.M.L., 2002, Advanced Technology Paths to Global Climate Stability: Energy for a Greenhouse Planet: Science, v. 298, no. 5595, p. 981-987.

IPCC Special Report on Carbon Dioxide Capture and Storage, 2005, ed. by B. Metz, O. Davidson, H. de Coninck, M. Loos, L. Meyer: Cambridge University Press, New York.

Lackner, K.S., 2003, A Guide to CO2 Sequestration: Science, v. 300, no. 5626, p. 1677-1678.

Lackner, K.S., Butt, D.P., and Wendt, C.H., 1997, Progress on binding CO2 in mineral substrates: Energy Conversion and Management, v. 38, no. Supplement 1, p. S259-S264.

Lackner, K.S., Wendt, C.H., Butt, D.P., Joyce, E.L., and Sharp, D.H., 1995, Carbon dioxide disposal in carbonate minerals: Energy, v. 20, no. 11, p. 1153-1170.

Le Bas, M.J., Le Maitre, R.W., Streckeisen, A., and Zanettin, B., 1986, A Chemical Classification of Volcanic Rocks Based on the Total Alkali-Silica Diagram: Journal of Petrology, v. 27, no. 3, p. 745-750.

Marini, L., 2007, Geological Sequestration of Carbon Dioxide: Thermodynamics, Kinetics, and Reaction Path Modeling: Elsevier Developments in Geochemistry 11: Elsevier, Amsterdam, 453 p.

Matter, J.M., Broecker, W.S., Stute, M., Gislason, S.R., Oelkers, E.H., Stefánsson, A., Wolff-Boenisch, D., Gunnlaugsson, E., Axelsson, G., and Björnsson, G., 2009, Permanent Carbon

Dioxide Storage into Basalt: The CarbFix Pilot Project, Iceland: Energy Procedia, v. 1, no. 1, p. 3641-3646.

McGrail, B.P., Schaef, H.T., Ho, A.M., Chien, Y.-J., Dooley, J.J., and Davidson, C.L., 2006, Potential for carbon dioxide sequestration in flood basalts: J. Geophys. Res., v. 111, no. B12, p. B12201.

Meschede, M., 1986, A method of discriminating between different types of mid-ocean ridge basalts and continental tholeiites with the Nb¸Zr¸Y diagram: Chemical Geology, v. 56, no. 3-4, p. 207-218.

Oelkers, E.H., Gislason, S.R., and Matter, J., 2008, Mineral Carbonation of CO2: Elements, v. 4, no. 5, p. 333-337.

Ojakangas, R.W., Morey, G.B., and Green, J.C., 2001, The Mesoproterozoic Midcontinent Rift System, Lake Superior Region, USA: Sedimentary Geology, v. 141-142, p. 421-442.

Paces, J.B., and Bornhorst, T.J., 1985, Geology and geochemistry of lava flows within the Copper Harbor Conglomerate, Keweenaw Peninsula, Michigan, in 31st Annual Institute on Lake Superior Geology Kenora, Ontario, p. 71-72.

Pueschner, U.R., 2001, Very low-grade metamorphism in the Portage Lake Volcanics on the Keweenaw Peninsula, Michigan, USA: Basel, Universitaet Basel, 163 p.

Rosenbauer, R.J., Thomas, B., Bischoff, J.L., and Palandri, J., 2012, Carbon sequestration via reaction with basaltic rocks: Geochemical modeling and experimental results: Geochimica et Cosmochimica Acta, v. 89, p. 116-133.

Stoiber, R.E., and Davidson, E.S., 1959, Amygdule mineral zoning in the Portage Lake Lava series, Michigan copper district; Part 1: Economic Geology, v. 54, no. 7, p. 1250-1277.

Wilson, S.A., Dipple, G.M., Power, I.M., Thom, J.M., Anderson, R.G., Raudsepp, M., Gabites, J.E., and Southam, G., 2009, Carbon Dioxide Fixation within Mine Wastes of Ultramafic-Hosted Ore Deposits: Examples from the Clinton Creek and Cassiar Chrysotile Deposits, Canada: Economic Geology, v. 104, no. 1, p. 95-112.

Wilson, S.A., Raudsepp, M., and Dipple, G.M., 2006, Verifying and quantifying carbon fixation in minerals from serpentine-rich mine tailings using the Rietveld method with X-ray powder diffraction data: American Mineralogist, v. 91, no. 8-9, p. 1331-1341.

Winchester, J.A., and Floyd, P.A., 1977, Geochemical discrimination of different magma series and their differentiation products using immobile elements: Chemical Geology, v. 20, p. 325-343.

Zevenhoven, R., Fagerlund, J., and Songok, J.K., 2011, CO2 mineral sequestration: developments toward large-scale application: Greenhouse Gases: Science and Technology, v. 1, no. 1, p. 48-57.

**APPENDIX A - Electron microprobe data**

**Hand Sample 11CLD001 (dry and wet)**


11CLD001

11CLD001_03 10-22_004 through 10-22_011

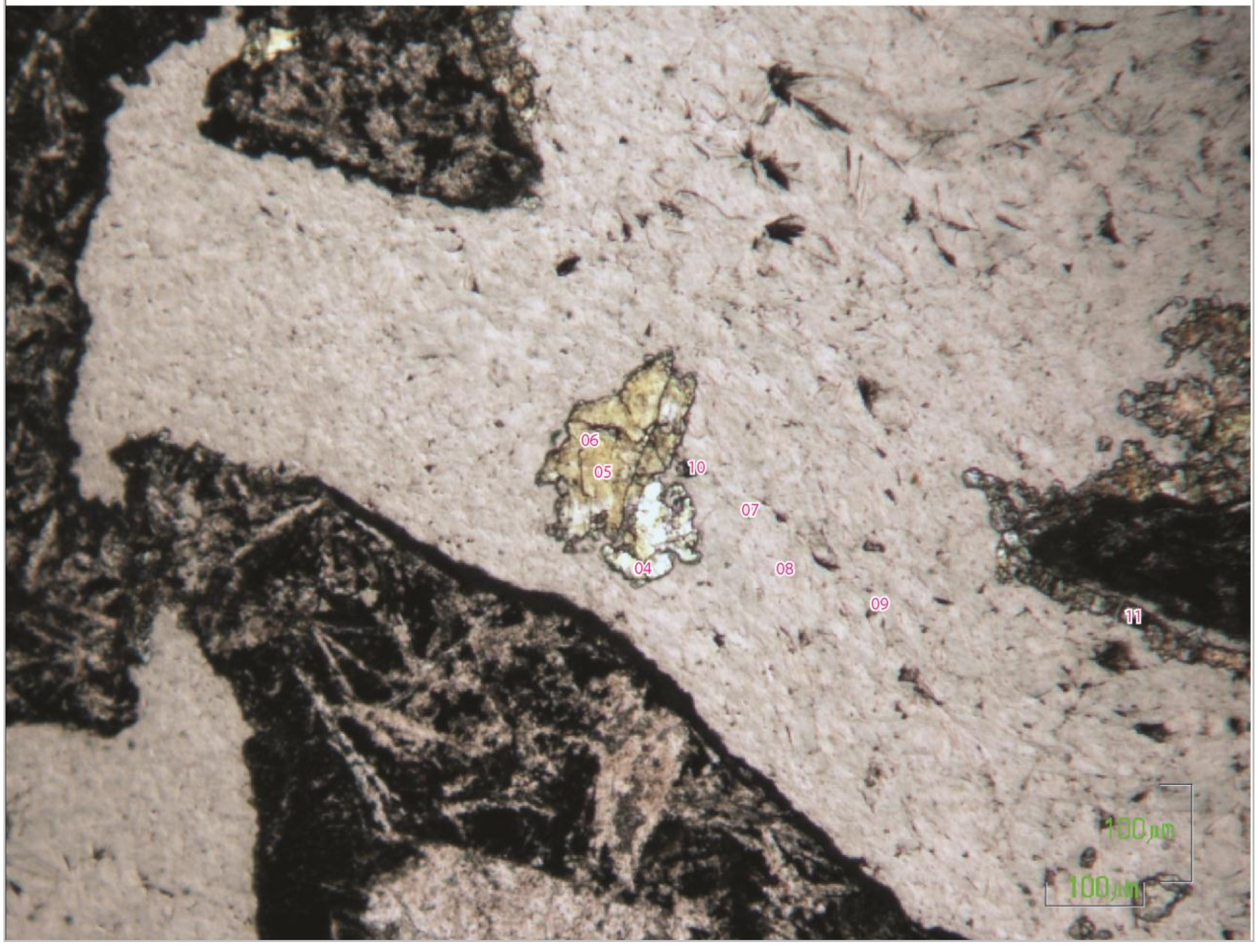


| Point | Mineral | wt % | | | | | | | | | | |
|---|---|---|---|---|---|---|---|---|---|---|---|---|
| | | Na2O | MgO | Al2O3 | SiO2 | K2O | CaO | TiO2 | MnO | FeO | CuO | Total |
| 04 | Epidote + Chlorite | 1.14 | 22.96 | 18.12 | 32.54 | - | 0.45 | - | 0.73 | 24.07 | - | 100 |
| 05 | Epidote + Chlorite | - | 22.62 | 18.21 | 33.48 | - | 0.55 | - | 0.75 | 24.39 | - | 100 |
| 06 | Epidote + Chlorite | 0.68 | 22.74 | 18.34 | 33.23 | - | 0.59 | - | 0.61 | 23.82 | - | 100 |
| 07 | Chlorite | - | 22.79 | 18.49 | 33.63 | - | - | - | - | 25.09 | - | 100 |
| 08 | Chlorite | - | 22.98 | 18.47 | 33.53 | - | - | - | - | 25.02 | - | 100 |
| 09 | Chlorite | - | 22.91 | 18.87 | 33.3 | - | - | - | 0.61 | 24.31 | - | 100 |
| 10 | Chlorite | - | 22.1 | 17.8 | 33.13 | - | - | - | | 26.97 | - | 100 |
| 11 | Epidote + Chlorite | - | 4.09 | 18.24 | 38.43 | 20 | - | - | 19.24 | - | - | 100 |

11CLD001_04    10-22_012 through 10-22_027 (10-22_028-031 opaques not shown)

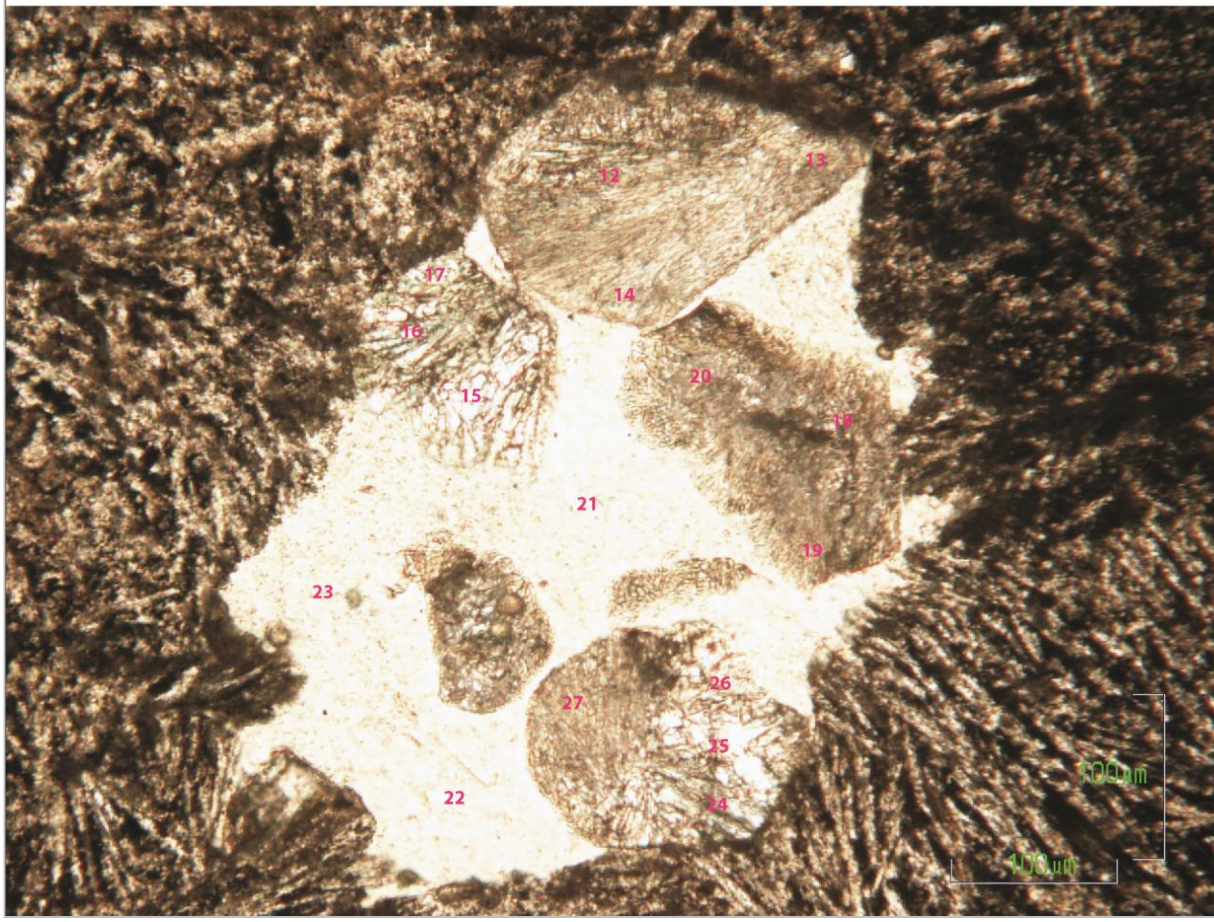

| Point | Mineral | wt % | | | | | | | | |
|---|---|---|---|---|---|---|---|---|---|---|
| | | $Na_2O$ | MgO | $Al_2O_3$ | $SiO_2$ | $Cl_2O$ | $K_2O$ | CaO | FeO | Total |
| 12 | Epidote + Chlorite | - | 24.32 | 16.2 | 44.28 | - | - | 6.21 | 9 | 100 |
| 13 | Epidote + Chlorite | - | 28.8 | 13.71 | 45.21 | - | - | 3.02 | 9.25 | 100 |
| 14 | Epidote + Chlorite | - | 19.87 | 17.64 | 43 | - | - | 9.7 | 9.79 | 100 |
| 15 | Pumpellyite | - | 2.93 | 22.33 | 39.6 | - | - | 23.02 | 12.13 | 100 |
| 16 | Pumpellyite | - | 3.67 | 21.7 | 40.54 | - | - | 21.31 | 12.77 | 100 |
| 17 | Pumpellyite | - | 2.95 | 21.72 | 40.24 | - | - | 22.62 | 12.46 | 100 |
| 18 | Epidote + Chlorite + Calcite | | 12.79 | 19.4 | 41.28 | - | - | 15.54 | 10.99 | 100 |
| 19 | Epidote + Chlorite + Calcite | 0.75 | 19.04 | 17.63 | 42.05 | - | - | 10.34 | 10.19 | 100 |
| 20 | Epidote + Chlorite + Calcite | - | 22.12 | 16.68 | 43.49 | - | - | 8.32 | 9.39 | 100 |
| 21 | Chlorite | - | 23.19 | 18.96 | 33.74 | - | - | - | 24.11 | 100 |
| 22 | Chlorite | - | 22.8 | 18.66 | 33.77 | - | - | - | 24.77 | 100 |
| 23 | Chlorite | - | 23.18 | 18.84 | 33.6 | - | - | - | 24.38 | 100 |
| 24 | Pumpellyite | - | 8.39 | 22.03 | 41.76 | - | - | 19.18 | 8.63 | 100 |
| 25 | Hole in slide | - | - | - | - | - | - | - | - | - |
| 26 | Pumpellyite | 4.81 | 22.89 | 40.98 | - | - | - | 21.26 | 10.06 | 100 |
| 27 | Epidote + Chlorite | 1.25 | 17.5 | 18.77 | 43.15 | 0.5 | 0.9 | 9.73 | 8.1 | 100 |
| 28 | FeOx | 1.49 | 10.4 | 7.66 | 14.04 | - | - | 1.53 | 62.1 | 100 |
| 29 | Sphene | - | 3.19 | 4.43 | 31.95 | - | - | 24.3 | 7.89 | 100 |
| 30 | FeOx + Sphene | - | 2.42 | 3.91 | 23.93 | - | - | 13.96 | 39.96 | 100 |
| 31 | Sphene | - | 3.33 | 4.4 | 33.25 | - | - | 24.61 | 5.29 | 100 |

11CLD001_02 10-22_032 through 10-22_044


| Point | Mineral | wt % | | | | | | | | | |
|---|---|---|---|---|---|---|---|---|---|---|---|
| | | $Na_2O$ | MgO | $Al_2O_3$ | $SiO_2$ | PtO | $K_2O$ | CaO | $TiO_2$ | FeO | Total |
| 32 | Albite | 11.32 | - | 19.58 | 69.1 | - | - | - | - | - | 100 |
| 33 | Chlorite + Sphene | - | 11.72 | 8.47 | 35.56 | - | - | 17.08 | 18.44 | 8.73 | 100 |
| 34 | Albite | 11.15 | - | 19.56 | 68.32 | - | 0.34 | - | - | 0.63 | 100 |
| 35 | Chlorite | - | 23.46 | 18.73 | 34.48 | - | - | - | - | 23.32 | 100 |
| 36 | Albite | 11.14 | - | 19.67 | 69.19 | - | - | - | - | - | 100 |
| 37 | K-spar | - | - | 18.26 | 65.82 | - | 15.91 | - | - | - | 100 |
| 38 | Epidote | - | - | 21.73 | 38.98 | - | - | 22.64 | - | 16.65 | 100 |
| 39 | Albite | 11.41 | - | 19.37 | 69.22 | - | - | - | - | - | 100 |
| 40 | Epidote | - | - | 20.80 | 39.07 | - | - | 22.91 | 0.60 | 16.62 | 100 |
| 41 | Epidote | - | - | 21.29 | 39.44 | - | - | 22.92 | - | 16.35 | 100 |
| 42 | Chlorite + Sphene | - | 11.53 | 10.97 | 35.22 | 0.93 | - | 16.3 | 14.64 | 10.41 | 100 |
| 43 | Epidote | - | - | 20.78 | 39.43 | - | - | 22.73 | - | 17.06 | 100 |
| 44 | Chlorite | - | 23.36 | 18.36 | 34.58 | - | - | - | - | 23.7 | 100 |

11CLD001_05 10-29_033 through 10-29_036


| Point | Mineral | wt % | | | | | | | | |
|---|---|---|---|---|---|---|---|---|---|---|
| | | $Na_2O$ | MgO | $Al_2O_3$ | $SiO_2$ | $SO_3$ | $K_2O$ | FeO | CuO | Total |
| 33 | Albite | 10.4 | - | 19.6 | 68.89 | - | 1.11 | - | - | 100 |
| 34 | K-spar | - | - | 18.41 | 65.8 | - | 15.79 | - | - | 100 |
| 35 | Copper | - | - | 0.85 | 2.07 | 0.88 | 0.35 | 0.36 | 95.49 | 100 |
| 36 | K-spar | - | 0.58 | 18.44 | 65.15 | - | 15.83 | - | - | 100 |

11CLD001_07 10-29_037 through 10-29_045


| Point | Mineral | wt % | | | | | | | | |
|---|---|---|---|---|---|---|---|---|---|---|
| | | $Na_2O$ | MgO | $Al_2O_3$ | $SiO_2$ | $K_2O$ | CaO | MnO | FeO | Total |
| 37 | Albite | 10.71 | - | 20.01 | 68.89 | 0.39 | - | - | - | 100 |
| 38 | K-spar | - | - | 18.15 | 65.68 | 16.17 | - | - | - | 100 |
| 39 | Chlorite | - | 23.1 | 19.38 | 33.94 | - | - | - | 23.58 | 100 |
| 40 | Chlorite + K-spar | - | 15.41 | 18.68 | 43.69 | 4.28 | - | - | 17.94 | 100 |
| 41 | Albite | 11.05 | - | 19.48 | 68.79 | - | - | - | 0.68 | 100 |
| 42 | Albite | 10.29 | - | 19.46 | 66.81 | 1.04 | 0.52 | - | 1.88 | 100 |
| 43 | Chlorite | - | 23.93 | 18.97 | 33.95 | - | - | 0.6 | 22.55 | 100 |
| 44 | Chlorite | - | 23.2 | 18.55 | 33.56 | - | - | 0.65 | 24.04 | 100 |
| 45 | K-spar | 5.09 | 1.22 | 18.8 | 65.68 | 9.21 | - | - | - | 100 |

11CLD001_08 10-29_046 through 10-29_057

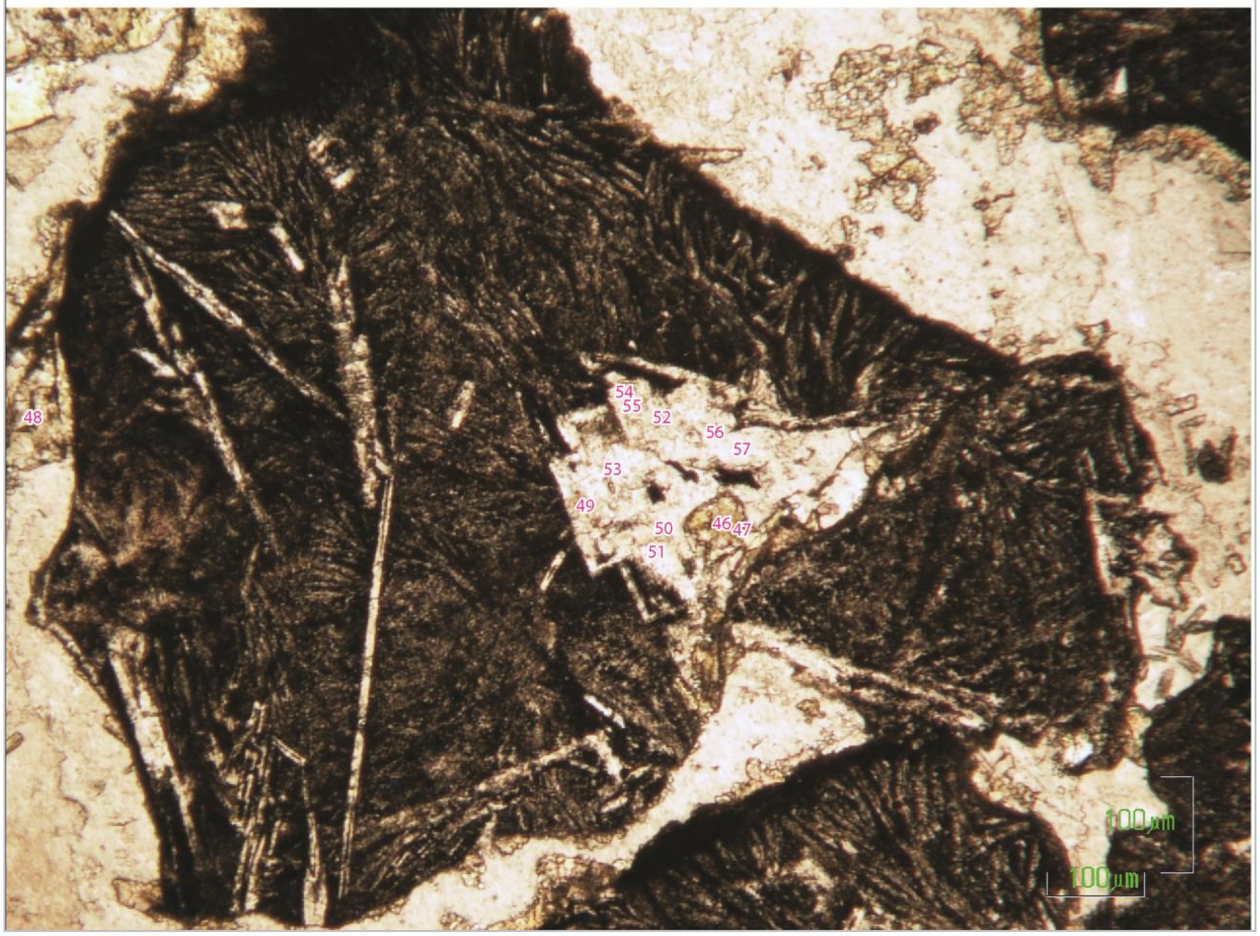


| Point | Mineral | wt % | | | | | | | | | |
|---|---|---|---|---|---|---|---|---|---|---|---|
| | | $Na_2O$ | MgO | $Al_2O_3$ | $SiO_2$ | $SO_3$ | $K_2O$ | CaO | MnO | FeO | Total |
| 46 | Epidote | - | - | 23.06 | 40.16 | - | 0.38 | 22.67 | - | 13.73 | 100 |
| 47 | Epidote | - | - | 20.06 | 38.83 | - | - | 22.45 | - | 18.66 | 100 |
| 48 | Epidote | - | - | 19.65 | 38.71 | - | - | 22.64 | - | 18.99 | 100 |
| 49 | K-spar | - | - | 18.19 | 65.7 | 16.11 | - | - | - | - | 100 |
| 50 | K-spar | - | - | 18.07 | 65.63 | 16.29 | - | - | - | - | 100 |
| 51 | Albite | 11.19 | - | 19.26 | 69.55 | - | - | - | - | - | 100 |
| 52 | Chlorite | - | 22.99 | 18.43 | 33.74 | - | - | - | 0.69 | 24.15 | 100 |
| 53 | Albite | 10.18 | - | 19.66 | 68.63 | 1.54 | - | - | - | - | 100 |
| 54 | Albite | 11.03 | - | 19.53 | 69.11 | 0.33 | - | - | - | - | 100 |
| 55 | Chlorite | - | 22.79 | 18.66 | 33.21 | - | - | - | 0.62 | 24.72 | 100 |
| 56 | Chlorite + K-spar | - | 4.42 | 18.23 | 59.79 | - | 12.29 | - | - | 5.27 | 100 |
| 57 | Chlorite | - | 22.14 | 18.39 | 32.7 | - | - | - | - | 26.77 | 100 |

**Hand Sample 11CLD003 (dry and wet)**

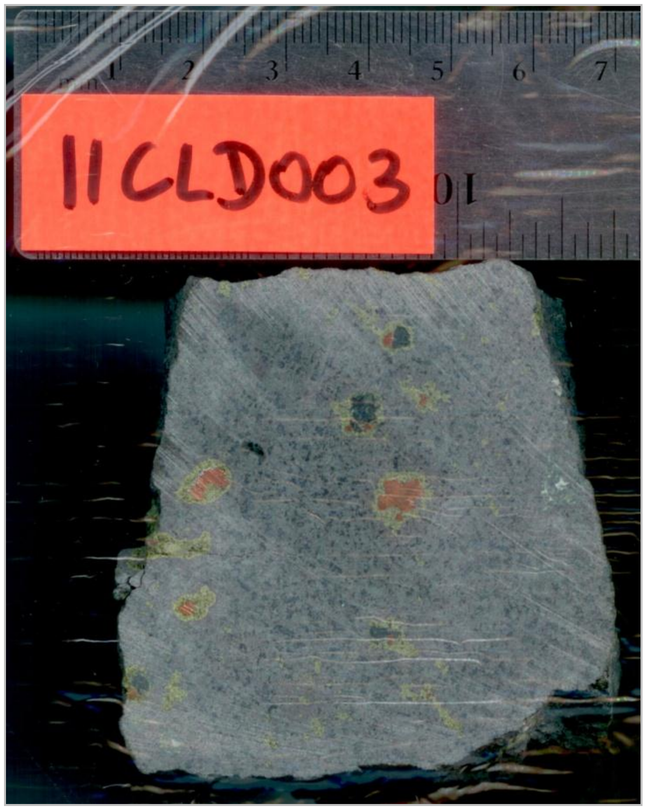


11CLD003

11CLD003_01 10-29_001 through 10-29_013

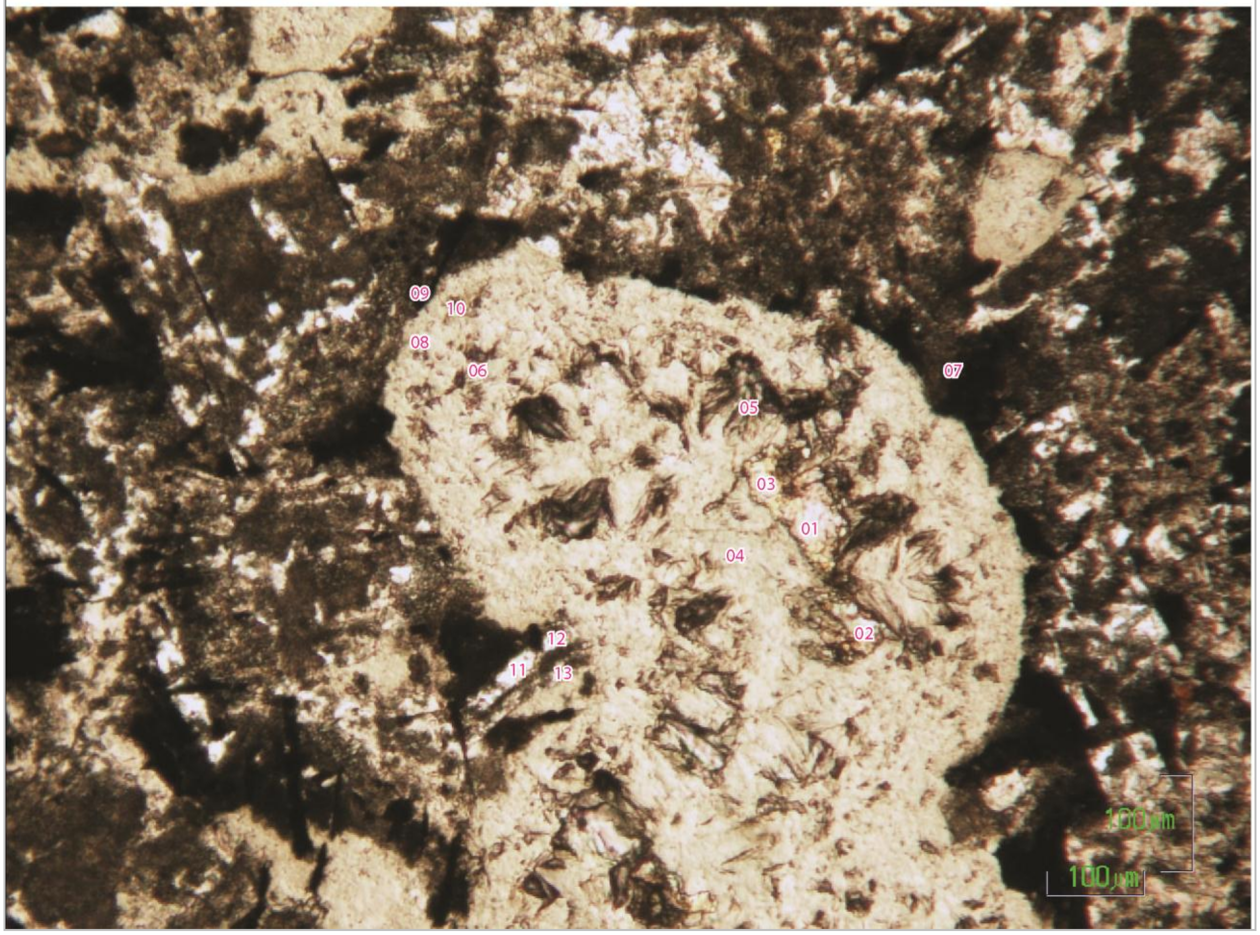


| Point | Mineral | wt % | | | | | | | | | |
|---|---|---|---|---|---|---|---|---|---|---|---|
| | | $Na_2O$ | MgO | $Al_2O_3$ | $SiO_2$ | P2O5 | CaO | $TiO_2$ | MnO | FeO | Total |
| 01 | Epidote | - | | 19.66 | 38.90 | - | 22.64 | - | - | 18.80 | 100 |
| 02 | Epidote | - | 1.29 | 19.85 | 38.71 | - | 21.84 | - | - | 18.30 | 100 |
| 03 | Epidote | - | 0.84 | 19.37 | 38.84 | - | 22.26 | - | - | 18.70 | 100 |
| 04 | Chlorite | - | 20.84 | 19.07 | 32.76 | - | - | - | 0.9 | 26.43 | 100 |
| 05 | Chlorite | - | 19.92 | 17.62 | 32.43 | - | - | - | 1.06 | 28.97 | 100 |
| 06 | Chlorite | - | 21.36 | 18.37 | 33.42 | - | 0.35 | - | 1.03 | 25.46 | 100 |
| 07 | FeOx | - | 2.58 | 2.31 | 4.25 | - | 0.89 | 2.13 | - | 87.84 | 100 |
| 08 | FeOx | - | 7.53 | 5.63 | 8.75 | - | 0.83 | 1.63 | - | 75.63 | 100 |
| 09 | Sphene + Apatite | 0.55 | 1.4 | 4.27 | 30 | 3.83 | 27.68 | 26.54 | - | 5.74 | 100 |
| 10 | Sphene | - | 0.52 | 4.73 | 33.6 | - | 27.81 | 30.21 | - | 3.14 | 100 |
| 11 | Albite | 11.34 | - | 20.03 | 68.3 | - | 0.33 | - | - | - | 100 |
| 12 | Albite | 10.96 | - | 19.83 | 69.21 | - | - | - | - | - | 100 |
| 13 | Albite | 10.55 | 1.74 | 19.61 | 66.71 | - | - | - | - | 1.39 | 100 |

11CLD003_02 10-29_014 through 10-29_021

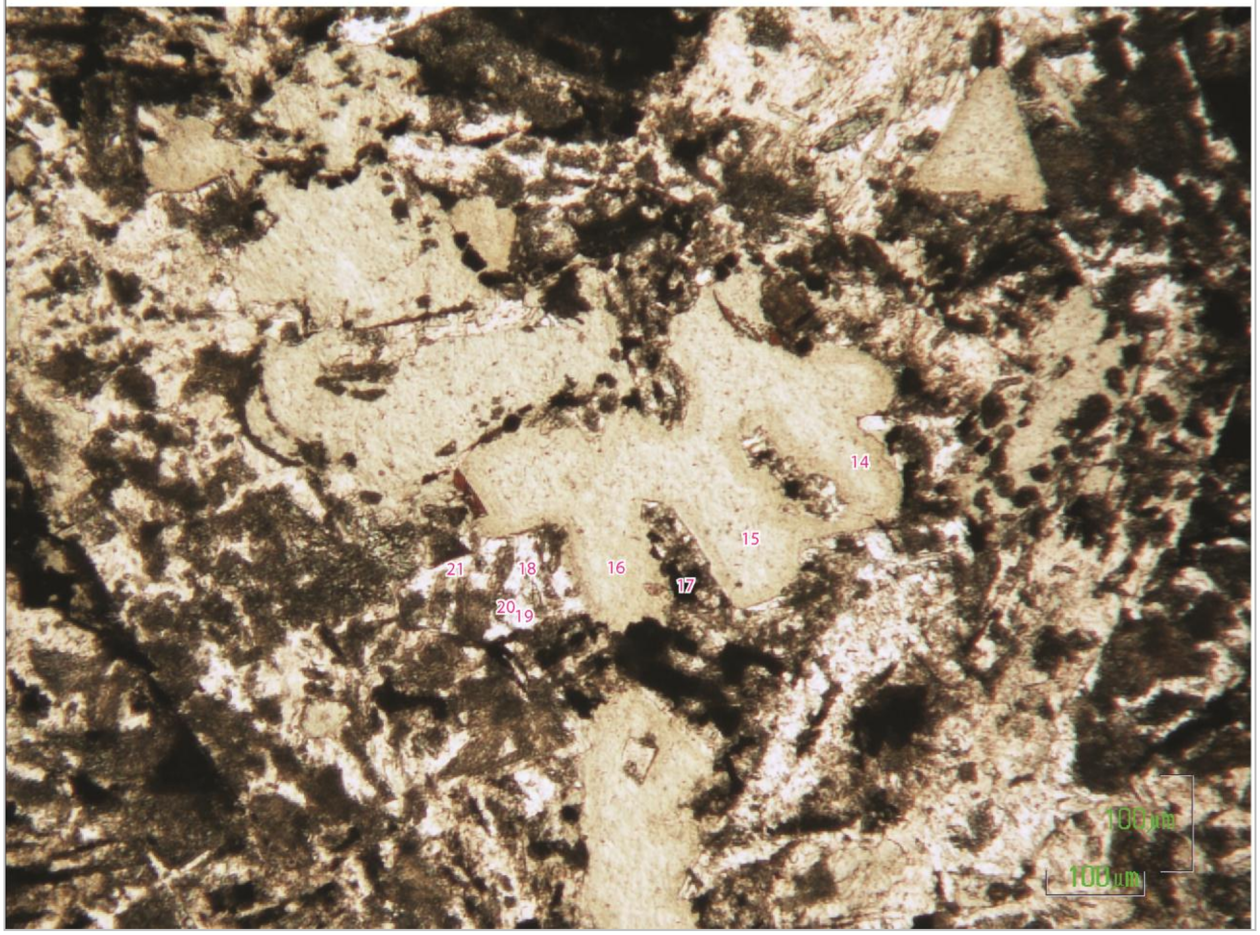


| Point | Mineral | wt % | | | | | | | | | |
|---|---|---|---|---|---|---|---|---|---|---|---|
| | | $Na_2O$ | MgO | $Al_2O_3$ | $SiO_2$ | $K_2O$ | CaO | $TiO_2$ | MnO | FeO | Total |
| 14 | Chlorite | - | 22.31 | 19.28 | 33.8 | - | - | - | - | 24.61 | 100 |
| 15 | Chlorite | 0.6 | 21.61 | 18.51 | 32.83 | - | 0.34 | - | 0.71 | 25.4 | 100 |
| 16 | Chlorite | 0.8 | 21.71 | 18.71 | 33.13 | - | - | - | 0.66 | 24.99 | 100 |
| 17 | Hematite + Ilmenite + Chlorite | - | 10.19 | 8.16 | 17.79 | - | 3.95 | 3.4 | - | 56.51 | 100 |
| 18 | Albite | 11.07 | - | 19.65 | 69.28 | - | - | - | - | - | 100 |
| 19 | Albite | 11.03 | - | 19.4 | 69.01 | 0.56 | - | - | - | - | 100 |
| 20 | Epidote + Chlorite | 0.77 | 3.9 | 22.69 | 41.28 | - | 21.48 | - | - | 9.88 | 100 |
| 21 | Albite | 11.21 | - | 19.56 | 68.84 | - | 0.39 | - | - | - | 100 |

| 11CLD003_04 | 10-29_022 through 10-29_032 |
|---|---|

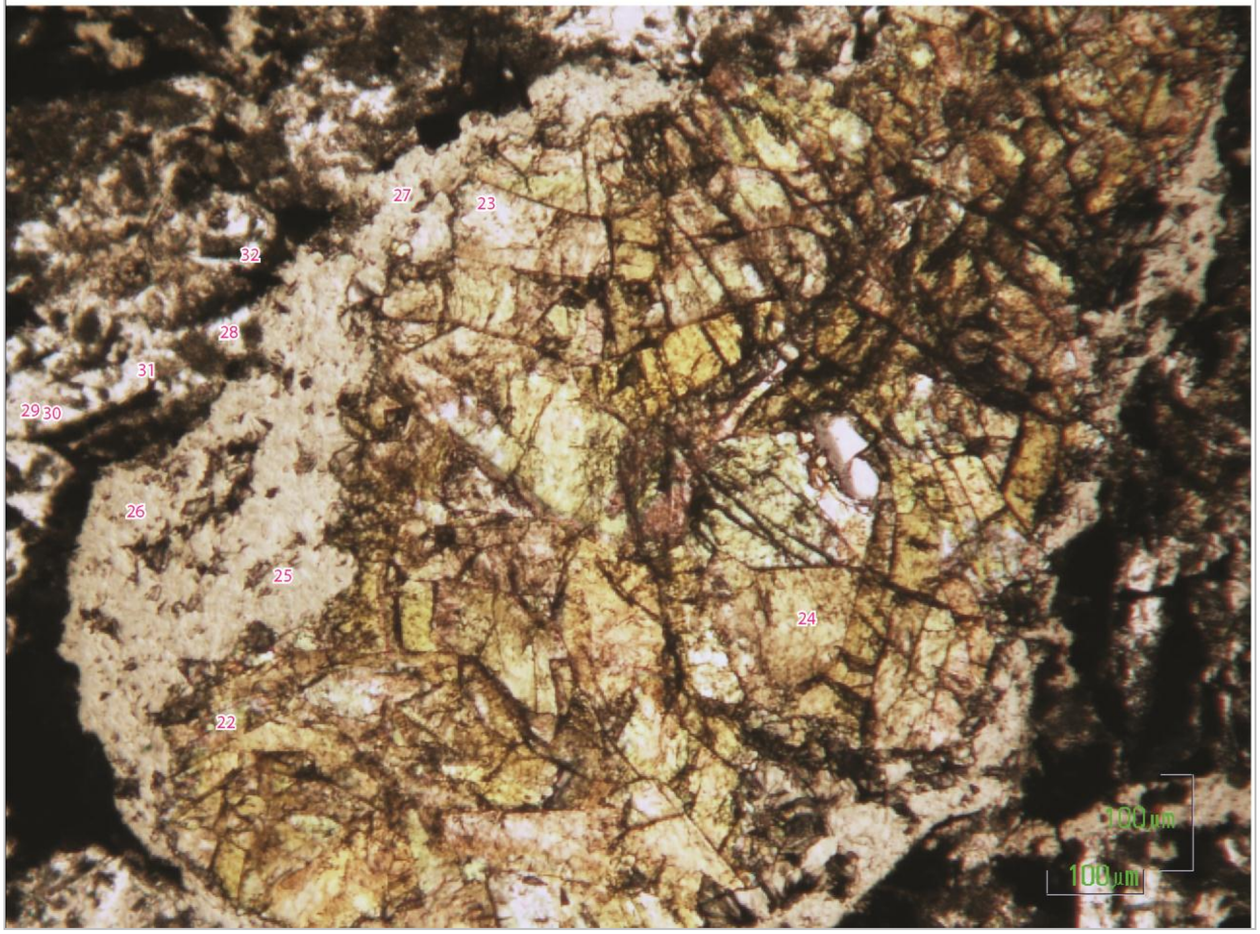


| Point | Mineral | wt % | | | | | | | | |
|---|---|---|---|---|---|---|---|---|---|---|
| | | $Na_2O$ | MgO | $Al_2O_3$ | $SiO_2$ | $K_2O$ | CaO | MnO | FeO | Total |
| 22 | Epidote | - | 0.84 | 20.13 | 39.23 | - | 22.04 | - | 17.76 | 100 |
| 23 | Epidote + Chlorite | - | 2.2 | 19.13 | 38.14 | - | 20.73 | - | 19.8 | 100 |
| 24 | Epidote | - | - | 18.87 | 39.00 | - | 22.21 | - | 19.91 | 100 |
| 25 | Chlorite | 0.83 | 21.68 | 18.47 | 33.1 | - | - | 0.68 | 25.24 | 100 |
| 26 | Chlorite | 0.75 | 21.22 | 18.6 | 32.83 | - | - | 0.75 | 25.85 | 100 |
| 27 | Chlorite | - | 20.83 | 18.09 | 33.3 | - | - | 0.68 | 27.09 | 100 |
| 28 | K-spar | 7.77 | - | 19.5 | 68.36 | 4.37 | - | - | - | 100 |
| 29 | Albite | 11.05 | - | 19.31 | 68.56 | 0.48 | 0.6 | - | - | 100 |
| 30 | Epidote + Chlorite + K-spar | - | 3.08 | 23.16 | 44.28 | 2.4 | 19.54 | - | 7.55 | 100 |
| 31 | Albite | 11.06 | - | 19.77 | 69.17 | - | - | - | - | 100 |
| 32 | Albite | 10.78 | - | 19.81 | 69.42 | - | - | - | - | 100 |

**Hand Sample 11CBF006**


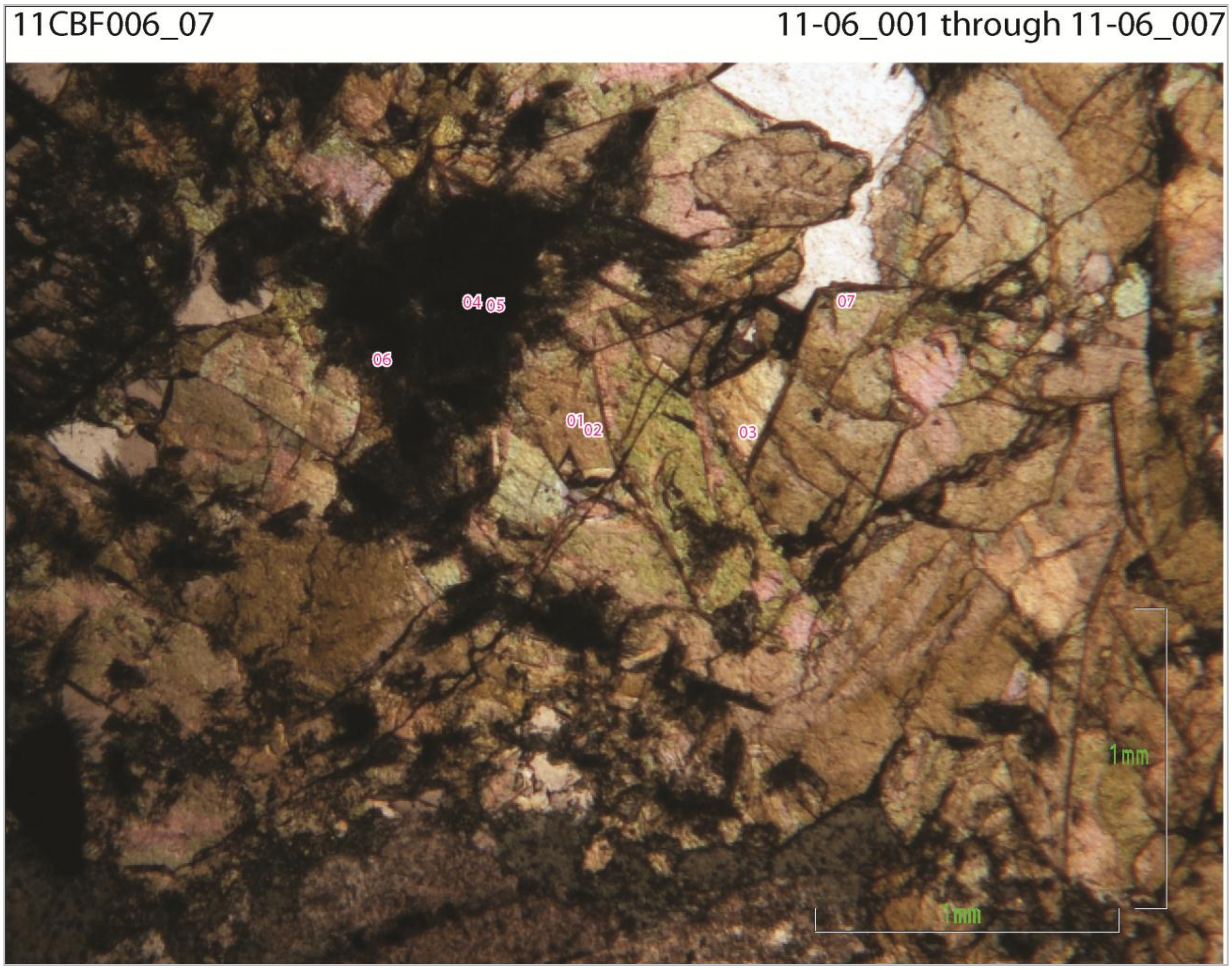


| Point | Mineral | wt % | | | | | | |
|---|---|---|---|---|---|---|---|---|
| | | MgO | $Al_2O_3$ | $SiO_2$ | CaO | MnO | FeO | Total |
| 01 | Epidote | - | 22.31 | 39.01 | 21.72 | 1.03 | 15.92 | 100 |
| 02 | Epidote | - | 24.52 | 39.57 | 22.74 | - | 13.17 | 100 |
| 03 | Epidote | - | 21.98 | 39.56 | 21.81 | 1.04 | 15.61 | 100 |
| 04 | Epidote + Chlorite | peak | 13.02 | 37.72 | 23.93 | - | 25.33 | 100 |
| 05 | Chlorite + Epidote | 29.32 | 12.65 | 42.3 | 2.67 | - | 13.07 | 100 |
| 06 | Chlorite + Epidote | 27.95 | 12.9 | 43.38 | 4.65 | - | 11.12 | 100 |
| 07 | Epidote | - | 21.40 | 39.24 | 23.13 | - | 16.23 | 100 |

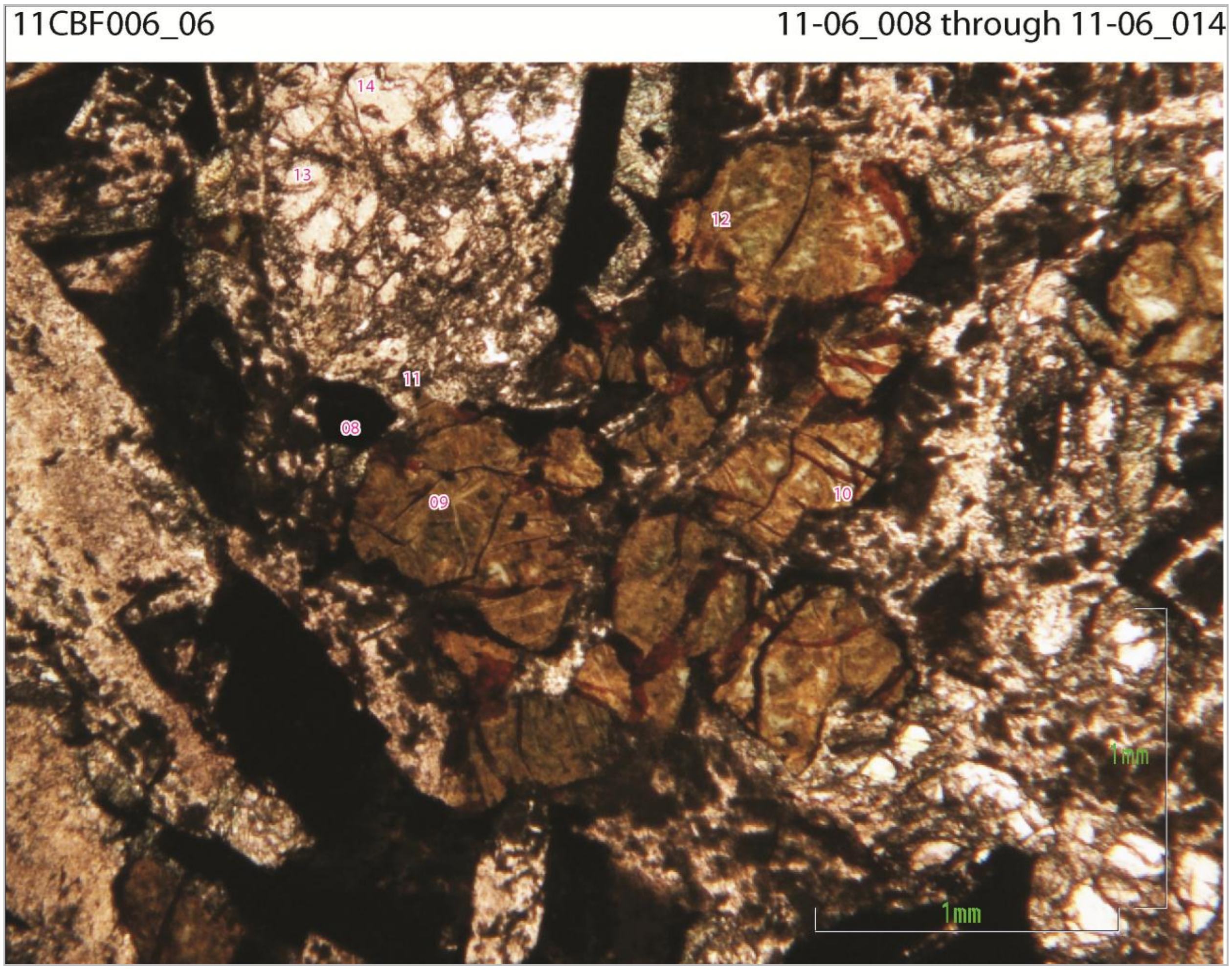


| Point | Mineral | wt % | | | | | | | |
|---|---|---|---|---|---|---|---|---|---|
| | | $Na_2O$ | MgO | $Al_2O_3$ | $SiO_2$ | CaO | $TiO_2$ | FeO | Total |
| 08 | FeOx | - | - | 1.03 | 5.95 | 4.13 | 21.66 | 67.23 | 100 |
| 09 | Chlorite + Epidote | - | 12.1 | 16.33 | 41.83 | 15.14 | - | 14.6 | 100 |
| 10 | Chlorite + Epidote | - | 14.28 | 19.05 | 36.83 | 7.75 | - | 22.1 | 100 |
| 11 | Pyroxene | - | 14.84 | 2.23 | 51.69 | 16.86 | 1.01 | 13.37 | 100 |
| 12 | Chlorite + Epidote | - | 15.15 | 16.27 | 42.95 | 12.76 | - | 12.86 | 100 |
| 13 | Pyroxene | - | 15.36 | 2.45 | 52.19 | 18.25 | 1.01 | 10.75 | 100 |
| 14 | Pyroxene | 0.77 | 15.54 | 2.38 | 52.39 | 18.15 | 0.77 | 9.99 | 100 |

11CBF006_05 11-06_015 through 11-06_029

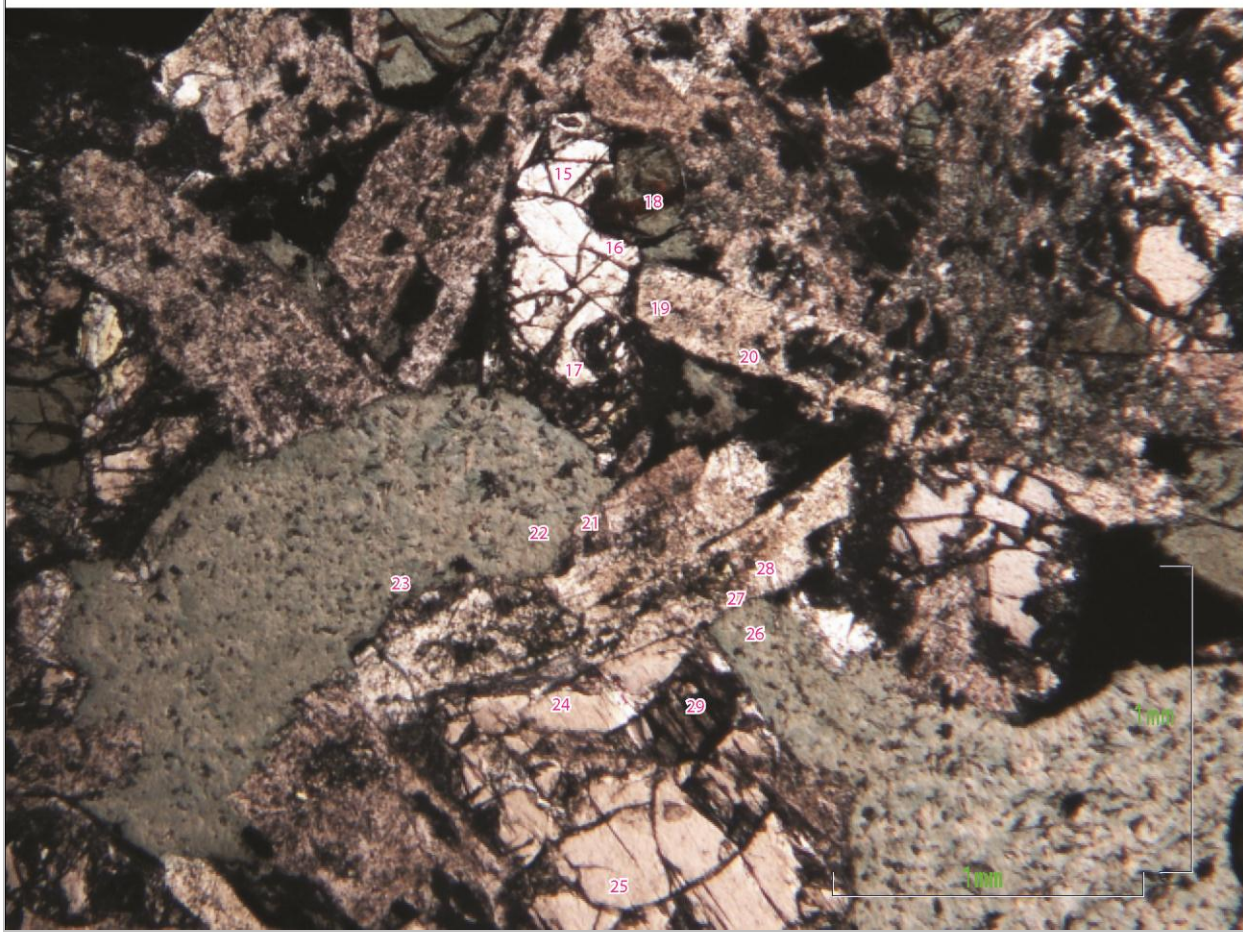

| Point | Mineral | wt % | | | | | | | | | |
|---|---|---|---|---|---|---|---|---|---|---|---|
| | | $Na_2O$ | MgO | $Al_2O_3$ | $SiO_2$ | CaO | $TiO_2$ | $Cr_2O_3$ | MnO | FeO | Total |
| 15 | Pyroxene | - | 15.06 | 2.91 | 51.58 | 19.36 | 0.95 | 0.65 | - | 9.49 | 100 |
| 16 | Pyroxene | - | 15.08 | 3.26 | 51.23 | 18.73 | 0.94 | 0.82 | - | 9.93 | 100 |
| 17 | Pyroxene | - | 13.56 | 2.78 | 50.59 | 18.26 | 1.21 | - | - | 13.6 | 100 |
| 18 | Chlorite | - | 18.86 | 18.3 | 31.99 | - | - | - | 0.76 | 30.1 | 100 |
| 19 | Albite | 11.41 | - | 19.66 | 68.93 | - | - | - | - | - | 100 |
| 20 | Albite | 11.15 | - | 19.62 | 69.23 | - | - | - | - | - | 100 |
| 21 | Albite | 11.45 | - | 19.33 | 69.22 | - | - | - | - | - | 100 |
| 22 | Chlorite | - | 18.08 | 18.69 | 31.91 | - | - | - | | 31.32 | 100 |
| 23 | Chlorite | - | 18.57 | 18.5 | 31.73 | - | - | - | 0.75 | 30.45 | 100 |
| 24 | Pyroxene | - | 15.84 | 2.6 | 52.2 | 18.83 | 0.76 | 0.61 | - | 9.15 | 100 |
| 25 | Pyroxene | - | 15.93 | 2.39 | 52.3 | 18.31 | 0.7 | 0.8 | - | 9.58 | 100 |
| 26 | Chlorite | - | 18.8 | 18.1 | 31.9 | - | - | - | 0.7 | 30.51 | 100 |
| 27 | Albite | 11.42 | | 19.59 | 69 | - | - | - | - | - | 100 |
| 28 | Epidote | - | - | 23.67 | 40.05 | 22.57 | - | - | - | 13.71 | 100 |
| 29 | Pyroxene | 0.85 | 14.33 | 3.73 | 50.14 | 18.39 | 1.26 | - | - | 11.3 | 100 |

11CBF006_04 11-06_030 through 11-06_041

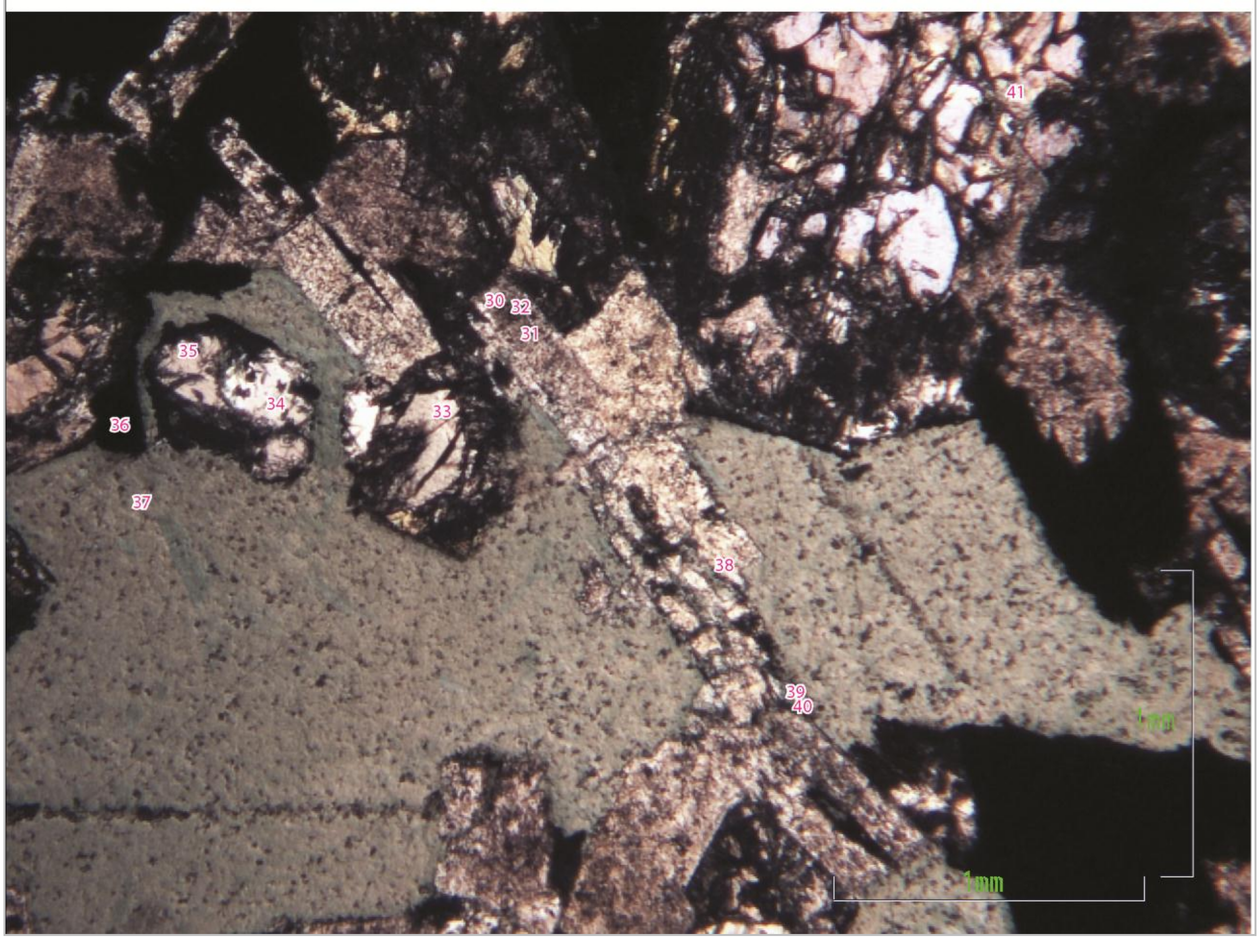

| Point | Mineral | wt % | | | | | | | | | |
|---|---|---|---|---|---|---|---|---|---|---|---|
| | | $Na_2O$ | MgO | $Al_2O_3$ | $SiO_2$ | CaO | $TiO_2$ | $Cr_2O_3$ | MnO | FeO | Total |
| 30 | Albite | 11.18 | - | 19.69 | 69.13 | - | - | - | - | - | 100 |
| 31 | Epidote + Chlorite + K-spar | 1.74 | 2.38 | 23.92 | 45.01 | 18.13 | - | - | - | 7.89 | 100 |
| 32 | K-spar | - | - | 20.06 | 63.52 | - | - | - | - | 1.1 | 100 |
| 33 | Pyroxene | 1.14 | 14.13 | 2.28 | 50.86 | 17.35 | 0.82 | - | - | 13.42 | 100 |
| 34 | Quartz | - | - | - | 100 | - | - | - | - | - | 100 |
| 35 | Quartz | - | - | - | 100 | - | - | - | - | - | 100 |
| 36 | FeOx + Ilmenite | 1.74 | 2.38 | 23.92 | 45.01 | 18.13 | - | - | - | 7.89 | 100 |
| 37 | Chlorite | - | 20.89 | 18.85 | 32.34 | - | - | - | 0.7 | 27.22 | 100 |
| 38 | Albite | 10.94 | - | 19.68 | 68.73 | - | - | - | - | - | 100 |
| 39 | Albite | 11.37 | - | 19.77 | 68.85 | - | - | - | - | - | 100 |
| 40 | K-spar | 1.97 | - | 18.54 | 65.46 | - | - | - | - | - | 100 |
| 41 | Pyroxene | - | 15.73 | 2.21 | 52.38 | 18.36 | 0.7 | 0.62 | - | 10.01 | 100 |

11CBF006_02 11-06_042 through 11-06_050

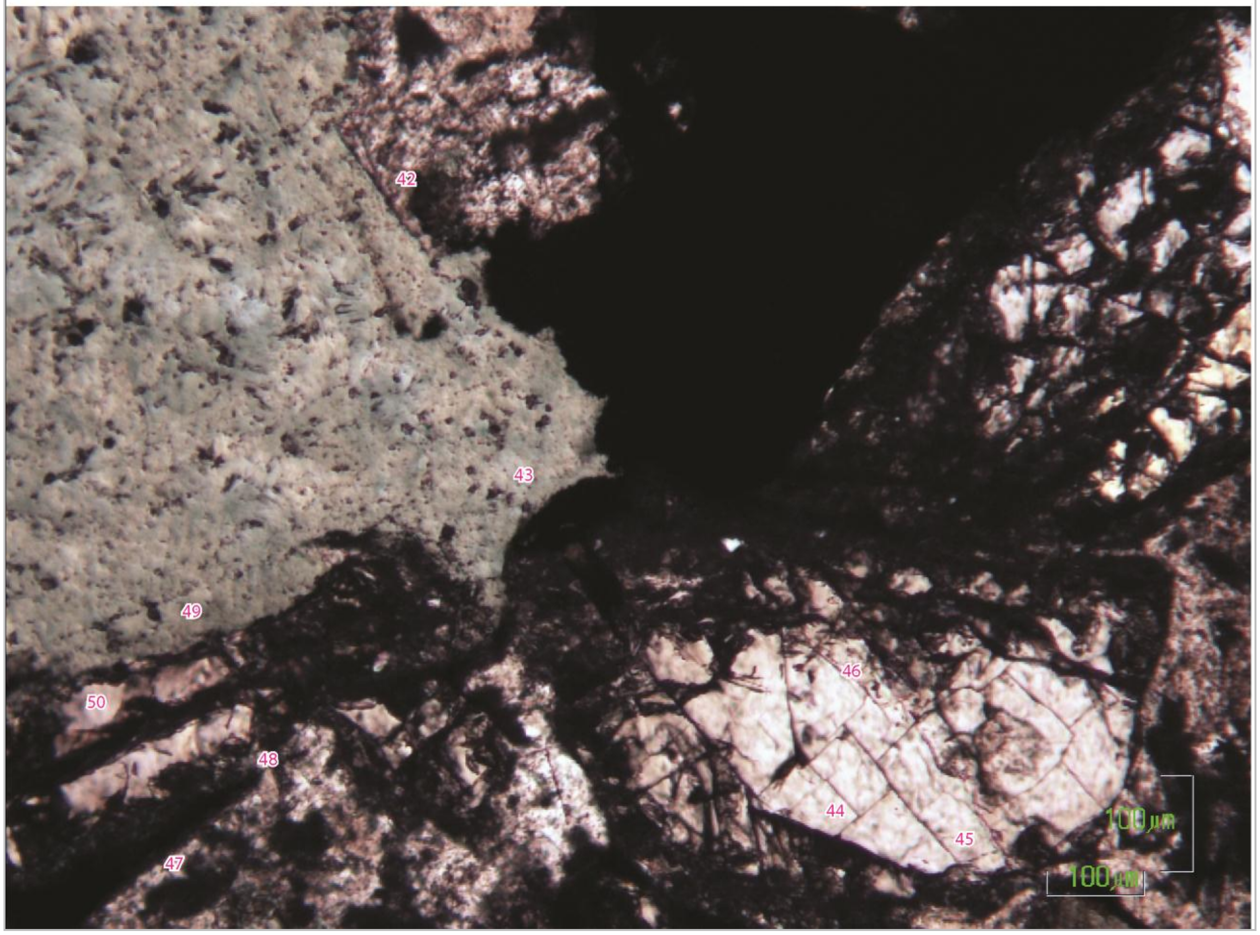


| Point | Mineral | wt % | | | | | | | | | |
|---|---|---|---|---|---|---|---|---|---|---|---|
| | | $Na_2O$ | MgO | $Al_2O_3$ | $SiO_2$ | CaO | $TiO_2$ | $Cr_2O_3$ | MnO | FeO | Total |
| 42 | Albite | 11.57 | - | 19.45 | 68.98 | - | - | - | - | - | 100 |
| 43 | Chlorite | - | 18.51 | 18.46 | 31.54 | - | - | - | 0.85 | 30.64 | 100 |
| 44 | Pyroxene | - | 15.32 | 2.37 | 52.19 | 18.87 | 0.79 | - | - | 10.47 | 100 |
| 45 | Pyroxene | - | 15.71 | 2.43 | 51.52 | 18.54 | 0.85 | 0.53 | - | 10.43 | 100 |
| 46 | Pyroxene | 0.88 | 14.6 | 3.25 | 51.09 | 18.76 | 0.95 | - | - | 10.46 | 100 |
| 47 | Albite | 11.58 | - | 19.47 | 68.95 | - | - | - | - | - | 100 |
| 48 | Albite | 11.18 | - | 19.7 | 69.12 | - | - | - | - | - | 100 |
| 49 | Chlorite | - | 20.32 | 18.49 | 32.24 | - | - | - | 0.8 | 28.15 | 100 |
| 50 | Pyroxene | - | 13.93 | 2.86 | 50.64 | 17.46 | 1.12 | - | - | 13.98 | 100 |

11CBF006_01 11-06_051 through 11-06_059

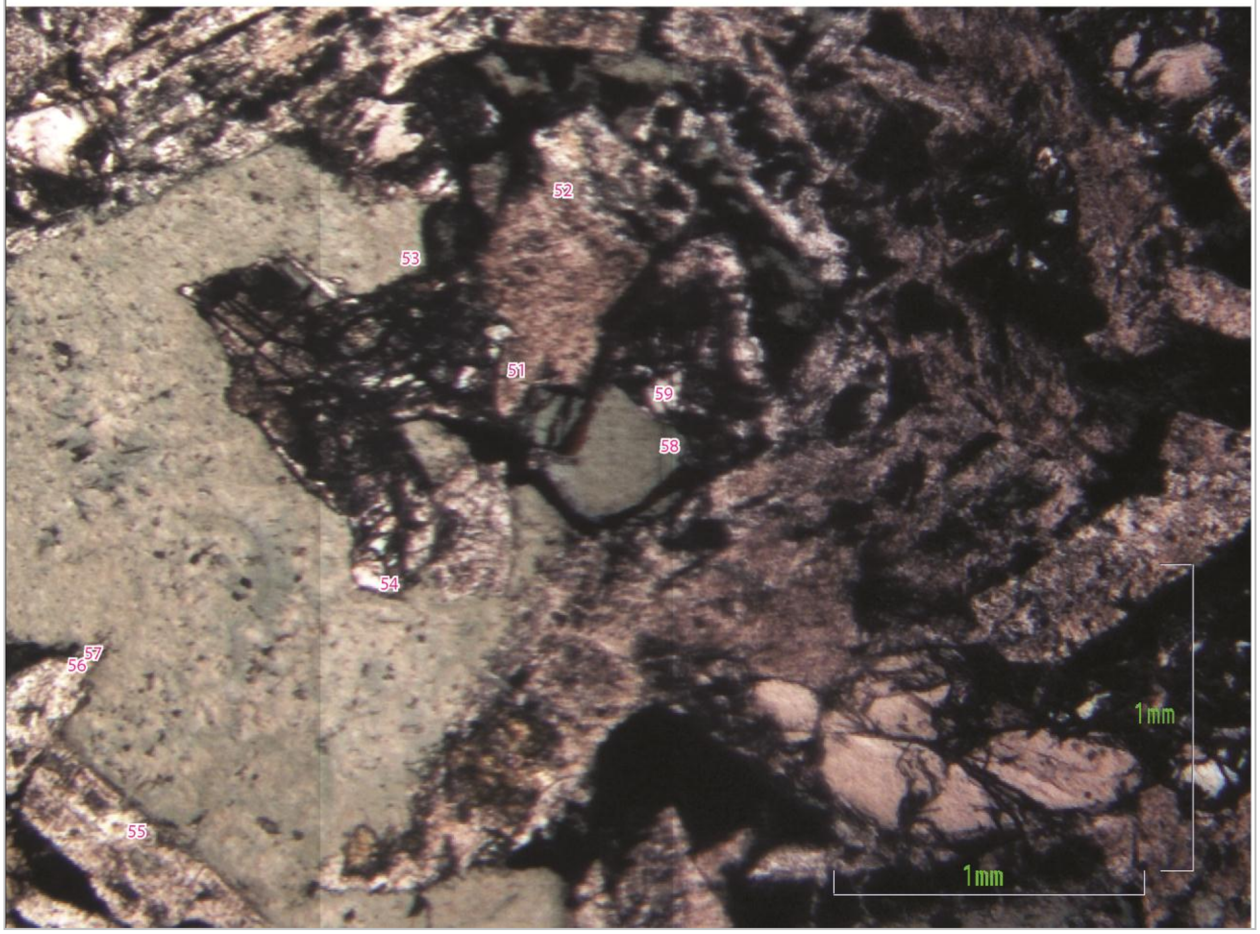


| Point | Mineral | wt % | | | | | | | | |
|---|---|---|---|---|---|---|---|---|---|---|
| | | $Na_2O$ | MgO | $Al_2O_3$ | $SiO_2$ | CaO | $TiO_2$ | MnO | FeO | Total |
| 51 | Albite | 11.47 | - | 19.49 | 69.04 | - | - | - | - | 100 |
| 52 | Albite | 11.43 | - | 19.52 | 69.06 | - | - | - | - | 100 |
| 53 | Chlorite | - | 18.44 | 18.71 | 31.86 | - | - | 0.88 | 30.11 | 100 |
| 54 | Quartz | - | - | - | 100 | - | - | - | - | 100 |
| 55 | Albite | 11.42 | - | 19.4 | 69.18 | - | - | - | - | 100 |
| 56 | Albite | 11.32 | - | 19.44 | 69.24 | - | - | - | - | 100 |
| 57 | Epidote | - | - | 21.82 | 39.50 | 22.25 | - | - | 16.43 | 100 |
| 58 | Chlorite | - | 18.56 | 18.26 | 32.23 | - | - | 0.74 | 30.21 | 100 |
| 59 | Pyroxene | - | 15.01 | 2.45 | 51.43 | 18.26 | 0.89 | - | 11.96 | 100 |

**Hand Sample 11CLD007 (dry and wet)**

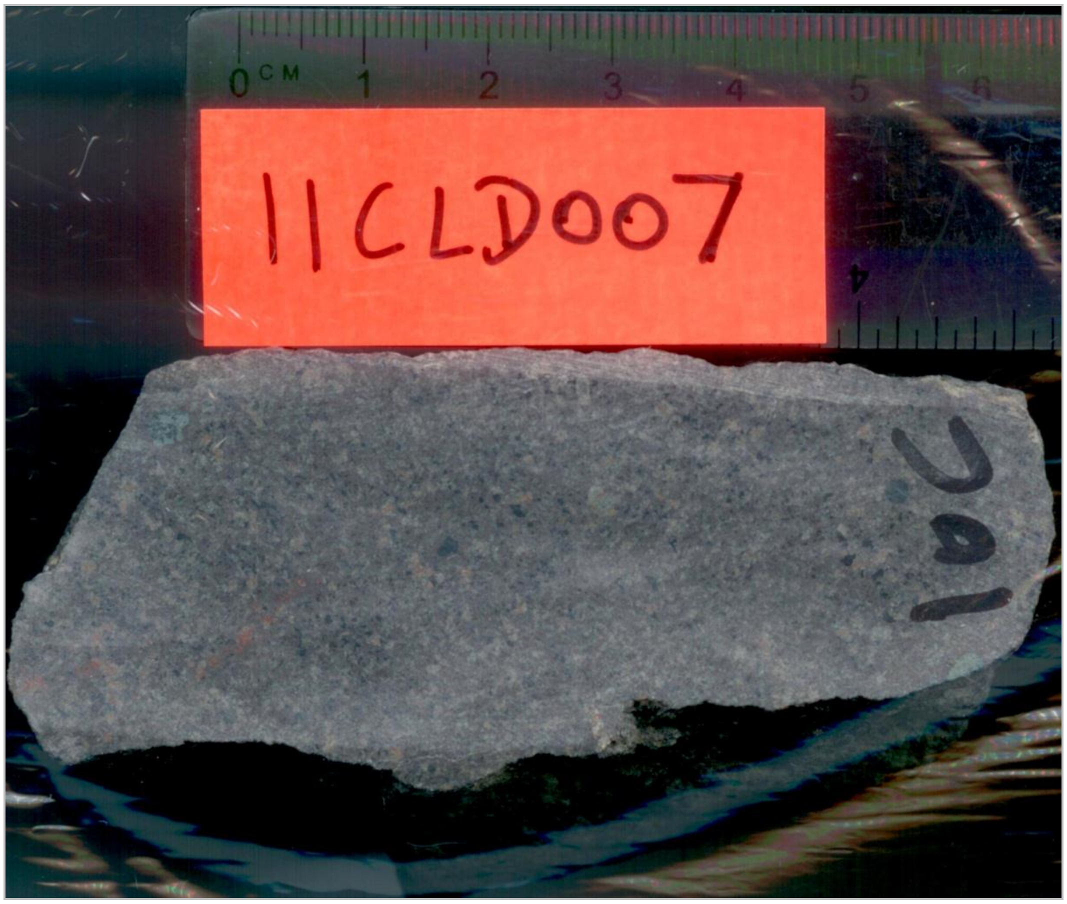

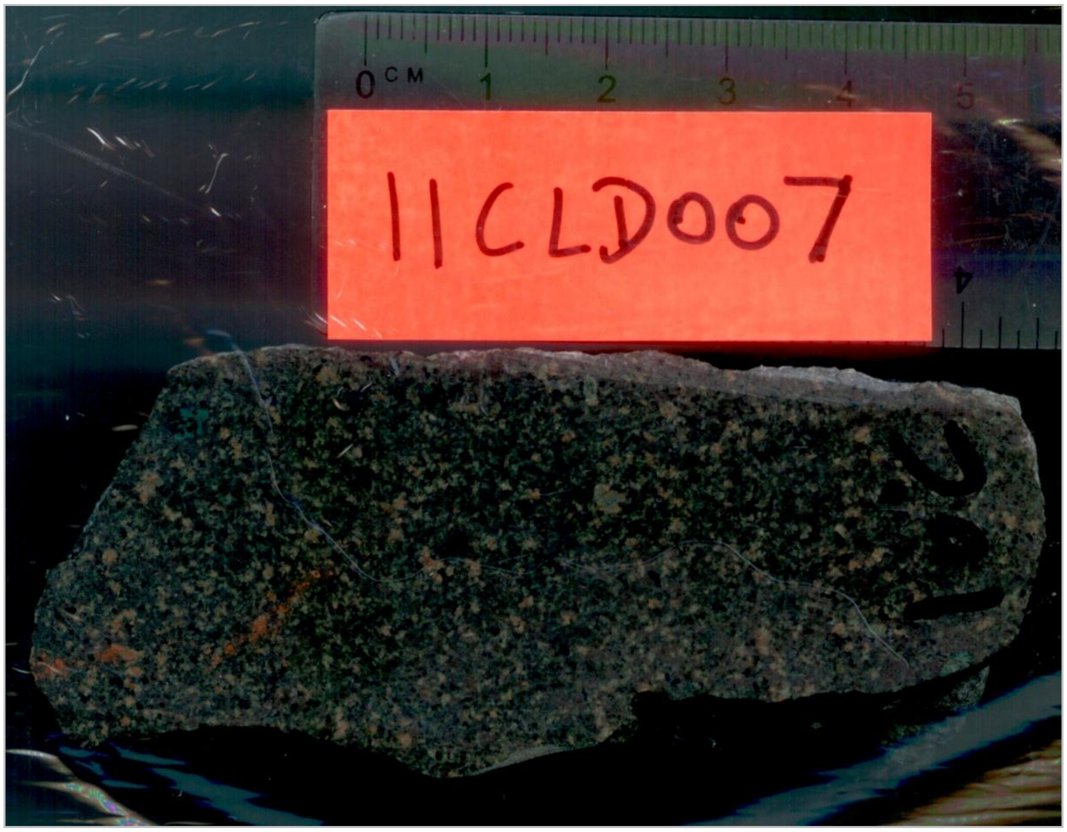
0 CM 1 2 3 4 5
11CLD007

11CLD007_06 11-06_060 through 11-06_070

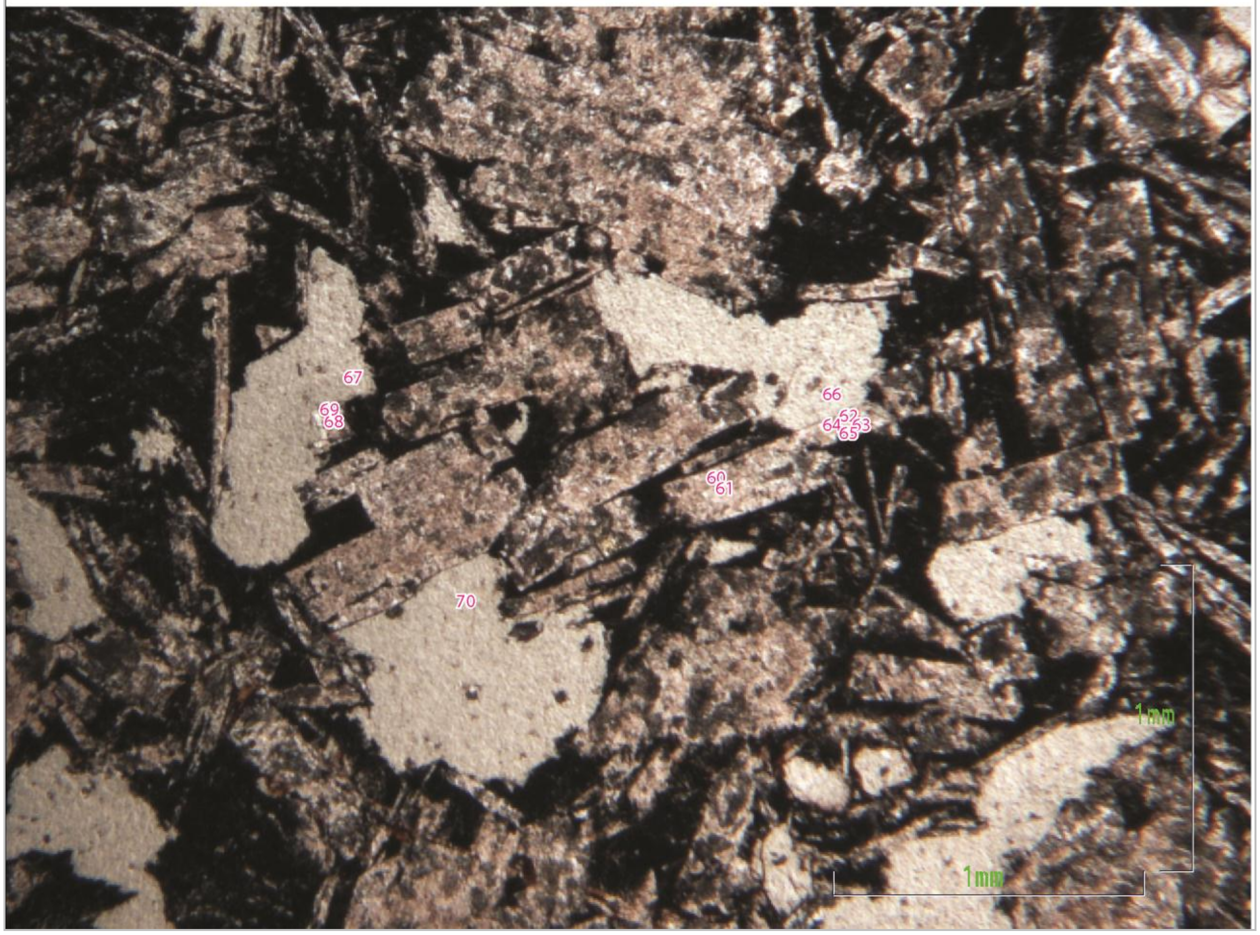


| Point | Mineral | wt % | | | | | | | | |
|---|---|---|---|---|---|---|---|---|---|---|
| | | $Na_2O$ | MgO | $Al_2O_3$ | $SiO_2$ | $K_2O$ | CaO | MnO | FeO | Total |
| 60 | Albite | 10.91 | - | 19.61 | 67.28 | 0.79 | - | - | 1.41 | 100 |
| 61 | K-spar | - | - | 18.54 | 65.65 | 15.82 | - | - | - | 100.01 |
| 62 | Albite | 11.07 | - | 19.63 | 69.29 | - | - | - | - | 100 |
| 63 | Epidote + Chlorite | 1.19 | 2.88 | 23.18 | 44.22 | - | 19.96 | - | 8.58 | 100 |
| 64 | K-spar | 0.67 | - | 18.38 | 65.26 | 15.7 | - | - | - | 100 |
| 65 | Epidote + Chlorite + K-spar | 0.84 | 3.91 | 22.06 | 40.19 | 0.51 | 22.17 | - | 10.32 | 100 |
| 66 | Chlorite | - | 25.02 | 19.01 | 34.62 | - | - | 0.66 | 20.68 | 100 |
| 67 | Chlorite | - | 24.69 | 18.95 | 34.06 | - | - | 0.76 | 21.54 | 100 |
| 68 | K-spar | - | - | 18.61 | 65.69 | 15.71 | - | - | - | 100 |
| 69 | Albite | 10.89 | - | 19.65 | 68.89 | 0.56 | - | - | - | 100 |
| 70 | Chlorite | - | 24.34 | 19.62 | 33.57 | - | - | 0.73 | 21.74 | 100 |

11CLD007_05 11-06_071 through 11-06_079

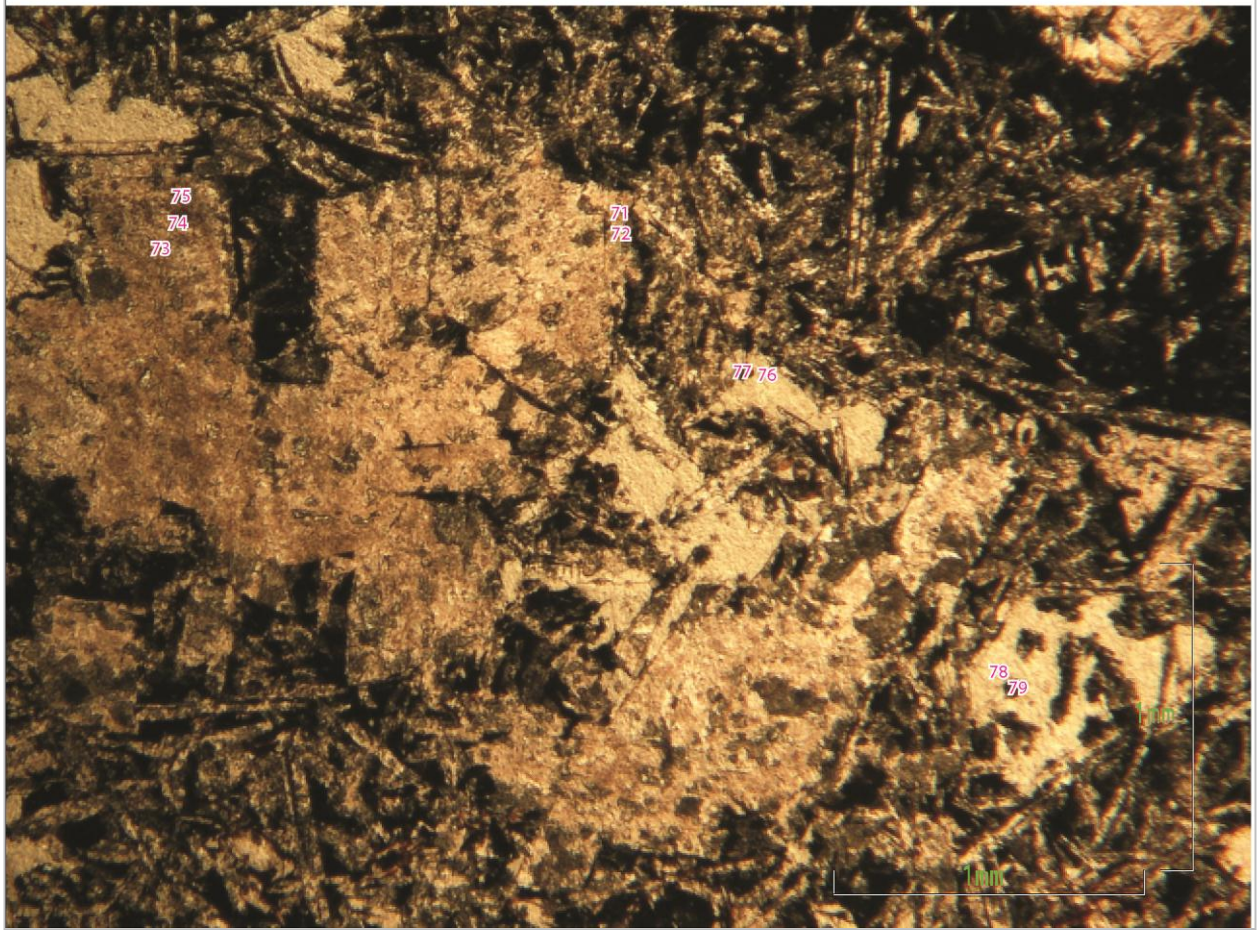


| Point | Mineral | wt % | | | | | | | | | |
|---|---|---|---|---|---|---|---|---|---|---|---|
| | | $Na_2O$ | MgO | $Al_2O_3$ | $SiO_2$ | $K_2O$ | CaO | $TiO_2$ | MnO | FeO | Total |
| 71 | Albite | 10.81 | - | 19.69 | 69.01 | 0.49 | - | - | - | - | 100 |
| 72 | K-spar | 1.18 | - | 18.68 | 65.56 | 14.58 | - | - | - | - | 100 |
| 73 | K-spar | - | - | 18.44 | 65.57 | 16 | - | - | - | - | 100 |
| 74 | Albite | 10.93 | - | 19.7 | 69.36 | - | - | - | - | - | 100 |
| 75 | Epidote + Chlorite | - | 2.93 | 24.17 | 40.47 | - | 22.95 | - | - | 9.47 | 100 |
| 76 | Chlorite | - | 24.95 | 18.68 | 34.78 | - | - | - | 0.68 | 20.9 | 100 |
| 77 | Sphene | - | - | 4.92 | 34.11 | - | 28.39 | 30.13 | - | 2.45 | 100 |
| 78 | Chlorite | - | 24.67 | 18.98 | 34.51 | - | - | - | - | 21.84 | 100 |
| 79 | Sphene + FeOx | - | 1.03 | 3.54 | 31.08 | - | 25.38 | 27.7 | - | 11.26 | 100 |

11CLD007_04 11-06_080 through 11-06_086

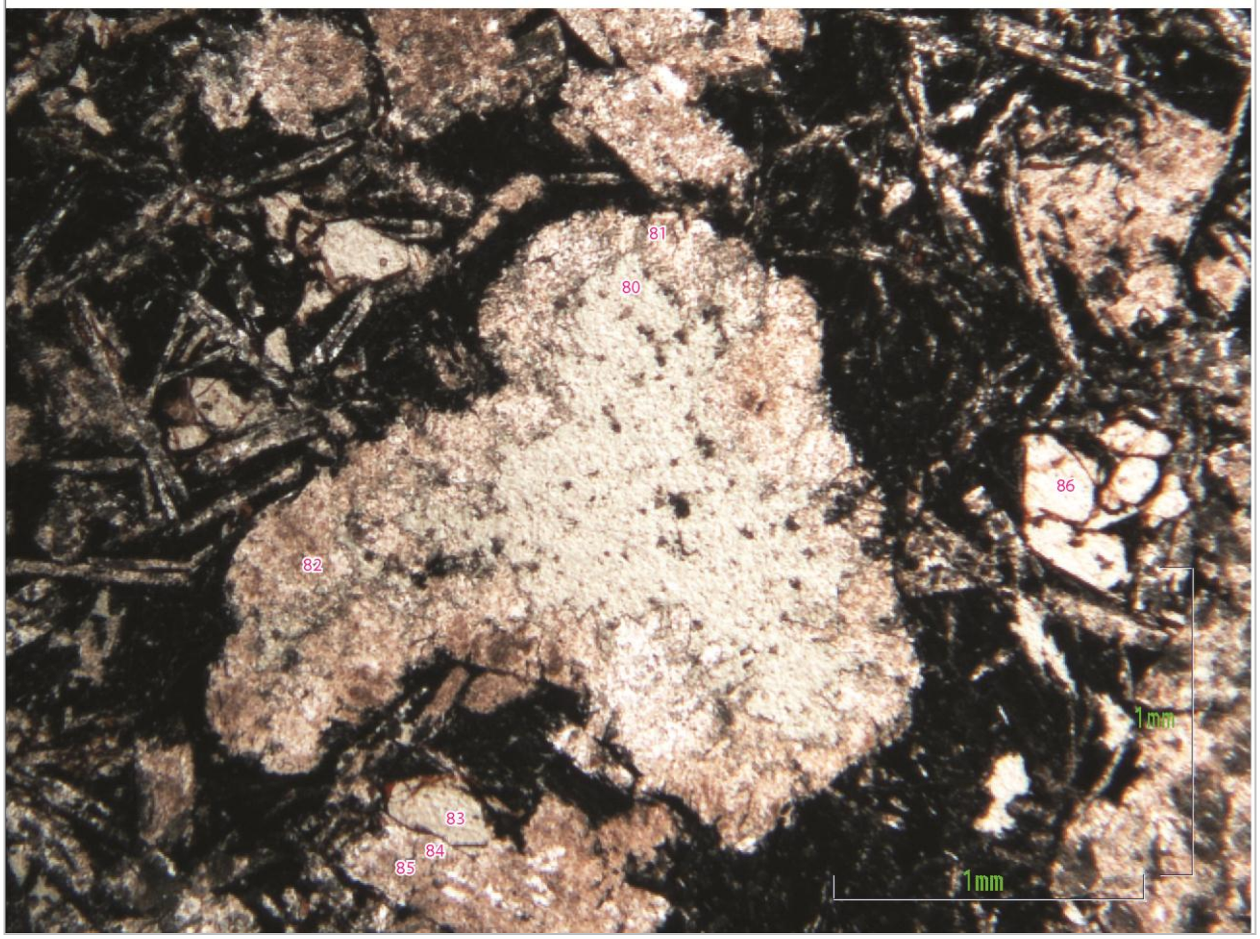


| Point | Mineral | wt % | | | | | | | |
|---|---|---|---|---|---|---|---|---|---|
| | | $Na_2O$ | MgO | $Al_2O_3$ | $SiO_2$ | $K_2O$ | MnO | FeO | Total |
| 80 | Chlorite | - | 22.85 | 18.54 | 33.02 | - | 0.64 | 24.94 | 100 |
| 81 | K-spar | - | - | 18.47 | 65.56 | 15.98 | - | - | 100 |
| 82 | K-spar | - | - | 18.34 | 65.73 | 15.93 | - | - | 100 |
| 83 | Chlorite | - | 23.72 | 18.44 | 34.09 | - | 0.78 | 22.97 | 100 |
| 84 | Albite | 11.2 | | 19.46 | 69.34 | - | - | - | 100 |
| 85 | K-spar | - | - | 18.33 | 65.69 | 15.98 | - | - | 100 |
| 86 | Chlorite | - | 24.9 | 18.36 | 34.89 | - | 0.81 | 21.04 | 100 |

11CLD007_02 11-06_087 through 11-06_090

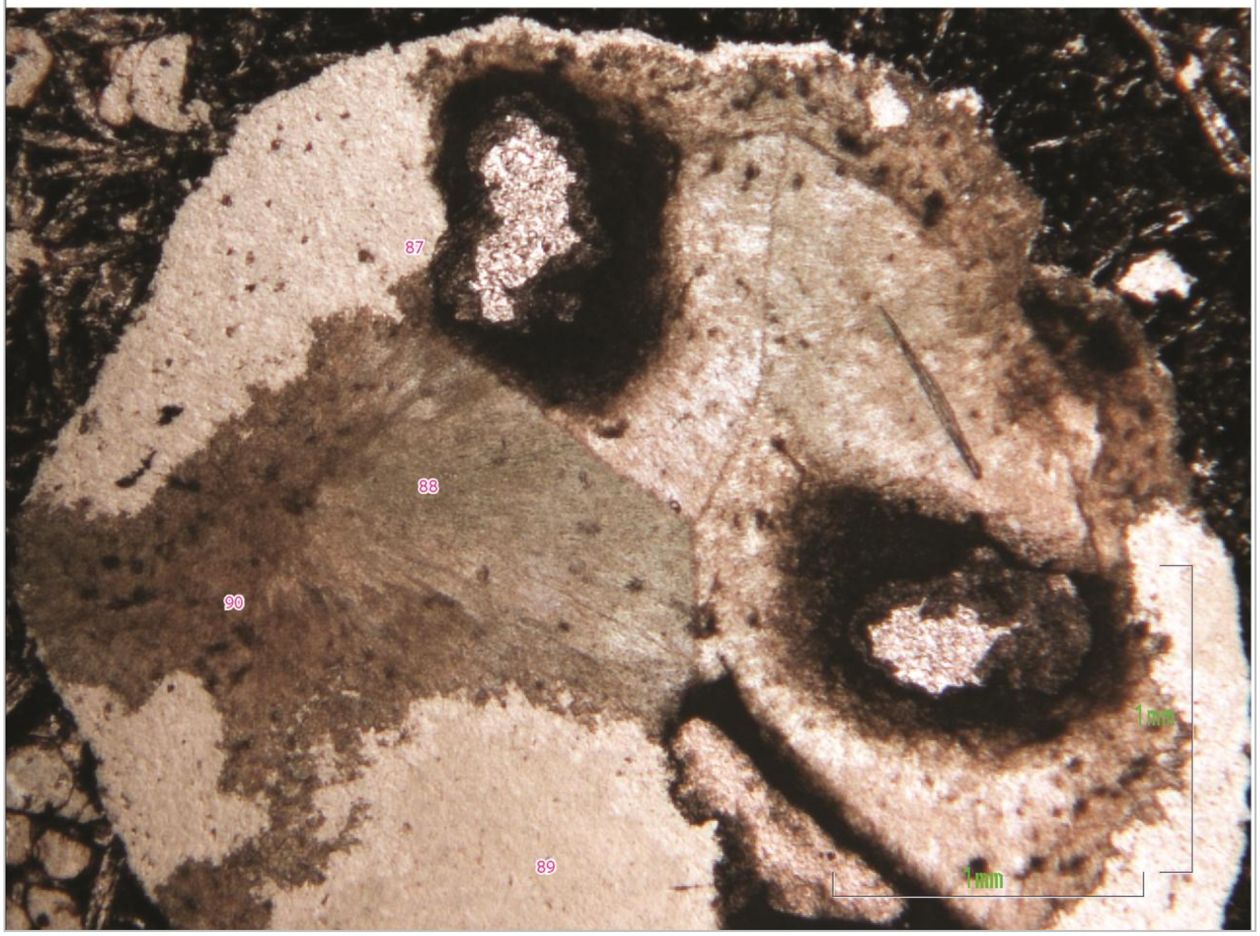


| Point | Mineral | wt % | | | | | | |
|---|---|---|---|---|---|---|---|---|
| | | MgO | $Al_2O_3$ | $SiO_2$ | CaO | MnO | FeO | Total |
| 87 | Chlorite | 24.64 | 18.58 | 34.52 | - | 0.74 | 21.51 | 100 |
| 88 | Pumpellyite | 3.39 | 23.77 | 40.3 | 23.7 | - | 8.89 | 100 |
| 89 | Chlorite | 25.08 | 18.93 | 34.23 | - | 0.7 | 21.05 | 100 |
| 90 | Pumpellyite | 7.17 | 22.76 | 41.6 | 20.5 | - | 8.05 | 100 |

11CLD007_01 11-06_091 through 11-06_100


| Point | Mineral | wt % | | | | | | | | | | |
|---|---|---|---|---|---|---|---|---|---|---|---|---|
| | | $Na_2O$ | MgO | $Al_2O_3$ | $SiO_2$ | $SO_3$ | $K_2O$ | CaO | $TiO_2$ | FeO | CuO | Total |
| 91 | Albite | 11.28 | - | 19.61 | 67.88 | - | - | 0.49 | - | 0.75 | - | 100 |
| 92 | K-spar | - | - | 18.87 | 65.62 | - | 15.51 | - | - | - | - | 100 |
| 93 | Chlorite | - | 23.67 | 18.96 | 33.93 | - | - | - | - | 23.43 | - | 100 |
| 94 | K-spar | - | - | 18.34 | 65.63 | - | 16.03 | - | - | - | - | 100 |
| 95 | Sphene | - | - | 5.35 | 33.11 | - | - | 27.97 | 30.42 | 3.15 | - | 100 |
| 96 | Copper | - | - | 0.99 | 2.26 | 2.07 | 0.43 | - | - | - | 94.25 | 100 |
| 97 | K-spar | - | - | 18.6 | 65.52 | - | 15.88 | - | - | - | - | 100 |
| 98 | K-spar | - | - | 18.45 | 65.54 | - | 16.01 | - | - | - | - | 100 |
| 99 | Quartz + K-spar | - | - | 4.4 | 95.4 | - | 0.19 | - | - | - | - | 100 |
| 100 | Chlorite | - | 23.18 | 18.99 | 33.91 | - | - | - | - | 23.93 | - | 100 |

**Hand Sample 11CLD005 (dry and wet)**


11CLD005 – extremely fine-grained dacite

No petrographic image included

BSE image for general reference

11CLD005 02-25-001 through 009 - image for general reference

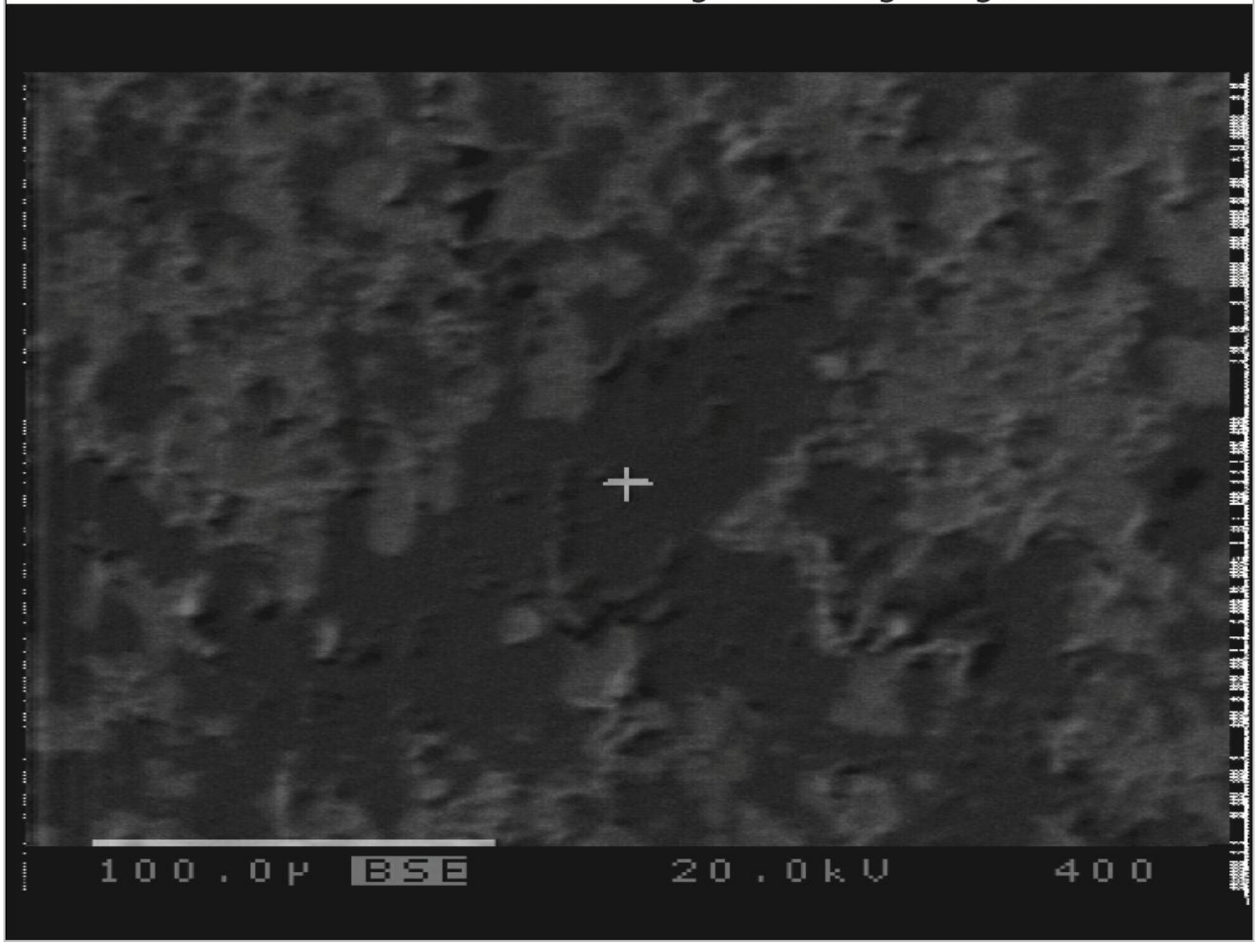


| Point | Mineral | wt % | | | | | |
|---|---|---|---|---|---|---|---|
| | | in BSE | $Al_2O_3$ | $SiO_2$ | CaO | FeO | Total |
| 01 | Quartz | dark area | - | 100 | - | - | 100 |
| 02 | Quartz | dark area | - | 100 | - | - | 100 |
| 03 | Epidote | light area | 22.57 | 39.71 | 23.11 | 14.6 | 100 |
| 04 | Epidote | light area | 20.87 | 38.8 | 23.16 | 17.18 | 100 |
| 05 | Epidote | light area | 22.73 | 39.78 | 23.15 | 14.34 | 100 |
| 06 | Quartz + Clay (?) | dark area | 0.75 | 99.16 | - | 0.1 | 100 |
| 07 | Epidote | light area | 21.40 | 39.24 | 23.13 | 16.23 | 100 |
| 08 | Epidote | light area | 23.67 | 40.05 | 22.57 | 13.71 | 100 |
| 09 | FeOx + Quartz | light area | 1.52 | 16.81 | - | 81.68 | 100 |

**Hand Sample 11CBF004 (dry and wet)**

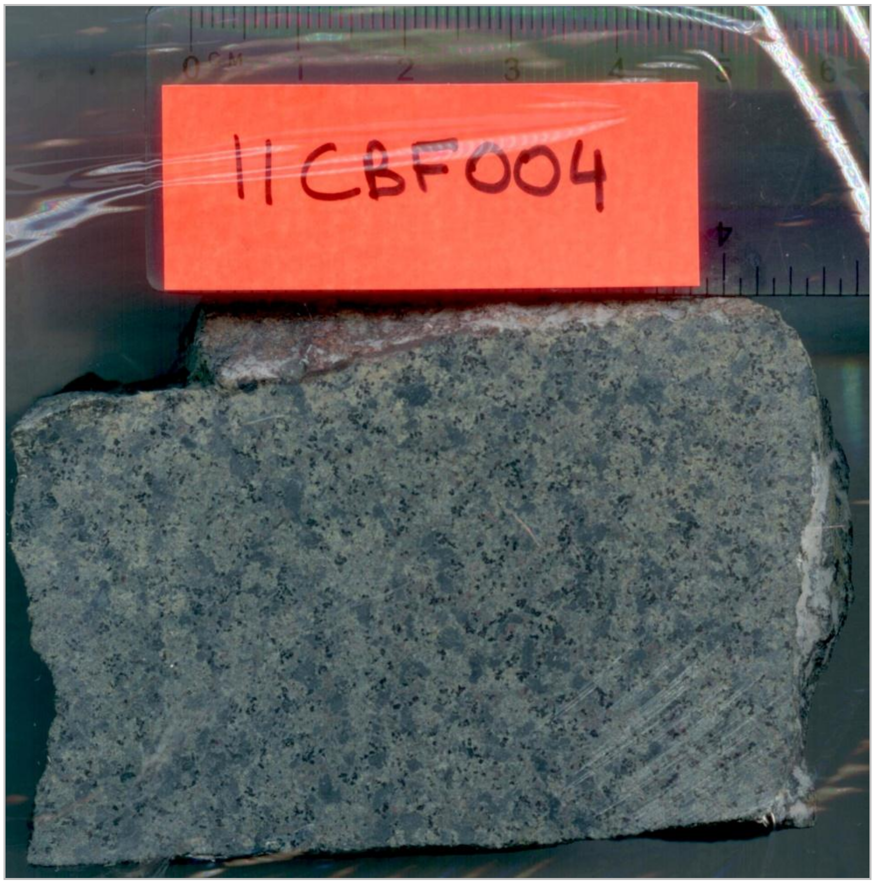
11CBF004

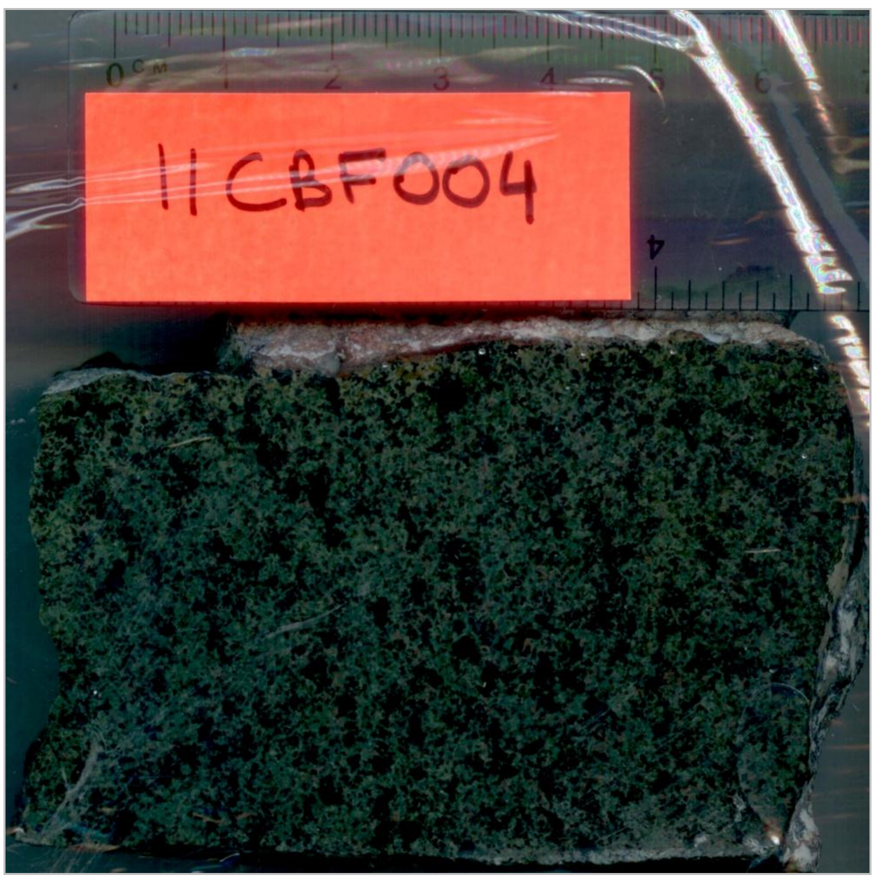
11CBF004

11CBF004_01 11-CBF004_001 through _025

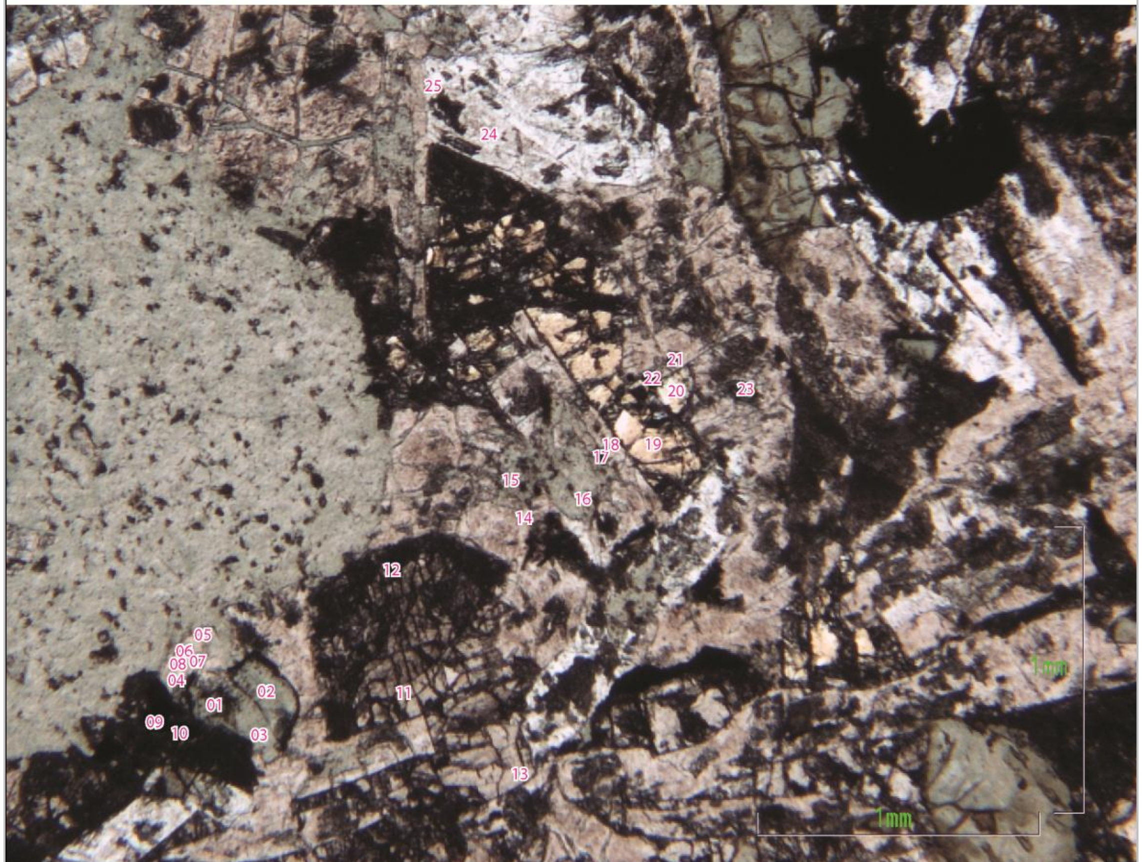


| Point | Mineral | wt % | | | | | | | | | | |
|---|---|---|---|---|---|---|---|---|---|---|---|---|
| | | $Na_2O$ | MgO | $Al_2O_3$ | $SiO_2$ | $K_2O$ | CaO | $TiO_2$ | $Cr_2O_3$ | MnO | FeO | Total |
| 01 | Chlorite | - | 20.02 | 17.41 | 33.04 | - | 0.85 | 0.63 | - | 0.66 | 27.4 | 100 |
| 02 | Chlorite | - | 19.53 | 18.81 | 32.34 | - | - | - | - | - | 29.32 | 100 |
| 03 | Chlorite | - | 20.62 | 17.11 | 33.26 | - | 0.54 | - | - | 0.72 | 27.75 | 100 |
| 04 | Albite | 10.55 | - | 19.37 | 70.08 | - | - | - | - | - | - | 100 |
| 05 | Albite | 10.4 | - | 19.66 | 69.51 | - | 0.42 | - | - | - | - | 100 |
| 06 | Albite | 10.39 | - | 19.66 | 69.95 | - | - | - | - | - | - | 100 |
| 07 | K-spar | 1.65 | - | 18.96 | 66.2 | 13.19 | - | - | - | - | - | 100 |
| 08 | K-spar | 2.82 | - | 18.87 | 65.55 | 12.75 | - | - | - | - | - | 100 |
| 09 | FeOx + Ilmenite | - | - | 0.7 | 4.39 | - | 2.94 | 15.97 | - | - | 76 | 100 |
| 10 | Sphene | - | 3.5 | 5.76 | 32.33 | - | 24 | 28.11 | - | - | 6.3 | 100 |
| 11 | Pyroxene | - | 14.04 | 3.02 | 51.19 | - | 19.41 | 1.23 | - | - | 11.11 | 100 |
| 12 | Pyroxene | - | 13.72 | 2.96 | 50.57 | - | 18.52 | 1.27 | - | - | 12.96 | 100 |
| 13 | Pyroxene | - | 15.29 | 2.06 | 52.28 | - | 18.55 | 0.97 | - | - | 10.85 | 100 |
| 14 | Albite | 10.15 | 1.56 | 19.44 | 66.55 | - | 0.45 | - | - | - | 1.9 | 100 |
| 15 | Chlorite | - | 19.94 | 17.71 | 33.28 | - | - | - | - | - | 29.07 | 100 |
| 16 | Chlorite | - | 20.5 | 17.79 | 33.82 | - | - | - | - | - | 27.88 | 100 |
| 17 | Sphene | - | 1 | 3.87 | 33.6 | - | 26.74 | 30.73 | - | - | 4.05 | 100 |
| 18 | Albite | 10.33 | - | 19.25 | 69.61 | 0.81 | - | - | - | - | - | 100 |
| 19 | Pyroxene | 0.9 | 14.3 | 3.31 | 50.38 | - | 18.82 | 1.08 | 0.55 | - | 10.65 | 100 |
| 20 | Pyroxene | 0.89 | 14.25 | 3.47 | 50.61 | - | 19.41 | 1.13 | - | - | 10.25 | 100 |
| 21 | Pumpellyite | - | 2.49 | 24.55 | 40.89 | - | 23.25 | - | - | - | 8.83 | 100 |
| 22 | Chlorite + Epidote? | - | 12.82 | 3.13 | 49.19 | - | 21.34 | 1.37 | - | - | 12.14 | 100 |
| 23 | Pumpellyite | - | 3.15 | 24.11 | 39.99 | - | 23.24 | - | - | - | 9.51 | 100 |
| 24 | K-spar | 0.95 | - | 18.21 | 64.98 | 15.33 | - | 0.53 | - | - | - | 100 |
| 25 | K-spar | 1.92 | - | 18.5 | 65.37 | 14.21 | - | - | - | - | - | 100 |

11CBF004_02 11-CBF004_026 through _035

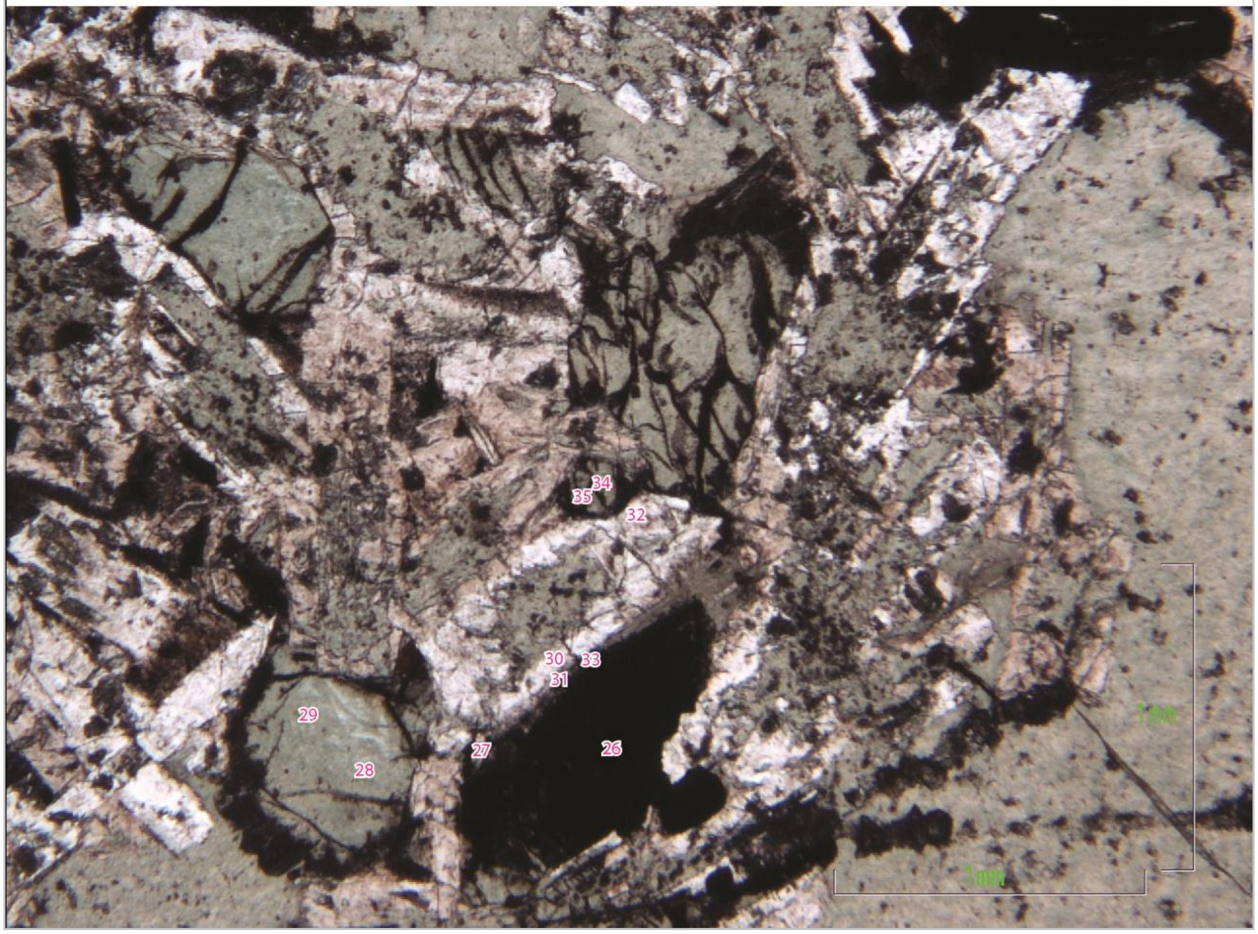


| Point | Mineral | | wt % | | | | | | | | | |
|---|---|---|---|---|---|---|---|---|---|---|---|---|
| | | $F_2O$ | $Na_2O$ | MgO | $Al_2O_3$ | $SiO_2$ | P2O5 | $K_2O$ | CaO | $TiO_2$ | MnO | FeO | Total |
| 26 | FeOx + Ilmenite | - | - | - | - | - | - | - | - | 37.3 | 0.82 | 61.88 | 100 |
| 27 | Sphene | - | 0.72 | 1.47 | 3.85 | 32.97 | - | - | 26.98 | 30.77 | - | 3.24 | 100 |
| 28 | Chlorite | - | 0.71 | 19.84 | 17.49 | 33.09 | - | - | 0.45 | - | - | 28.43 | 100 |
| 29 | Sphene | - | - | 3.18 | 5.04 | 33.25 | - | - | 24.56 | 28.33 | - | 5.63 | 100 |
| 30 | Albite | - | 10.51 | | 19.36 | 70.14 | - | - | - | - | - | - | 100 |
| 31 | Apatite | 3.13 | 0.63 | 1.79 | 2.59 | 6.42 | 36.98 | 1.18 | 45.52 | - | - | 1.77 | 100 |
| 32 | Albite | - | 10.3 | - | 19.85 | 69.24 | - | - | 0.61 | - | - | - | 100 |
| 33 | Apatite | 3.14 | - | 1.15 | 1.07 | 2.87 | 40.66 | - | 49.8 | - | - | 1.3 | 100 |
| 34 | Chlorite | - | - | 19.54 | 18.12 | 32.76 | - | - | - | - | 0.66 | 28.92 | 100 |
| 35 | Sphene | - | - | 1.11 | 3.64 | 33.28 | - | - | 27.48 | 30.93 | - | 3.55 | 100 |

## Analyses by Mineral

## Albite

| Sample | Point | $Na_2O$ | MgO | $Al_2O_3$ | $SiO_2$ | $K_2O$ | CaO | FeO | Total |
|---|---|---|---|---|---|---|---|---|---|
| 10CLD001 | 10-22_032 | 11.32 | - | 19.58 | 69.1 | - | - | - | 100 |
| 10CLD001 | 10-22_034 | 11.15 | - | 19.56 | 68.32 | 0.34 | - | 0.63 | 100 |
| 10CLD001 | 10-22_036 | 11.14 | - | 19.67 | 69.19 | - | - | - | 100 |
| 10CLD001 | 10-22_039 | 11.41 | - | 19.37 | 69.22 | - | - | - | 100 |
| 10CLD001 | 10-29_33 | 10.4 | - | 19.6 | 68.89 | 1.11 | - | - | 100 |
| 10CLD001 | 10-29_37 | 10.71 | - | 20.01 | 68.89 | 0.39 | - | - | 100 |
| 10CLD001 | 10-29_41 | 11.05 | - | 19.48 | 68.79 | - | - | 0.68 | 100 |
| 10CLD001 | 10-29_42 | 10.29 | - | 19.46 | 66.81 | 1.04 | 0.52 | 1.88 | 100 |
| 10CLD001 | 10-29_51 | 11.19 | - | 19.26 | 69.55 | - | - | - | 100 |
| 10CLD001 | 10-29_53 | 10.18 | - | 19.66 | 68.63 | 1.54 | - | - | 100 |
| 10CLD001 | 10-29_54 | 11.03 | - | 19.53 | 69.11 | 0.33 | - | - | 100 |
| 10CLD003 | 10-29_11 | 11.34 | - | 20.03 | 68.3 | - | 0.33 | - | 100 |
| 10CLD003 | 10-29_12 | 10.96 | - | 19.83 | 69.21 | - | - | - | 100 |
| 10CLD003 | 10-29_13 | 10.55 | 1.74 | 19.61 | 66.71 | - | - | 1.39 | 100 |
| 10CLD003 | 10-29_18 | 11.07 | - | 19.65 | 69.28 | - | - | - | 100 |
| 10CLD003 | 10-29_19 | 11.03 | - | 19.4 | 69.01 | 0.56 | - | - | 100 |
| 10CLD003 | 10-29_21 | 11.21 | - | 19.56 | 68.84 | - | 0.39 | - | 100 |
| 10CLD003 | 10-29_29 | 11.05 | - | 19.31 | 68.56 | 0.48 | 0.6 | - | 100 |
| 10CLD003 | 10-29_31 | 11.06 | - | 19.77 | 69.17 | - | - | - | 100 |
| 10CLD003 | 10-29_32 | 10.78 | - | 19.81 | 69.42 | - | - | - | 100 |
| 10CBF006 | 11-06_019 | 11.41 | - | 19.66 | 68.93 | - | - | - | 100 |
| 10CBF006 | 11-06_020 | 11.15 | - | 19.62 | 69.23 | - | - | - | 100 |
| 10CBF006 | 11-06_021 | 11.45 | - | 19.33 | 69.22 | - | - | - | 100 |
| 10CBF006 | 11-06_027 | 11.42 | - | 19.59 | 69 | - | - | - | 100 |
| 10CBF006 | 11-06_030 | 11.18 | - | 19.69 | 69.13 | - | - | - | 100 |
| 10CBF006 | 11-06_038 | 10.94 | - | 19.68 | 68.73 | 0.65 | - | - | 100 |
| 10CBF006 | 11-06_039 | 11.37 | - | 19.77 | 68.85 | - | - | - | 100 |
| 10CBF006 | 11-06_042 | 11.57 | - | 19.45 | 68.98 | - | - | - | 100 |
| 10CBF006 | 11-06_047 | 11.58 | - | 19.47 | 68.95 | - | - | - | 100 |
| 10CBF006 | 11-06_048 | 11.18 | - | 19.7 | 69.12 | - | - | - | 100 |
| 10CBF006 | 11-06_051 | 11.47 | - | 19.49 | 69.04 | - | - | - | 100 |
| 10CBF006 | 11-06_052 | 11.43 | - | 19.52 | 69.06 | - | - | - | 100 |
| 10CBF006 | 11-06_055 | 11.42 | - | 19.4 | 69.18 | - | - | - | 100 |
| 10CBF006 | 11-06_056 | 11.32 | - | 19.44 | 69.24 | - | - | - | 100 |
| 10CLD007 | 11-06_060 | 10.91 | - | 19.61 | 67.28 | 0.79 | - | 1.41 | 100 |
| 10CLD007 | 11-06_062 | 11.07 | - | 19.63 | 69.29 | - | - | - | 100 |
| 10CLD007 | 11-06_069 | 10.89 | - | 19.65 | 68.89 | 0.56 | - | - | 100 |

| Sample | Point | $Na_2O$ | MgO | $Al_2O_3$ | $SiO_2$ | $K_2O$ | CaO | FeO | Total |
|---|---|---|---|---|---|---|---|---|---|
| 10CLD007 | 11-06_071 | 10.81 | - | 19.69 | 69.01 | 0.49 | - | - | 100 |
| 10CLD007 | 11-06_074 | 10.93 | - | 19.7 | 69.36 | - | - | - | 100 |
| 10CLD007 | 11-06_084 | 11.2 | - | 19.46 | 69.34 | - | - | - | 100 |
| 10CLD007 | 11-06_091 | 11.28 | - | 19.61 | 67.88 | - | 0.49 | 0.75 | 100 |
| 11CBF004 | 11CBF004-004 | 10.55 | - | 19.37 | 70.08 | - | - | - | 100 |
| 11CBF004 | 11CBF004-005 | 10.4 | - | 19.66 | 69.51 | - | 0.42 | - | 100 |
| 11CBF004 | 11CBF004-006 | 10.39 | - | 19.66 | 69.95 | - | - | - | 100 |
| 11CBF004 | 11CBF004-014 | 10.15 | 1.56 | 19.44 | 66.55 | - | 0.45 | 1.9 | 100 |
| 11CBF004 | 11CBF004-018 | 10.33 | - | 19.25 | 69.61 | 0.81 | - | - | 100 |
| 11CBF004 | 11CBF004-030 | 10.51 | - | 19.36 | 70.14 | - | - | - | 100 |
| 11CBF004 | 11CBF004-032 | 10.3 | - | 19.85 | 69.24 | - | 0.61 | - | 100 |

## K-spar

| Sample | Point | $Na_2O$ | MgO | $Al_2O_3$ | $SiO_2$ | $K_2O$ | $TiO_2$ | FeO | Total |
|---|---|---|---|---|---|---|---|---|---|
| 10CLD001 | 10-22_037 | - | - | 18.26 | 65.82 | 15.91 | - | - | 100.0 |
| 10CLD001 | 10-29_34 | - | - | 18.41 | 65.8 | 15.79 | - | - | 100.0 |
| 10CLD001 | 10-29_36 | - | 0.58 | 18.44 | 65.15 | 15.83 | - | - | 100.0 |
| 10CLD001 | 10-29_38 | - | - | 18.15 | 65.68 | 16.17 | - | - | 100.0 |
| 10CLD001 | 10-29_45 | 5.09 | 1.22 | 18.8 | 65.68 | 9.21 | - | - | 100.0 |
| 10CLD001 | 10-29_49 | - | - | 18.19 | 65.7 | 16.11 | - | - | 100.0 |
| 10CLD001 | 10-29_50 | - | - | 18.07 | 65.63 | 16.29 | - | - | 100.0 |
| 10CLD003 | 10-29_28 | 7.77 | - | 19.5 | 68.36 | 4.37 | - | - | 100.0 |
| 10CBF006 | 11-06_032 | - | - | 20.06 | 63.52 | 15.33 | - | 1.1 | 100.0 |
| 10CBF006 | 11-06_040 | 1.97 | - | 18.54 | 65.46 | 14.02 | - | - | 100.0 |
| 10CLD007 | 11-06_061 | - | - | 18.54 | 65.65 | 15.82 | - | - | 100.0 |
| 10CLD007 | 11-06_064 | 0.67 | - | 18.38 | 65.26 | 15.7 | - | - | 100.0 |
| 10CLD007 | 11-06_068 | - | - | 18.61 | 65.69 | 15.71 | - | - | 100.0 |
| 10CLD007 | 11-06_072 | 1.18 | - | 18.68 | 65.56 | 14.58 | - | - | 100.0 |
| 10CLD007 | 11-06_073 | - | - | 18.44 | 65.57 | 16 | - | - | 100.0 |
| 10CLD007 | 11-06_081 | - | - | 18.47 | 65.56 | 15.98 | - | - | 100.0 |
| 10CLD007 | 11-06_082 | - | - | 18.34 | 65.73 | 15.93 | - | - | 100.0 |
| 10CLD007 | 11-06_085 | - | - | 18.33 | 65.69 | 15.98 | - | - | 100.0 |
| 10CLD007 | 11-06_092 | - | - | 18.87 | 65.62 | 15.51 | - | - | 100.0 |
| 10CLD007 | 11-06_094 | - | - | 18.34 | 65.63 | 16.03 | - | - | 100.0 |
| 10CLD007 | 11-06_097 | - | - | 18.6 | 65.52 | 15.88 | - | - | 100.0 |
| 10CLD007 | 11-06_098 | - | - | 18.45 | 65.54 | 16.01 | - | - | 100.0 |
| 11CBF004 | 11CBF004-007 | 1.65 | - | 18.96 | 66.2 | 13.19 | - | - | 100.0 |
| 11CBF004 | 11CBF004-008 | 2.82 | - | 18.87 | 65.55 | 12.75 | - | - | 100.0 |
| 11CBF004 | 11CBF004-024 | 0.95 | - | 18.21 | 64.98 | 15.33 | 0.53 | - | 100.0 |
| 11CBF004 | 11CBF004-025 | 1.92 | - | 18.5 | 65.37 | 14.21 | - | - | 100.0 |

## Epidote

| Sample | Point | MgO | $Al_2O_3$ | $SiO_2$ | $K_2O$ | CaO | $TiO_2$ | MnO | FeO | Total |
|---|---|---|---|---|---|---|---|---|---|---|
| 10CLD001 | 10-22_038 | - | 21.73 | 38.98 | - | 22.64 | - | - | 16.65 | 100.0 |
| 10CLD001 | 10-22_040 | - | 20.80 | 39.07 | - | 22.91 | 0.60 | - | 16.62 | 100.0 |
| 10CLD001 | 10-22_041 | - | 21.29 | 39.44 | - | 22.92 | - | - | 16.35 | 100.0 |
| 10CLD001 | 10-22_043 | - | 20.78 | 39.43 | - | 22.73 | - | - | 17.06 | 100.0 |
| 10CLD001 | 10-29_46 | - | 23.06 | 40.16 | 0.38 | 22.67 | - | - | 13.73 | 100.0 |
| 10CLD001 | 10-29_47 | - | 20.06 | 38.83 | - | 22.45 | - | - | 18.66 | 100.0 |
| 10CLD001 | 10-29_48 | - | 19.65 | 38.71 | - | 22.64 | - | - | 18.99 | 100.0 |
| 10CLD003 | 10-29_01 | - | 19.66 | 38.90 | - | 22.64 | - | - | 18.80 | 100.0 |
| 10CLD003 | 10-29_02 | 1.29 | 19.85 | 38.71 | - | 21.84 | - | - | 18.30 | 100.0 |
| 10CLD003 | 10-29_03 | 0.84 | 19.37 | 38.84 | - | 22.26 | - | - | 18.70 | 100.0 |
| 10CLD003 | 10-29_22 | 0.84 | 20.13 | 39.23 | - | 22.04 | - | - | 17.76 | 100.0 |
| 10CLD003 | 10-29_24 | - | 18.87 | 39.00 | - | 22.21 | - | - | 19.91 | 100.0 |
| 10CBF006 | 11-06_001 | - | 22.31 | 39.01 | - | 21.72 | - | 1.03 | 15.92 | 100.0 |
| 10CBF006 | 11-06_002 | - | 24.52 | 39.57 | - | 22.74 | - | - | 13.17 | 100.0 |
| 10CBF006 | 11-06_003 | - | 21.98 | 39.56 | - | 21.81 | - | 1.04 | 15.61 | 100.0 |
| 10CBF006 | 11-06_007 | - | 21.40 | 39.24 | - | 23.13 | - | - | 16.23 | 100.0 |
| 10CBF006 | 11-06_028 | - | 23.67 | 40.05 | - | 22.57 | - | - | 13.71 | 100.0 |
| 10CBF006 | 11-06_057 | - | 21.82 | 39.50 | - | 22.25 | - | - | 16.43 | 100.0 |
| 11CLD005 | 02-25-003 | - | 22.57 | 39.71 | - | 23.11 | - | - | 14.6 | 100.0 |
| 11CLD005 | 02-25-004 | - | 20.87 | 38.8 | - | 23.16 | - | - | 17.18 | 100.0 |
| 11CLD005 | 02-25-005 | - | 22.73 | 39.78 | - | 23.15 | - | - | 14.34 | 100.0 |
| 11CLD005 | 02-25-007 | - | 25.93 | 40 | - | 22.75 | - | 0.7 | 10.61 | 100.0 |
| 11CLD005 | 02-25-008 | - | 25.88 | 40.22 | - | 23.25 | - | - | 10.65 | 100.0 |

## Pumpellyite

| Sample | Point | MgO | $Al_2O_3$ | $SiO_2$ | CaO | FeO | Total |
|---|---|---|---|---|---|---|---|
| 10CLD001 | 10-22_015 | 2.93 | 22.33 | 39.6 | 23.02 | 12.13 | 100.0 |
| 10CLD001 | 10-22_016 | 3.67 | 21.7 | 40.54 | 21.31 | 12.77 | 100.0 |
| 10CLD001 | 10-22_017 | 2.95 | 21.72 | 40.24 | 22.62 | 12.46 | 100.0 |
| 10CLD001 | 10-22_024 | 8.39 | 22.03 | 41.76 | 19.18 | 8.63 | 100.0 |
| 10CLD001 | 10-22_026 | 4.81 | 22.89 | 40.98 | 21.26 | 10.06 | 100.0 |
| 11CLD007 | 11-06_088 | 3.39 | 23.77 | 40.3 | 23.7 | 8.89 | 100.1 |
| 11CLD007 | 11-06_090 | 7.17 | 22.76 | 41.6 | 20.5 | 8.05 | 100.1 |
| 11CBF004 | 11CBF004-021 | 2.49 | 24.55 | 40.89 | 23.25 | 8.83 | 100.0 |
| 11CBF004 | 11CBF004-023 | 3.15 | 24.11 | 39.99 | 23.24 | 9.51 | 100.0 |

# Chlorite

| Sample | Point | $Na_2O$ | MgO | $Al_2O_3$ | $SiO_2$ | CaO | $TiO_2$ | MnO | FeO | Total |
|---|---|---|---|---|---|---|---|---|---|---|
| 10CLD001 | 10-22_007 | - | 22.79 | 18.49 | 33.63 | - | - | - | 25.09 | 100.0 |
| 10CLD001 | 10-22_008 | - | 22.98 | 18.47 | 33.53 | - | - | - | 25.02 | 100.0 |
| 10CLD001 | 10-22_009 | - | 22.91 | 18.87 | 33.3 | - | - | 0.61 | 24.31 | 100.0 |
| 10CLD001 | 10-22_010 | - | 22.1 | 17.8 | 33.13 | - | - | - | 26.97 | 100.0 |
| 10CLD001 | 10-22_021 | - | 23.19 | 18.96 | 33.74 | - | - | - | 24.11 | 100.0 |
| 10CLD001 | 10-22_022 | - | 22.8 | 18.66 | 33.77 | - | - | - | 24.77 | 100.0 |
| 10CLD001 | 10-22_023 | - | 23.18 | 18.84 | 33.6 | - | - | - | 24.38 | 100.0 |
| 10CLD001 | 10-22_035 | - | 23.46 | 18.73 | 34.48 | - | - | - | 23.32 | 100.0 |
| 10CLD001 | 10-22_044 | - | 23.36 | 18.36 | 34.58 | - | - | - | 23.7 | 100.0 |
| 10CLD001 | 10-29_39 | - | 23.1 | 19.38 | 33.94 | - | - | - | 23.58 | 100.0 |
| 10CLD001 | 10-29_43 | - | 23.93 | 18.97 | 33.95 | - | - | 0.6 | 22.55 | 100.0 |
| 10CLD001 | 10-29_44 | - | 23.2 | 18.55 | 33.56 | - | - | 0.65 | 24.04 | 100.0 |
| 10CLD001 | 10-29_52 | - | 22.99 | 18.43 | 33.74 | - | - | 0.69 | 24.15 | 100.0 |
| 10CLD001 | 10-29_55 | - | 22.79 | 18.66 | 33.21 | - | - | 0.62 | 24.72 | 100.0 |
| 10CLD001 | 10-29_57 | - | 22.14 | 18.39 | 32.7 | - | - | - | 26.77 | 100.0 |
| 10CLD003 | 10-29_04 | - | 20.84 | 19.07 | 32.76 | - | - | 0.9 | 26.43 | 100.0 |
| 10CLD003 | 10-29_05 | - | 19.92 | 17.62 | 32.43 | - | - | 1.06 | 28.97 | 100.0 |
| 10CLD003 | 10-29_06 | - | 21.36 | 18.37 | 33.42 | 0.35 | - | 1.03 | 25.46 | 100.0 |
| 10CLD003 | 10-29_14 | - | 22.31 | 19.28 | 33.8 | - | - | - | 24.61 | 100.0 |
| 10CLD003 | 10-29_15 | 0.6 | 21.61 | 18.51 | 32.83 | 0.34 | - | 0.71 | 25.4 | 100.0 |
| 10CLD003 | 10-29_16 | 0.8 | 21.71 | 18.71 | 33.13 | - | - | 0.66 | 24.99 | 100.0 |
| 10CLD003 | 10-29_25 | 0.83 | 21.68 | 18.47 | 33.1 | - | - | 0.68 | 25.24 | 100.0 |
| 10CLD003 | 10-29_26 | 0.75 | 21.22 | 18.6 | 32.83 | - | - | 0.75 | 25.85 | 100.0 |
| 10CLD003 | 10-29_27 | - | 20.83 | 18.09 | 33.3 | - | - | 0.68 | 27.09 | 100.0 |
| 10CBF006 | 11-06_018 | - | 18.86 | 18.3 | 31.99 | - | - | 0.76 | 30.1 | 100.0 |
| 10CBF006 | 11-06_022 | - | 18.08 | 18.69 | 31.91 | - | - | - | 31.32 | 100.0 |
| 10CBF006 | 11-06_023 | - | 18.57 | 18.5 | 31.73 | - | - | 0.75 | 30.45 | 100.0 |
| 10CBF006 | 11-06_026 | - | 18.8 | 18.1 | 31.9 | - | - | 0.7 | 30.51 | 100.0 |
| 10CBF006 | 11-06_037 | - | 20.89 | 18.85 | 32.34 | - | - | 0.7 | 27.22 | 100.0 |
| 10CBF006 | 11-06_043 | - | 18.51 | 18.46 | 31.54 | - | - | 0.85 | 30.64 | 100.0 |
| 10CBF006 | 11-06_049 | - | 20.32 | 18.49 | 32.24 | - | - | 0.8 | 28.15 | 100.0 |
| 10CBF006 | 11-06_053 | - | 18.44 | 18.71 | 31.86 | - | - | 0.88 | 30.11 | 100.0 |
| 10CBF006 | 11-06_058 | - | 18.56 | 18.26 | 32.23 | - | - | 0.74 | 30.21 | 100.0 |
| 10CLD007 | 11-06_066 | - | 25.02 | 19.01 | 34.62 | - | - | 0.66 | 20.68 | 100.0 |
| 10CLD007 | 11-06_067 | - | 24.69 | 18.95 | 34.06 | - | - | 0.76 | 21.54 | 100.0 |
| 10CLD007 | 11-06_070 | - | 24.34 | 19.62 | 33.57 | - | - | 0.73 | 21.74 | 100.0 |
| 10CLD007 | 11-06_076 | - | 24.95 | 18.68 | 34.78 | - | - | 0.68 | 20.9 | 100.0 |
| 10CLD007 | 11-06_078 | - | 24.67 | 18.98 | 34.51 | - | - | - | 21.84 | 100.0 |
| 10CLD007 | 11-06_080 | - | 22.85 | 18.54 | 33.02 | - | - | 0.64 | 24.94 | 100.0 |
| 10CLD007 | 11-06_083 | - | 23.72 | 18.44 | 34.09 | - | - | 0.78 | 22.97 | 100.0 |
| 10CLD007 | 11-06_086 | - | 24.9 | 18.36 | 34.89 | - | - | 0.81 | 21.04 | 100.0 |

| Sample | Point | $Na_2O$ | MgO | $Al_2O_3$ | $SiO_2$ | CaO | $TiO_2$ | MnO | FeO | Total |
|---|---|---|---|---|---|---|---|---|---|---|
| 10CLD007 | 11-06_087 | - | 24.64 | 18.58 | 34.52 | - | - | 0.74 | 21.51 | 100.0 |
| 10CLD007 | 11-06_089 | - | 25.08 | 18.93 | 34.23 | - | - | 0.7 | 21.05 | 100.0 |
| 10CLD007 | 11-06_093 | - | 23.67 | 18.96 | 33.93 | - | - | - | 23.43 | 100.0 |
| 10CLD007 | 11-06_100 | - | 23.18 | 18.99 | 33.91 | - | - | - | 23.93 | 100.0 |
| 11CBF004 | 11CBF004_001 | - | 20.02 | 17.41 | 33.04 | 0.85 | 0.63 | 0.66 | 27.4 | 100.0 |
| 11CBF004 | 11CBF004_002 | - | 19.53 | 18.81 | 32.34 | - | - | - | 29.32 | 100.0 |
| 11CBF004 | 11CBF004_003 | - | 20.62 | 17.11 | 33.26 | 0.54 | - | 0.72 | 27.75 | 100.0 |
| 11CBF004 | 11CBF004_015 | - | 19.94 | 17.71 | 33.28 | - | - | - | 29.07 | 100.0 |
| 11CBF004 | 11CBF004_016 | - | 20.5 | 17.79 | 33.82 | - | - | - | 27.88 | 100.0 |
| 11CBF004 | 11CBF004_028 | 0.71 | 19.84 | 17.49 | 33.09 | 0.45 | - | - | 28.43 | 100.0 |
| 11CBF004 | 11CBF004_034 | - | 19.54 | 18.12 | 32.76 | - | - | 0.66 | 28.92 | 100.0 |

# Pyroxene (Augite)

| Sample | Point | $Na_2O$ | MgO | $Al_2O_3$ | $SiO_2$ | CaO | $TiO_2$ | $Cr_2O_3$ | FeO | Total |
|---|---|---|---|---|---|---|---|---|---|---|
| 11CBF006 | 11-06_011 | - | 14.84 | 2.23 | 51.69 | 16.86 | 1.01 | - | 13.37 | 100.0 |
| 11CBF006 | 11-06_013 | - | 15.36 | 2.45 | 52.19 | 18.25 | 1.01 | - | 10.75 | 100.0 |
| 11CBF006 | 11-06_014 | 0.77 | 15.54 | 2.38 | 52.39 | 18.15 | 0.77 | - | 9.99 | 100.0 |
| 11CBF006 | 11-06_015 | - | 15.06 | 2.91 | 51.58 | 19.36 | 0.95 | 0.65 | 9.49 | 100.0 |
| 11CBF006 | 11-06_016 | - | 15.08 | 3.26 | 51.23 | 18.73 | 0.94 | 0.82 | 9.93 | 100.0 |
| 11CBF006 | 11-06_017 | - | 13.56 | 2.78 | 50.59 | 18.26 | 1.21 | - | 13.6 | 100.0 |
| 11CBF006 | 11-06_024 | - | 15.84 | 2.6 | 52.2 | 18.83 | 0.76 | 0.61 | 9.15 | 100.0 |
| 11CBF006 | 11-06_025 | - | 15.93 | 2.39 | 52.3 | 18.31 | 0.7 | 0.8 | 9.58 | 100.0 |
| 11CBF006 | 11-06_029 | 0.85 | 14.33 | 3.73 | 50.14 | 18.39 | 1.26 | - | 11.3 | 100.0 |
| 11CBF006 | 11-06_033 | 1.14 | 14.13 | 2.28 | 50.86 | 17.35 | 0.82 | - | 13.42 | 100.0 |
| 11CBF006 | 11-06_041 | - | 15.73 | 2.21 | 52.38 | 18.36 | 0.7 | 0.62 | 10.01 | 100.0 |
| 11CBF006 | 11-06_044 | - | 15.32 | 2.37 | 52.19 | 18.87 | 0.79 | - | 10.47 | 100.0 |
| 11CBF006 | 11-06_045 | - | 15.71 | 2.43 | 51.52 | 18.54 | 0.85 | 0.53 | 10.43 | 100.0 |
| 11CBF006 | 11-06_046 | 0.88 | 14.6 | 3.25 | 51.09 | 18.76 | 0.95 | - | 10.46 | 100.0 |
| 11CBF006 | 11-06_050 | - | 13.93 | 2.86 | 50.64 | 17.46 | 1.12 | - | 13.98 | 100.0 |
| 11CBF006 | 11-06_059 | - | 15.01 | 2.45 | 51.43 | 18.26 | 0.89 | - | 11.96 | 100.0 |
| 11CBF004 | 11CBF004-011 | - | 14.04 | 3.02 | 51.19 | 19.41 | 1.23 | - | 11.11 | 100.0 |
| 11CBF004 | 11CBF004-012 | - | 13.72 | 2.96 | 50.57 | 18.52 | 1.27 | - | 12.96 | 100.0 |
| 11CBF004 | 11CBF004-013 | - | 15.29 | 2.06 | 52.28 | 18.55 | 0.97 | - | 10.85 | 100.0 |
| 11CBF004 | 11CBF004-019 | 0.9 | 14.3 | 3.31 | 50.38 | 18.82 | 1.08 | 0.55 | 10.65 | 100.0 |
| 11CBF004 | 11CBF004-020 | 0.89 | 14.25 | 3.47 | 50.61 | 19.41 | 1.13 | - | 10.25 | 100.0 |
| 11CBF004 | 11CBF004-022 | - | 12.82 | 3.13 | 49.19 | 21.34 | 1.37 | - | 12.14 | 100.0 |

## Sphene

| Sample | Point | $Na_2O$ | MgO | $Al_2O_3$ | $SiO_2$ | CaO | $TiO_2$ | FeO | Total |
|---|---|---|---|---|---|---|---|---|---|
| 10CLD001 | 10-22_029 | - | 3.19 | 4.43 | 31.95 | 24.3 | 28.25 | 7.89 | 100.0 |
| 10CLD001 | 10-22_031 | - | 3.33 | 4.4 | 33.25 | 24.61 | 29.12 | 5.29 | 100.0 |
| 10CLD003 | 10-29_10 | - | 0.52 | 4.73 | 33.6 | 27.81 | 30.21 | 3.14 | 100.0 |
| 10CLD007 | 11-06_077 | - | - | 4.92 | 34.11 | 28.39 | 30.13 | 2.45 | 100.0 |
| 10CLD007 | 11-06_079 | - | 1.03 | 3.54 | 31.08 | 25.38 | 27.7 | 11.26 | 100.0 |
| 10CLD007 | 11-06_095 | - | - | 5.35 | 33.11 | 27.97 | 30.42 | 3.15 | 100.0 |
| 11CBF004 | 11CBF004-010 | - | 3.5 | 5.76 | 32.33 | 24 | 28.11 | 6.3 | 100.0 |
| 11CBF004 | 11CBF004-017 | - | 1 | 3.87 | 33.6 | 26.74 | 30.73 | 4.5 | 100.4 |
| 11CBF004 | 11CBF004-027 | 0.72 | 1.47 | 3.85 | 32.97 | 26.98 | 30.77 | 3.24 | 100.0 |
| 11CBF004 | 11CBF004-029 | - | 3.18 | 5.04 | 33.25 | 24.56 | 28.33 | 5.63 | 100.0 |
| 11CBF004 | 11CBF004-034 | - | 1.11 | 3.64 | 33.28 | 27.48 | 30.93 | 3.55 | 100.0 |

# Apatite

| Sample | Point | $F_2O$ | $Na_2O$ | MgO | $Al_2O_3$ | $SiO_2$ | $P_2O_5$ | $K_2O$ | CaO | FeO | Total |
|---|---|---|---|---|---|---|---|---|---|---|---|
| 11CBF004 | 11CBF004-031 | 3.13 | 0.63 | 1.79 | 2.59 | 6.42 | 36.98 | 1.18 | 45.52 | 1.77 | 100 |
| 11CBF004 | 11CBF004-033 | 3.14 | - | 1.15 | 1.07 | 2.87 | 40.66 | - | 49.8 | 1.3 | 99.99 |

## Alteration

| Sample | Point | Guess | $Na_2O$ | MgO | $Al_2O_3$ | $SiO_2$ | $Cl_2O$ | $K_2O$ | CaO | MnO | FeO | Total |
|---|---|---|---|---|---|---|---|---|---|---|---|---|
| 10CLD001 | 10-22_004 | Ep + chl | 1.14 | 22.96 | 18.12 | 32.54 | - | - | 0.45 | 0.73 | 24.07 | 100.0 |
| 10CLD001 | 10-22_005 | Ep + chl | - | 22.62 | 18.21 | 33.48 | - | - | 0.55 | 0.75 | 24.39 | 100.0 |
| 10CLD001 | 10-22_006 | Ep + chl | 0.68 | 22.74 | 18.34 | 33.23 | - | - | 0.59 | 0.61 | 23.82 | 100.0 |
| 10CLD001 | 10-22_011 | Ep + chl | - | 4.09 | 18.24 | 38.43 | - | - | 20 | - | 19.24 | 100.0 |
| 10CLD001 | 10-22_012 | Ep + chl | - | 24.32 | 16.2 | 44.28 | - | - | 6.21 | - | 9 | 100.0 |
| 10CLD001 | 10-22_013 | Ep + chl | - | 28.8 | 13.71 | 45.21 | - | - | 3.02 | - | 9.25 | 100.0 |
| 10CLD001 | 10-22_014 | Ep + chl | - | 19.87 | 17.64 | 43 | - | - | 9.7 | - | 9.79 | 100.0 |
| 10CLD001 | 10-22_018 | Ep + chl + ca | - | 12.79 | 19.4 | 41.28 | - | - | 15.54 | - | 10.99 | 100.0 |
| 10CLD001 | 10-22_019 | Ep + chl + ca | 0.75 | 19.04 | 17.63 | 42.05 | - | - | 10.34 | - | 10.19 | 100.0 |
| 10CLD001 | 10-22_020 | Ep + chl + ca | - | 22.12 | 16.68 | 43.49 | - | - | 8.32 | - | 9.39 | 100.0 |
| 10CLD001 | 10-22_027 | Ep + chl + ca | 1.25 | 17.5 | 18.77 | 43.15 | 0.5 | 0.9 | 9.73 | - | 8.1 | 99.9 |
| 10CLD001 | 10-29_40 | chl + k-spar | - | 15.41 | 18.68 | 43.69 | - | 4.28 | - | - | 17.94 | 100.0 |
| 10CLD001 | 10-29_56 | chl + k-spar | - | 4.42 | 18.23 | 59.79 | - | 12.29 | - | - | 5.27 | 100.0 |
| 10CLD003 | 10-29_20 | Ep + chl + ca | 0.77 | 3.9 | 22.69 | 41.28 | - | - | 21.48 | - | 9.88 | 100.0 |
| 10CLD003 | 10-29_24 | Ep + chl + ca | - | 2.2 | 19.13 | 38.14 | - | - | 20.73 | - | 19.8 | 100.0 |
| 10CLD003 | 10-29_30 | Ep + chl + k-spar + ca | - | 3.08 | 23.16 | 44.28 | - | 2.4 | 19.54 | - | 7.55 | 100.0 |
| 10CBF006 | 11-06_005 | Ep + chl | - | 29.32 | 12.65 | 42.3 | - | - | 2.67 | - | 13.07 | 100.0 |
| 10CBF006 | 11-06_006 | Ep + chl | - | 27.95 | 12.9 | 43.38 | - | - | 4.65 | - | 11.12 | 100.0 |
| 10CBF006 | 11-06_009 | Ep + chl + ca | - | 12.1 | 16.33 | 41.83 | - | - | 15.14 | - | 14.6 | 100.0 |
| 10CBF006 | 11-06_010 | Ep + chl | - | 14.28 | 19.05 | 36.83 | - | - | 7.75 | - | 22.1 | 100.0 |
| 10CBF006 | 11-06_012 | Ep + chl + ca | - | 15.15 | 16.27 | 42.95 | - | - | 12.76 | - | 12.86 | 100.0 |
| 10CBF006 | 11-06_031 | Ep + chl + k-spar + ca | 1.74 | 2.38 | 23.92 | 45.01 | - | 0.92 | 18.13 | - | 7.89 | 100.0 |
| 10CLD007 | 11-06_063 | Ep + chl + ca | 1.19 | 2.88 | 23.18 | 44.22 | - | - | 19.96 | - | 8.58 | 100.0 |
| 10CLD007 | 11-06_065 | Ep + chl + k-spar + ca | 0.84 | 3.91 | 22.06 | 40.19 | - | 0.51 | 22.17 | - | 10.32 | 100.0 |
| 10CLD007 | 11-06_075 | Ep + chl + ca | - | 2.93 | 24.17 | 40.47 | - | - | 22.95 | - | 9.47 | 100.0 |

## Opaques

| Sample | Point | Guess | $Na_2O$ | MgO | $Al_2O_3$ | $SiO_2$ | $SO_3$ | $P_2O_5$ | $K_2O$ | CaO | $TiO_2$ | MnO | FeO | CuO | Total |
|---|---|---|---|---|---|---|---|---|---|---|---|---|---|---|---|
| 10CLD001 | 10-22_028 | FeOx | 1.49 | 10.4 | 7.66 | 14.04 | - | 1.19 | - | 1.53 | 1.6 | - | 62.1 | - | 100.0 |
| 10CLD001 | 10-22_030 | FeOx | - | 2.42 | 3.91 | 23.93 | - | - | - | 13.96 | 15.82 | - | 39.96 | - | 100.0 |
| 10CLD001 | 10-29_35 | Copper | - | - | 0.85 | 2.07 | 0.88 | - | 0.35 | - | - | - | 0.36 | 95.49 | 100.0 |
| 10CLD003 | 10-29_07 | FeOX | - | 2.58 | 2.31 | 4.25 | - | - | - | 0.89 | 2.13 | - | 87.84 | - | 100.0 |
| 10CLD003 | 10-29_08 | FeOx | - | 7.53 | 5.63 | 8.75 | - | - | - | 0.83 | 1.63 | - | 75.63 | - | 100.0 |
| 10CLD003 | 10-29_17 | FeOx + ilm | - | 10.19 | 8.16 | 17.79 | - | - | - | 3.95 | 3.4 | - | 56.51 | - | 100.0 |
| 10CBF006 | 11-06_008 | FeOx | - | - | 1.03 | 5.95 | - | - | - | 4.13 | 21.66 | - | 67.23 | - | 100.0 |
| 10CBF006 | 11-06_036 | FeOx + ilm | - | - | - | - | - | - | - | - | 7.89 | 0.89 | 89.58 | 1.64 | 100.0 |
| 10CLD007 | 11-06_096 | copper | - | - | 0.99 | 2.26 | 2.07 | - | 0.43 | - | - | - | - | 94.25 | 100.0 |
| 11CLD005 | 02-25-009 | ht + qtz +clay | - | - | 1.52 | 16.81 | - | - | - | - | - | - | 81.68 | - | 100.0 |
| 11CBF004 | 11CBF004-009 | FeOx + ilm | - | - | 0.7 | 4.39 | - | - | - | 2.94 | 15.97 | - | 76 | - | 100.0 |
| 11CBF004 | 11CBF004-026 | FeOx + ilm | - | - | - | - | - | - | - | - | 37.3 | 0.82 | 61.88 | - | 100.0 |

**Appendix B: Assumptions and Cost Estimate for Caledonia Mine Carbon Dioxide Direct Injection Demonstration Project (Cost data from RS Means and vender quotations)**

1. **Storage of 100 tons of carbon dioxide as carbonate minerals.**
2. **Density of carbonate minerals = 2 kg/$m^3$**
3. **Injection into stopes backfilled with crushed mine tailings**
4. **Porosity of mine tailings is estimated at 20%**
5. **Stope cross sections are 3 x 3 meters**
6. **Required total volume of voids in stopes = 500 $m^3$**
7. **Backfill volume = 60%**
8. **Length of each stope = 60 meters**

| | *Component*<br>*Structures/Materials/Supplies* | *Quantity* | *Unit* | *Unit Cost*<br>*($)* | *Item Total*<br>*($)* | *Sub-totals*<br>*($)* |
|---|---|---|---|---|---|---|
| 1 | Reinforced concrete barrier walls | 2 | ea | 25,000 | 50,000 | |
| 2 | High pressure portals | 2 | ea | 5,000 | 10,000 | |
| 3 | Furnace | 1 | ea | 100,000 | 100,000 | |
| 4 | Pipeline system | 1 | ea | 100,000 | 100,000 | |
| 5 | Compressor (rental 750 cfm) | 24 | mo | 3,000 | 72,000 | |
| 6 | Power transmission line to grid | 1 | ea | 70,000 | 70,000 | |
| 7 | Fuel (wood chips @ 8,000 Btu) | 80 | tons | 50 | 4,000 | |
| 8 | Carbon dioxide | 500 | tanks | 85 | 42,500 | |
| 9 | Nitrogen | 2,000 | tanks | 85 | 170,000 | |
| 10 | Instrumentation & sample anal. | 1 | ea | 250,000 | 250,000 | |
| | Sub-total | | | | 868,500 | 868,500 |
| | *Professional Staff & Student* | | | | | |
| 11 | Co-PI, Geological Engineer | 6 | mo | 13,500 | 81,000 | |
| 12 | Co-PI ,Civil Engineer | 6 | mo | 13,500 | 81,000 | |
| 13 | Ph.D Candidate | 24 | mo | 5625 | 135,000 | |
| | Sub-total | | | | | 297,000 |
| 14 | Staff Benefits (0.35 x 297,000) | | | | | 103,950 |
| 15 | F&A (0.50 x sum of items 1-14) | | | | | 634,725 |
| | Project Total | | | | | $1,904,175 |